ISTANBUL TECHNICAL UNIVERSITY * INSTITUTE OF ENERGY

INVESTIGATION OF THERMAL DECOMPOSITION BEHAVIOR OF SOME LIGNOCELLULOSIC MATERIALS

M.Sc. Thesis by
MUSTAFA CAN CELEBI

Department: Energy Science and Technology
Programme: Energy Science and Technology

Supervisor: Assoc. Prof. Nilgun Karatepe YAVUZ

JANUARY 2011

ISTANBUL TECHNICAL UNIVERSITY * INSTITUTE OF ENERGY

INVESTIGATION OF THERMAL DECOMPOSITION BEHAVIOR OF SOME LIGNOCELLULOSIC MATERIALS

M.Sc. Thesis by
MUSTAFA CAN CELEBI
(301081021)

Date of submission : 20 December 2010
Date of defence examination: 26 January 2011

Supervisor (Chairman) : Assoc. Prof. Dr. Nilgun Yavuz Karatepe (ITU)

Members of the Examining Committee : Assis. Prof. Dr.Sevilay Haciyakupoglu (ITU)

Assoc. Prof. Dr. Sevil Yucel (YTU)

JANUARY 2011

İSTANBUL TEKNİK ÜNİVERSİTESİ * ENERJİ ENSTİTÜSÜ

BAZI LİGNOSELÜLOZİK MALZEMELERİN ISIL BOZUNMA DAVRANIMLARININ İNCELENMESİ

YÜKSEK LİSANS TEZİ

MUSTAFA CAN ÇELEBİ

(301081021)

Tezin Enstitüye Verildiği Tarih : 20 Aralık 2010
Tezin Savunulduğu Tarih : 26 Ocak 2011

Tez Danışmanı : Doç. Dr. Nilgün Karatepe Yavuz (İTÜ)
Diğer Jüri Üyeleri : Yrd. Doç. Dr. Sevilay Hacıyakupoğlu (İTÜ)
Doç. Dr. Sevil Yücel (YTÜ)

OCAK 2011

FOREWORD

I would like to express my deepest gratitude to my supervisor Assoc. Prof. Dr. Nilgün Yavuz Karatepe for her guidance, advice, criticism, encouragement and insight throughout the research.

I also would like to thank Assist. Prof. Gulnur Mertoglu Elmas for her guidance in structural analysis of biomass samples. I am also grateful to my colleague, Neslihan Yuca from Istanbul Technical University Energy Institute, for her assistance in preparation of biomass samples used in the experiments.

I also thank to "TÜBİTAK MAM Energy Institute, Coal and Biomass Combustion and Gasification Laboratory" research group members, Assist. Prof. Dr. Hayati Olgun, Berrin Bay, Hakan Karatas, Yeliz Durak for their support during the experiments.

Last but not least, sincere thanks to my parents for their endless support during all the study and especially for their lifetime confidence in me.

December 2010

Mustafa Can Celebi

Chemical Engineer

TABLE OF CONTENTS

Page

ABBREVIATIONS

T	: temperature (K)
t	: time (s)
mtons	: million tons
mtoe	: million ton of oil equivalent
E_a	: activation energy (kJ/mol)
A	: frequency factor (1/s)
n	: order of reaction
f(α)	: differential form of the kinetic model
k	: reaction rate constant (s^{-1})
α	: conversion factor
R	: gas constant (kJ/mol.K)
b	: constant heating rate (K/s)
T_o	: initial temperature (K)
W	: weight of sample at any time
W_o	: initial weight of the sample
W_∞	: weight of sample at the end of the decomposition
TG	: thermogravimetry
TGA	: thermogravimetrical analysis
R^2	: coefficient of variation

LIST OF TABLES

Page

LIST OF FIGURES

Page

INVESTIGATION OF THERMAL DECOMPOSITION BEHAVIOR OF SOME LIGNOCELLULOSIC MATERIALS

SUMMARY

The fact that fosil fuels would deplete in foreseeable future, requires the utilization of alternative energy sources. Renewable energy sources are mainly comprised of solar, wind, hydraulic, geothermal, biomass. The biomass potential is ten times the global energy consumption and two hundred times that of food energy consumption. Subsequent to 1970s oil crisis, research studies on utilization of biomass as energy source have been conducted. Since biomass stores the solar energy in via photosynthesis, it is considered to be an important energy source.

The energy content of biomass is extracted by means of thermochemical, biological and physical processes. Carbonization and pyrolysis are the two thermochemical conversion processes that are used to obtain solid, liquid and uncondensable gas products by heating biomass under inert atmospheres. The process is carried out at low temperatures and high heating rates if the aim is to produce high liquid yield products; whereas it should be conducted under low heating rates if the desired products are high yield gases. The process is named as carbonization if it is utilized to obtain high yield solid products, and it is carried out both at low heating rates and under low temperature.

In this study, the thermal decomposition behavior of four different biomass samples, namely olive cake, hazelnut shell, sugarcane bagasse and corn cob are investigated under N_2 atmosphere at four different heating rates, namely 5, 20, 50 and 100 K/min. Kinetic parameters have been calculated according to Coats Redfern, by partitioning the decomposition into three regions since biomass samples are composed of hemicelluse, cellulose and lignin.

BAZI LİGNOSELÜLOZİK MALZEMELERİN ISIL BOZUNMA DAVRANIMLARININ İNCELENMESİ

ÖZET

Enerji ihtiyacımızın büyük bölümünü karşılayan fosil enerji kaynaklarının yakın bir gelecekte tükenecek olması, alternatif enerji kaynaklarının yaygın olarak kullanımını gerektirmektedir. Yenilenebilir enerji kaynakları; güneş, rüzgar, hidrolik, jeotermal, dalga ve biyokütle gibi kaynakları kapsamaktadır. Biyokütle kaynak potansiyeli, bugünkü küresel ticari enerji kullanımının on katı ve besin enerjisi tüketiminin iki yüz katına eşdeğerdir. 1970'li yıllarda gerçekleşen enerji (petrol) krizinden sonra dünya enerji ihtiyacının karşılanması için biyokütle kullanımı üzerinde araştırmalar yapılmıştır. Biyokütle kaynakları fotosentez yoluyla güneş enerjisini depolamaktadır. Düşük yoğunluğa sahip olan güneş enerjisinin depolanması hassas kolektörler aracılığıyla bile zordur. Ancak, biyokütle bu enerjiyi yapısında depoladığından önemli bir alternatif enerji kaynağıdır.

Biyokütlenin enerji içeriği termokimyasal, fiziksel ve biyolojik prosesler ile belirlenir. Karbonizasyon ve piroliz, biyokütlelerin inert ortamda ısıtılarak sıvı, katı ve yoğunlaşmayan gaz ürünlere dönüşmesini sağlayan termokimyasal dönüşüm prosesleridir. Prosesin amacı, yüksek sıvı ürün verimi elde etmek ise düşük sıcaklık, yüksek ısıtma hızı; yüksek gaz ürün verimi elde etmek ise düşük ısıtma hızı uygulanmalıdır. Eğer yüksek katı ürün verimi elde edilmek isteniyorsa, ısıl bozundurma işlemi düşük sıcaklık ve düşük ısıtma hızında gerçekleştirilir ve proses karbonizasyon adını alır.

Bu çalışmada, biyokütle kaynakları olan mısır küspesi, şeker pancarı küspesi, fındık kabuğu ile zeytin çekirdeği numunelerinin farklı koşullardaki (5,20,50 ve 100 K/dak ısıtma hızlarında, 50 ve 100 cm^3/dak gaz akış debilerinde) ısıl bozunum davranımları termogravimetrik analiz sisteminde incelenmiş ve ısıl bozunum kinetik parametreleri diferansiyel termal gravimetri verilerinden yararlanılarak Coats-Redfern yöntemi ile hesaplanmıştır.

1. INTRODUCTION

1.1 Nature of the problem

In today's world sustainable development has become the main focus of the human being. Sustainable development could be defined as, "utilizing the natural sources in order to develop the economical and social status in such a manner that, the coming generations would also be able to increase their life standards in a safe and healthy environment. Global warming, the average rise in temperature of the seas and land areas, is the most threatening issue regarding the sustainable development since the end of the last century. This is mainly due to the increasing concentration of greenhouse gases namely, CO_2, NO_x, H_2O, CFC-s, CH_4 and O_3 in the atmosphere [1].

Many sciencetists have been working on this subject in order to find out whether this global warming phenomenon has been resulted from anthropogenic forcing or natural forcing. Debates concerning the sustainable development began in 1972 in Stockholm Conference [2] Until the second half of 1980s, the government policies all over the world had been focused on providing economic and social development by increasing GNDP. In order to provide GNDP increase, production has to be increased thus leading an enormous amount of fossile fuel usage. There was a common belief that natural sources would be eternal. Besides this fossile fuel usage has negative impacts on the environment, nonetheless economic programmes were put into force without taking any precaution. In spite of the fact that the global warming phenomenon has been under observation by the scientists during the 20^{th} century, it was the 1^{st} World Climate Change Conference organized by WMO in 1979 where the importance of the topic was emphasized for the first time in international platform [3].

As expressed above development requires energy resources to be utilized, mainly the fossile fuels, which contradicts with the environmental sustainability and protection

of natural sources. In addition to that, world population is displaying an increase and according to IEA, the trend would be increasing linearly in the upcoming years [4].

2. ENERGY REVIEW

2.1 Future energy scenarios

Energy utilization is believed to be the reflection of development stage of a country. Thus, as population grows each and every year it is inevitable that energy sources utilization would show an increasing trend in order to provide economic welfare.

In Figure 2.1, the result of the IEA annual outlook report 2009, the energy demand trend is displayed with respect to years.

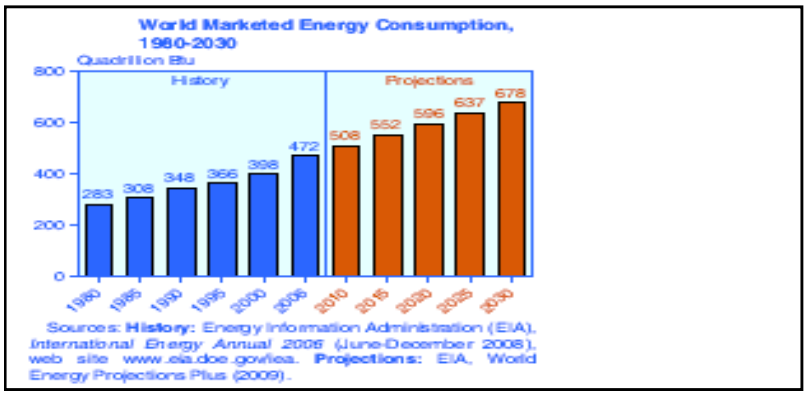

Figure 2.1: World marketed energy consumption between 1980-2030 [5]

In addition to IEA, corporate oil companies namely, Shell, Exxon Mobil have also reported similar market trends for the foreseeable future according to different scenarios.

“Shell Energy Scenarios to 2050” published in 2008 has two different energy policy scenarios regarding energy utilization in 2050. The scramble scenario in which ecnomic growth is relied on fosil fuels focuses on national energy security, thereby decision-makers would concentrate on secure energy supply. Action against global warming is not taken seriously as well as the energy efficieny measures.

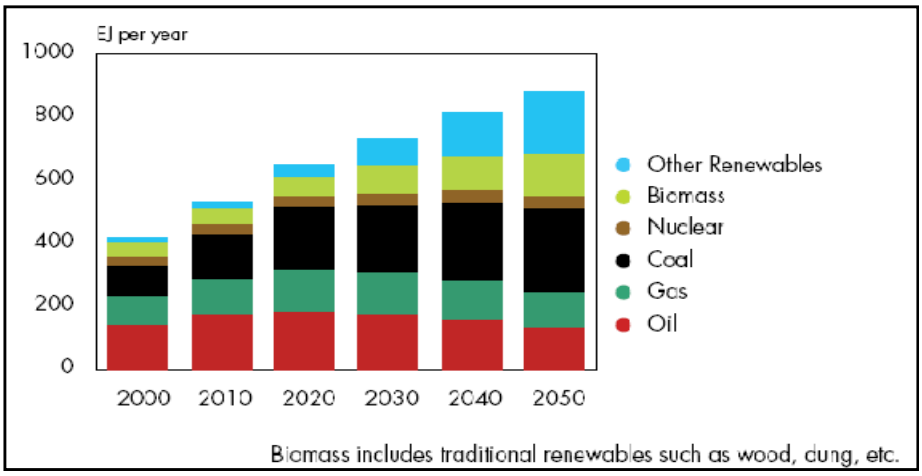

Figure 2.2: Primary energy source in 2050 according to scramble scenario[6]

In this scenario, energy companies take important roles where the politicians would be affected by rivalry between the consumer and the producer. Therefore, actions for preventing global warming and utilizing energy in a more effcient manner would not be taken most probably.

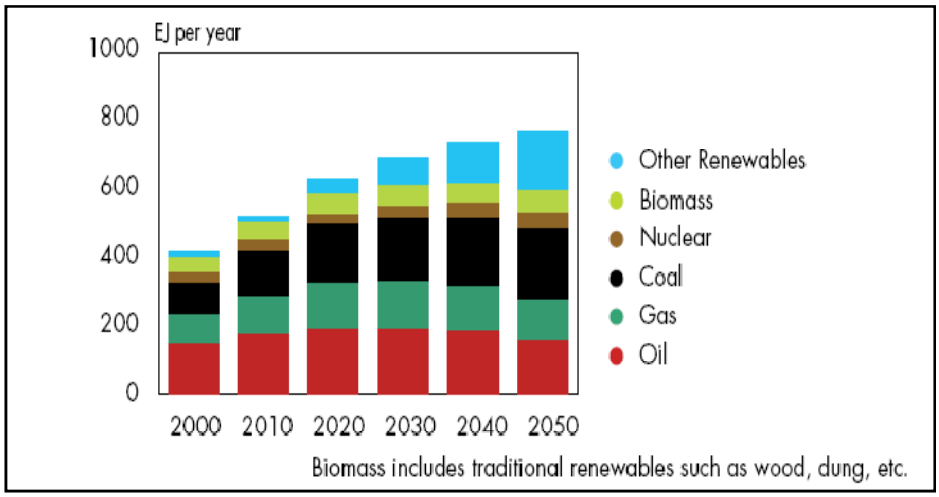

Figure 2.3: Primary energy source in 2050 according to blueprint scenario[6]

In contrast to scramble scenario, blueprint scenario addresses to a change in energy utilisation habits. It is predicted that both developing and developed countries will be less energy intensive in the course of activities sustaining economic growth. As compared to Figure 2.2, less energy utilisation is observed meaning that less CO_2 emission could be achieved by integrating CCS, fuel-cell and hybrid technologies. Government mandated energy policies together with the fiscal incentives would lead to energy efficient technologies to be developed and spred not only in the OECD members but also in Non-OECD member countries [6]. Furthermore, the comparison

of the two scenarios expressed above are displayed in Figure 2.4 in order to provide clear understanding of the general view.

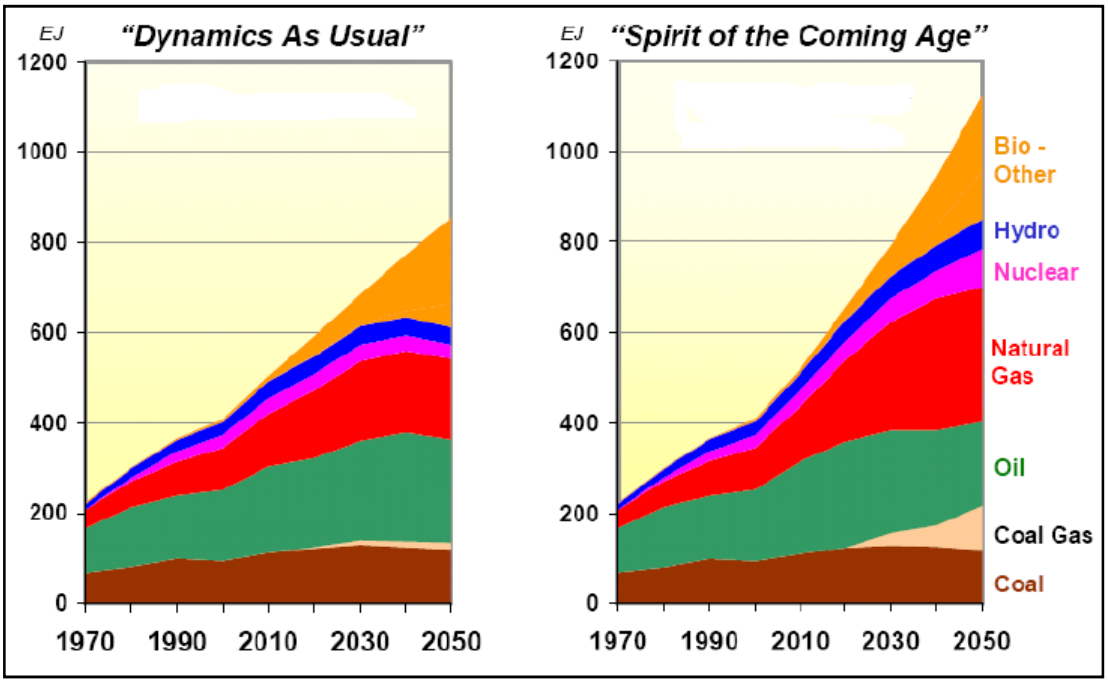

Figure 2.4: Comparison of global primary energy demand projections [6]

Another giant oil company that has been in the sector more than a century Exxon Mobil, published a report in 2007 with the title "The Outlook for Energy A View to 2030". Projections that took part in this outlook addresses the importance of fosil fuels in spite of the fact that the incentives and mandatory policies would be expected to increase the share of renewables. Thus, it is obvious that mankind would be using fosil fuels in the short to medium term in order to sustain the economic growth. In energy sector there is no "best" solution, rather than the possible solutions are intertwined and several factors are to be taken into account in finding an optimum way of providing energy. These factors are abbreviated as 3A and those are namely, accessibility, availability and acceptability in World Energy Council's Report published in 2007 with the title Deciding the Future: Energy Policy Scenarios to 2050. In order to make it clear, the following definitions are taken from the WEC report.

"Accessibility means that a minimum level of commercial energy services (in the form of electricity, stationary uses, and transport) is available at prices that are both affordable (low enough to meet the needs of the poor) and sustainable (prices reflecting the full marginal costs of energy production, transmission, and distribution

to support the financial ability of suppliers to maintain and develop these energy services). Availability relates to the long-term continuity of supply as well as to the short-term quality of service. Energy shortages can disrupt economic development, so a well-diversified portfolio of domestic or imported (or regionally) traded fuels and energy services is required. Acceptability addresses public attitudes and the environment, covering many issues: deforestation, land degradation or soil acidification at the regional level; indoor or local pollution such as that from the burning of traditional biomass fuels, or because of poor quality coal briquettes or charcoal production; greenhouse gas emissions and climate change on a global scale; nuclear security, safety, waste management, and proliferation; and the possible negative impact of the large dams or large-scale modern biomass developments" [7].

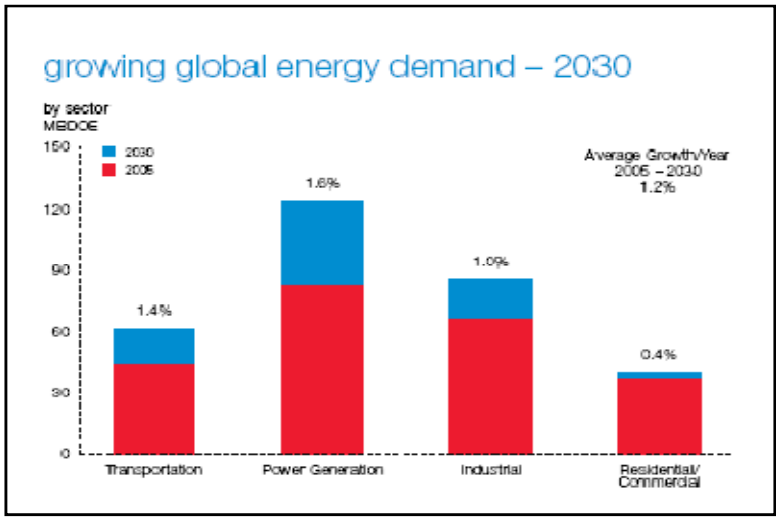

Figure 2.5: Global energy demand projection according to sectors [8]

Under the light of the above discussion and facts, it is clear that fosil fuels will play vital importance in development. Several international companies' reports and the independent associations such as WEC, IEA data have been collected in order to reflect the world energy review. It is not a surprising fact that utilization of fosil fuels will lead an increase in CO_2 emissions. Therefore there is a trade off between the welfare of mankind and the environmental sustainability. Focusing on financial affairs would create big problems in the next few decades; but the dynamics of the life itself necessitates production of goods by using raw materials. So, the possible outcomes of each and every anthropogenic activities should be modelled and estimated.

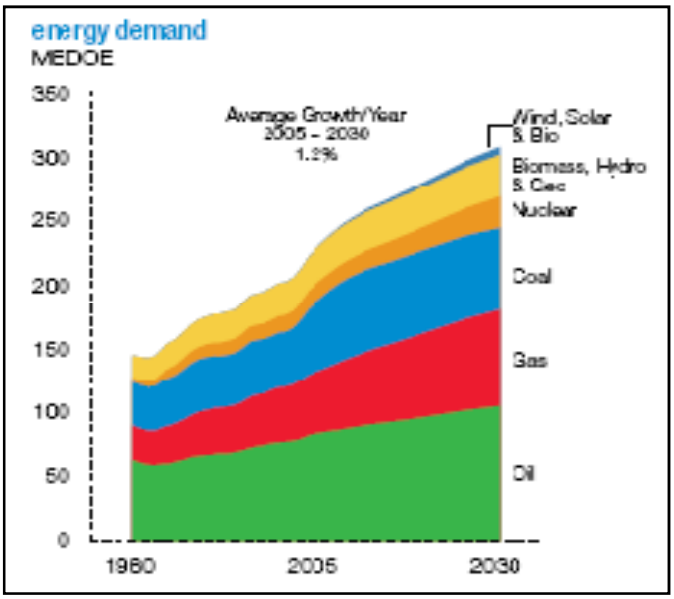

Figure 2.6: General global energy demand projection [8]

Below there are three graphs showing the population, GDP and primary energy demand projections that took place in "The Outlook for Energy A View to 2030".

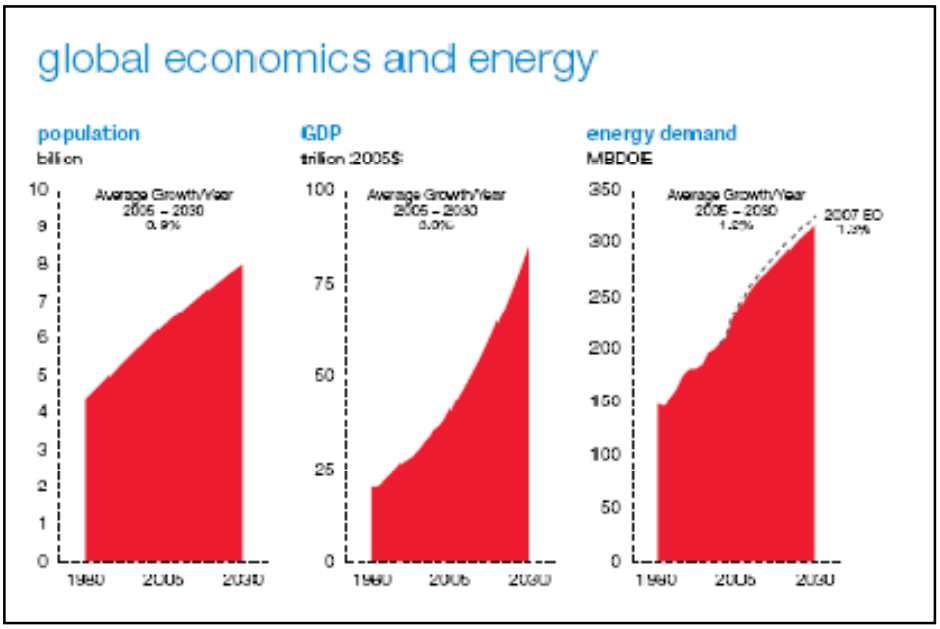

Figure 2.7: An overall view to global energy and economics up to 2030 [8]

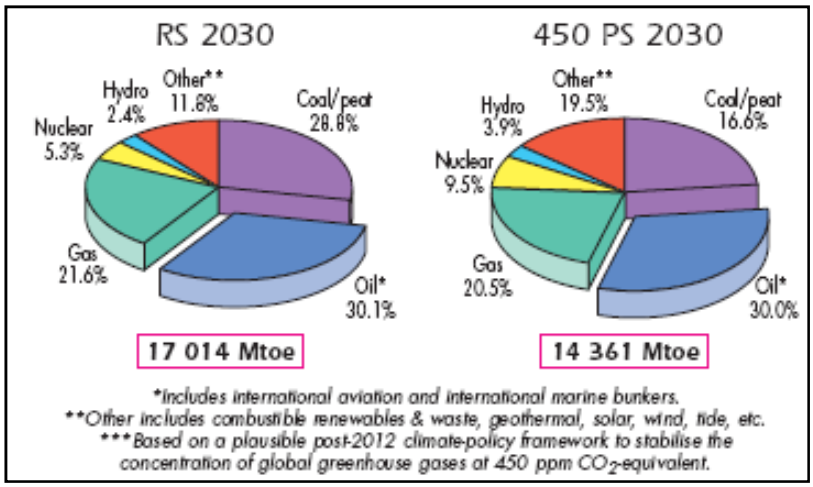

Figure 2.8: Fuel shares in 2030 for reference and alternative scenarios [9]

2.2 Energy review of the world

The future energy scenarios addresses the dominance of fosil fuels and its importance in the foreseeable future in almost all reliable association's outlook reports. It is mandatory to investigate the current energy situation of the world in order to clearly understand and take precautions against global warming without damaging the development trend.

As impressed before world is based on fosil fuels, and in Figure 2.8 the worldwide energy consumption according to primary energy sources data is displayed.

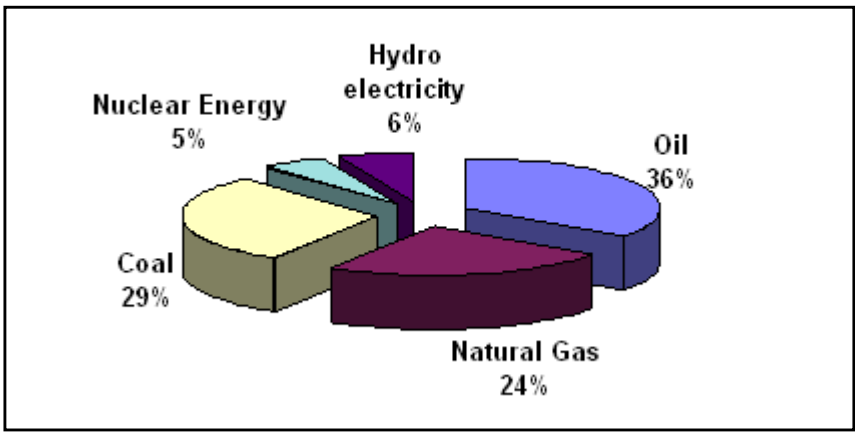

Figure 2.9: Global primary energy consumption by the end of 2008 [10]

Fosil fuels have always dominated the primary energy sources since the beginning of the 20th century. In Figure 2.10 comparison based on the primary energy supply between 1973 and 2007 is shown.

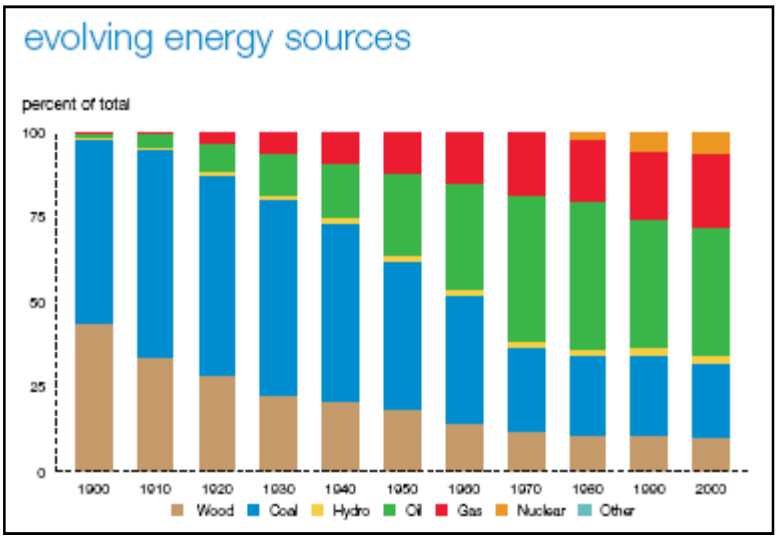

Figure 2.10: World's energy sources over the 20th and 21st centuries [8]

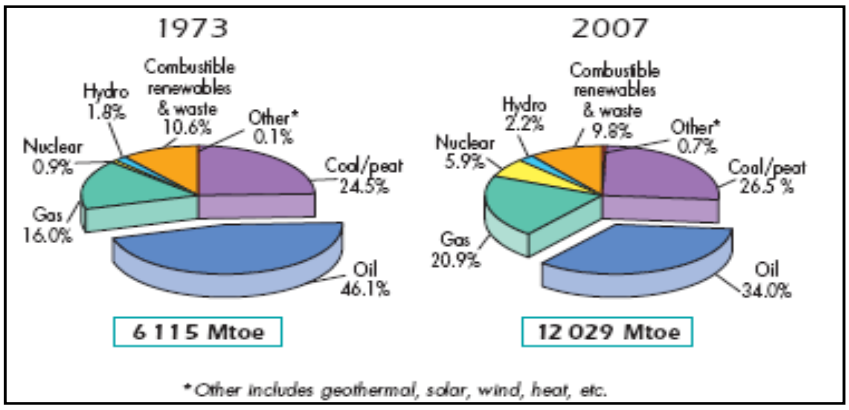

Figure 2.11: 1973 and 2007 shares of total primary energy supply [9]

Another interesting point is the fosil fuel producing regions in the world. This data is actually indicative in understanding the energy politics of developed countries and international conflicts, also the related wars in the last century.

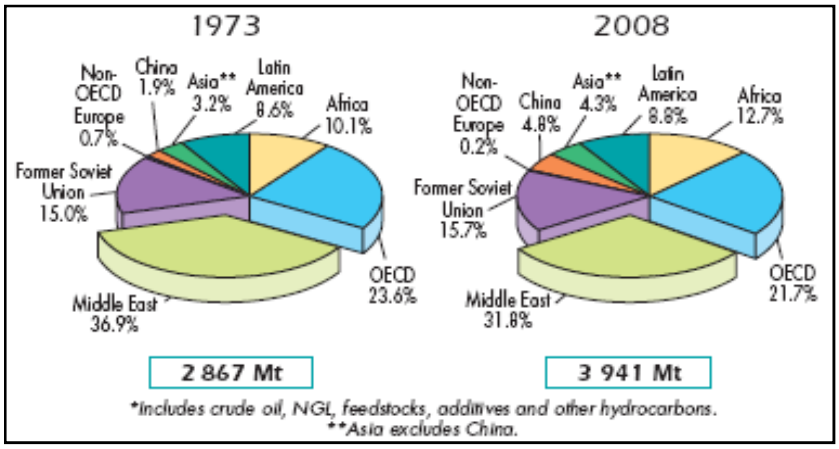

Figure 2.12: 1973 and 2008 regional shares of oil production [9]

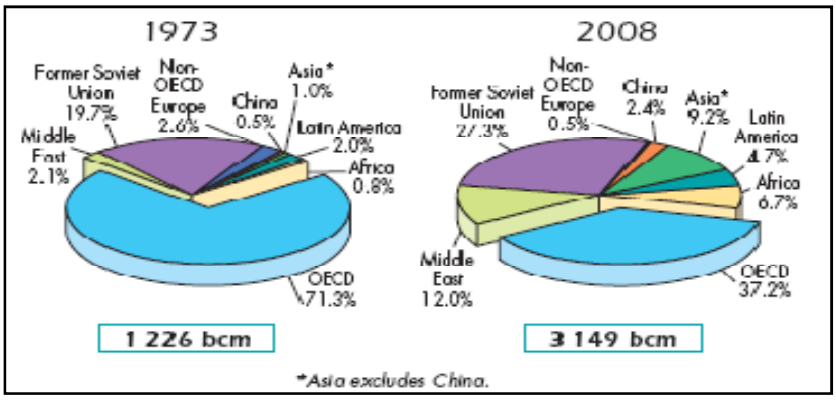

Figure 2.13: 1973 and 2008 regional shares of natural gas production [9]

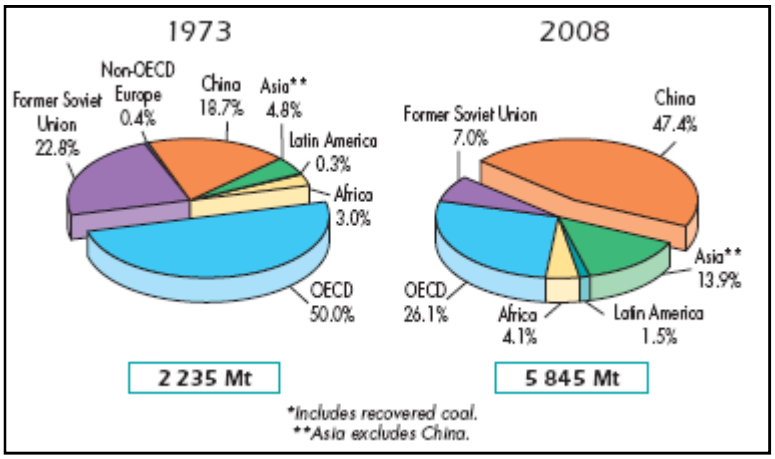

Figure 2.14: 1973 and 2008 regional shares of hard coal production [9]

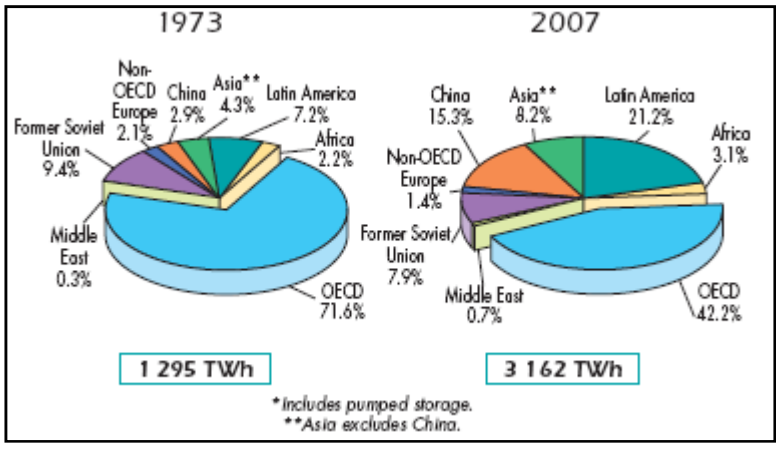

Figure 2.15: 1973 and 2007 regional shares of nuclear production [9]

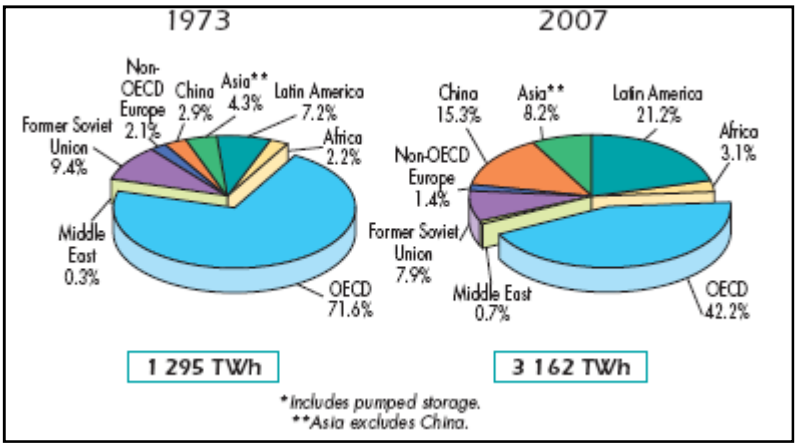

Figure 2.16: 1973 and 2007 regional shares of hydro production [9]

2.3 Prices of energy sources and commodities

As long as energy is accessible in a safe and sustainable way, the next consideration is its cost. Since energy is the raw material of all biotic activities its unit price has vital importance for both residential and industrial purpose. Due to that reason, several price data have been displayed in various graphs.

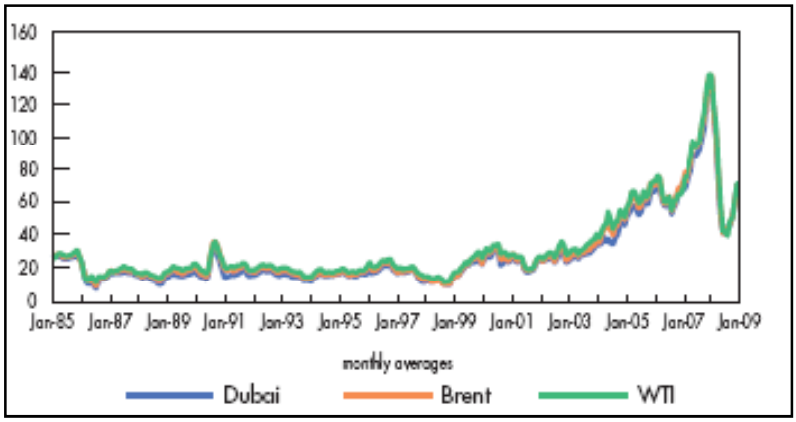

Figure 2.17: Key crude oil spot prices(US $/barrel) [9]

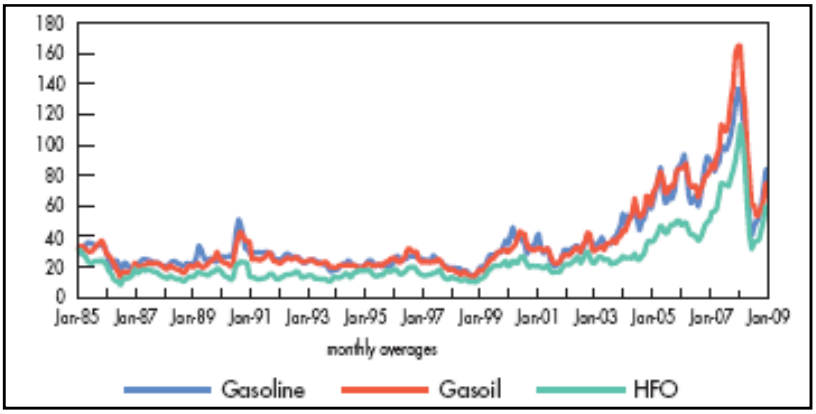

Figure 2.18: Rotterdam oil product spot prices (US $/barrel) [9]

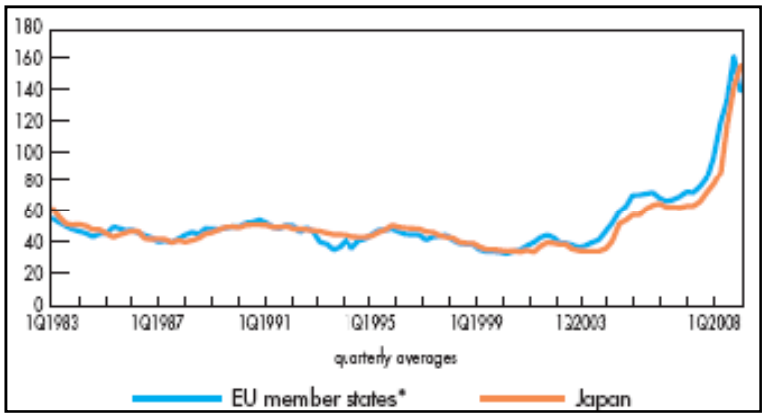

Figure 2.19: Steam coal import costs (US $/tonnes) [9]

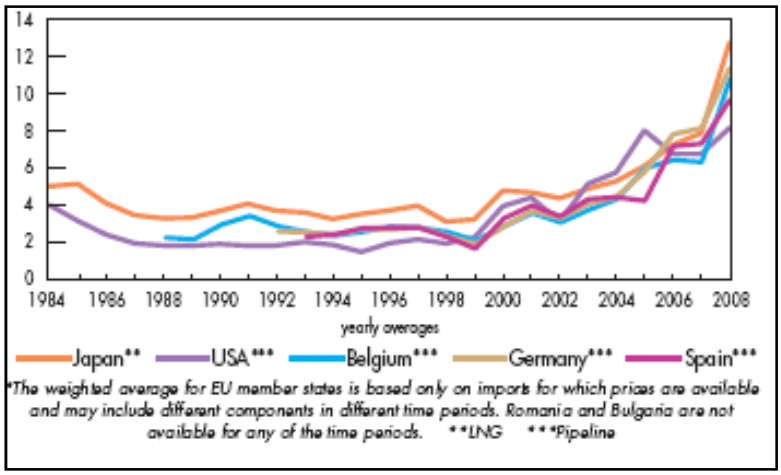

Figure 2.20: Natural gas import prices (US $/MBtu) [9]

In Figures 2.17 through 2.21 there exist sharp increases, almost all of which could not be controlled by countries itself. Looking deeply into the world history, this could easily be seen as well. So, countries have to find out a way of producing sustainable, economically acceptable and also accessible energy. Local energy sources such as wind, biomass, geothermal are of vital importance when the vulnerability of energy prices are considered. CO_2 emissions creates a serious problem that needs to be handled in a convenient manner, such that the living standards would be maintained while protection of the environment is also achieved. Thus, as expressed in advance increasing GDP by producing more requires utilization of energy sources, mainly the fosil fuels which as a result ends up with globa warming phenomenon. That is the reason of the existence of this sub chapter. Making more money while producing via sustainable energy resources is a very difficult task and there are only a few ways of doing this:

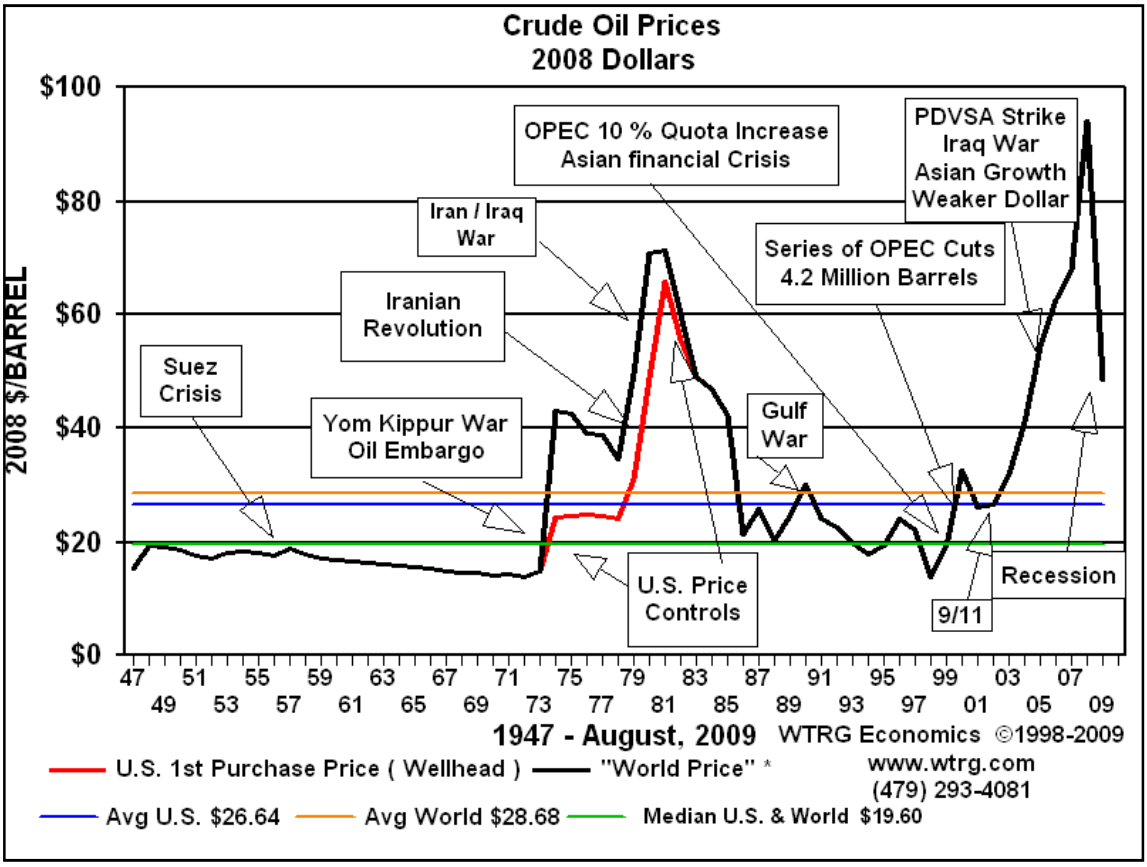

Figure 2.21: Worldwide crude oil prices between 1947-2008 [11]

- Using less energy (contradiction with economical development)
- More energy efficient industrial & residential facilities (needs important amount of investment)
- Clean Technologies (e.g gasification, IGCC, fluidized bed co-combustion of fosil fuels via biomass, supercritical processes, oxy-combustion, CCS)
- Renewables (wind, solar, hydro, geothermal, wave, hydrogen, biomass which are generally expensive than the conventional energy producing technologies)

In order to make an objective and concrete judgement, unit cost of electricity production via diffent technologies. Although the conventional techniques (especially fosil fuel utilizing thermal power plants) are genereally more cheaper on both investment and operational costs basis; after the Kyoto Protocol has put into force it has become a common belief that carbon taxes or penalties will become a reality in very near future. This means, for the production of required amount of energy fosil fuels will not be favored anymore. Instead renewables will come into big

picture. In Table 2.1 and Figure 2.22 those projections depicted in conferences or notable agencies' reports could be seen.

Table 2.1 is taken from an international conference that has been helding in Istanbul since 1994. A Turkish bank giving credit to energy projects presented the unit costs of energy Technologies whereas; Figure 2.22 is taken from the annual report of European Wind Energy Association.

The meaning of the figures presented in this section and how this thesis can contribute to those is mainly covered in the coming section.

Table 2.1: Investment and unit electricity cost of various Technologies [12]

Technology	**Unit Electricity Cost ($cent/kWh)**	**Investment Cost ($/kW)**
Natural gas	5.6-6.8	571-
Natural gas combined cycle	3.5-4.1	466-590
Coal	3.6-4.9	1,094-1,350
Geothermal	2.5-8.0	1,150-2,500
Wind		
20 kW	8.0-12.0	1,500-2,500
500 kW		
Solar photovoltaic		
2 kW	18.0-36.0	6,500-13,000
20 kW	15.0-21.0	5,300-7,500
Solar thermal	16.0-23.0	2,800-5,000
Hydroelectricity	0.2-0.5	750-1,500
Biomass	6.0-20.0	1,700-

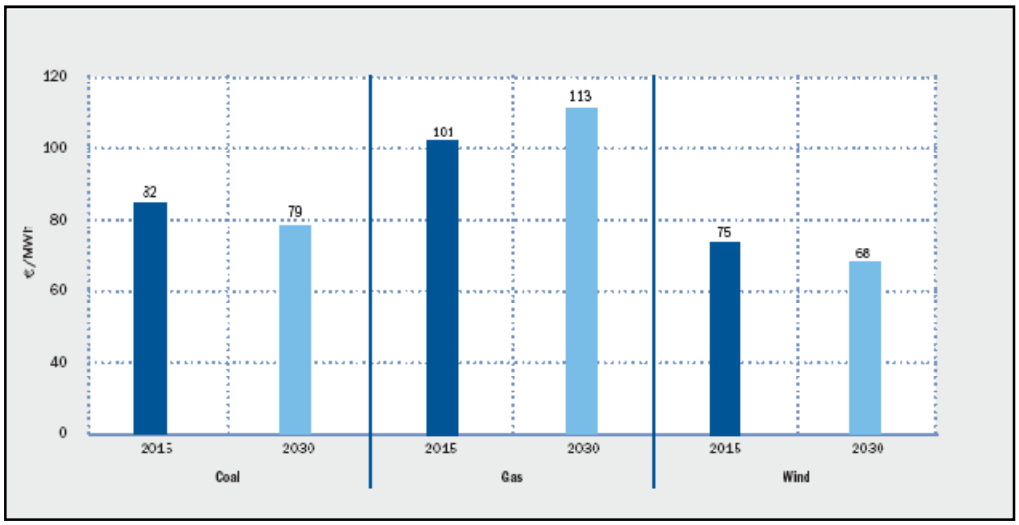

Figure 2.22: Electricity generating costs in the European Union, 2015 and 2030 [13]

2.4 Energy Review of Turkey

On the primary energy resources basis, Turkey is 73% dependent on imported energy sources. In addition to that, in terms of energy technologies degree of reliance on imported energy increases up to even more drastic values. Due to the fact that global energy demand increase would be 60% in 2030 while the national energy investments will be 120 billion € during that period it is clear that the energy policies of the country has to be revised [14]. Dependency of Turkey on imported fuel and is demonstrated in Figure 2.23.

As the world is focused more on supply security, availability and accessibility it is of vital importance to have an energy policy based primarily on the natural sources. Another crucial point in determining the utilization of the energy source is the environmental effect occurring at the end of the process as well as its unit price, and accessibility.

Under the light of all information expressed above, it is believed that the importance of biomass in energy technologies would be understood and special attention would be given to the utilization of biomass in Turkey for energy production.

Although detailed information is provided in section three, it would be beneficial to have a little bit background information about the biomass, and how could it be so important for contributing Turkey's energy production. The most attractive point is that the biomass combustion and gasification is considered to be CO_2 neutral which makes it favorable against the global warming phenomenon. There are more

advantages of biomass utilization in energy production that will be covered in section three.

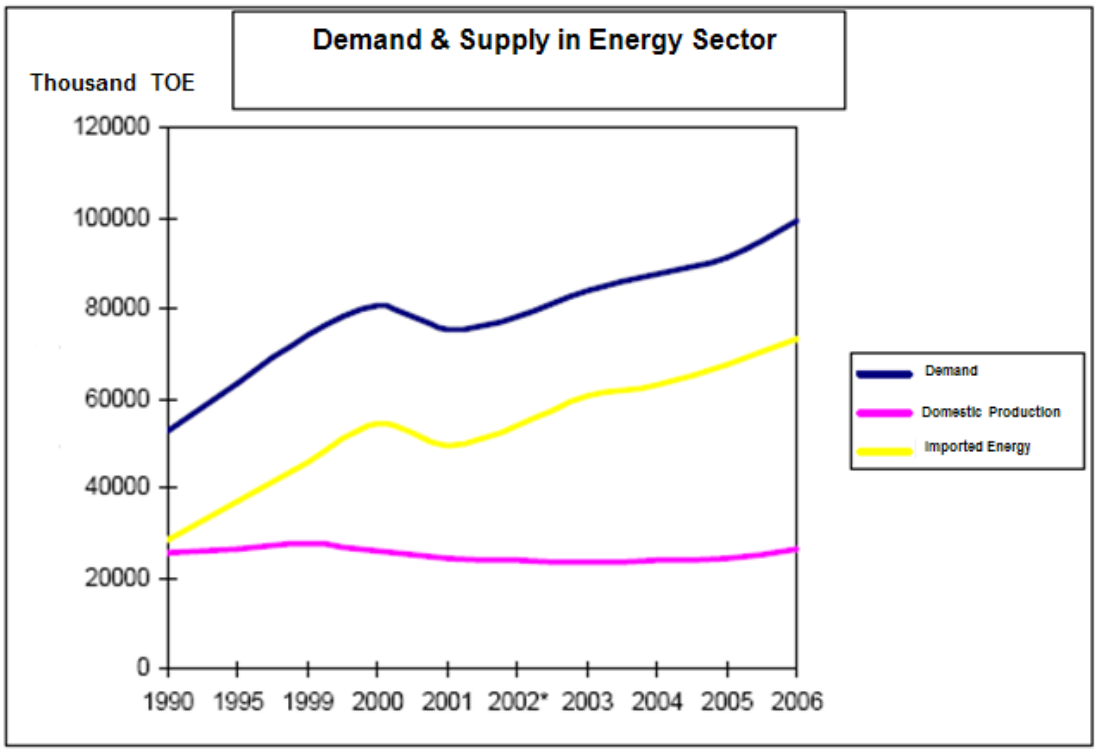

Figure 2.23: Turkey's energy gap between production & imported energy [13]

Up to this point, pojection about the energy situation in 2030, and a brief summary about the advantages of biomass utilization is presented. The remaining of the section is devoted to the current energy situation in Turkey.

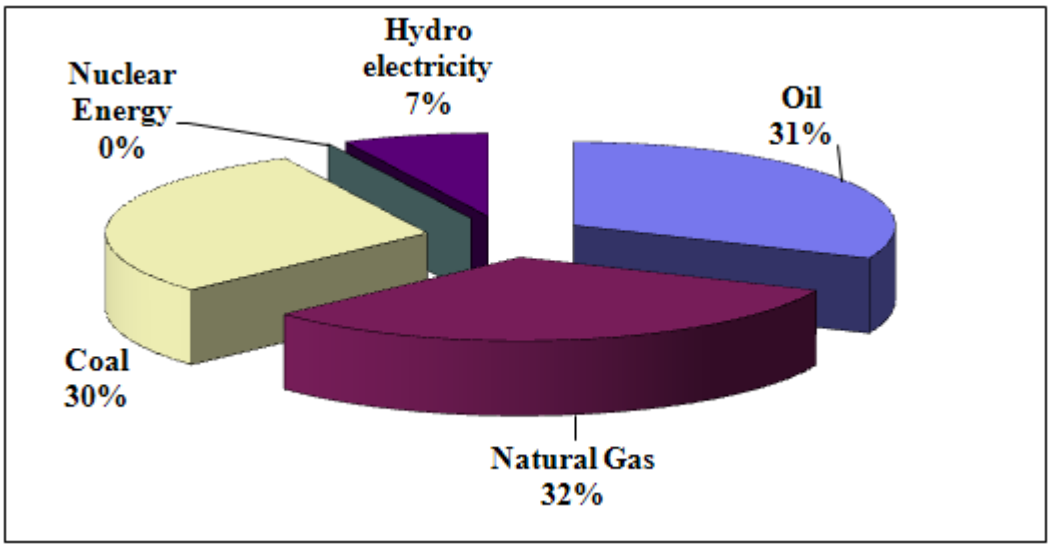

Figure 2.24: National primary energy consumption by the end of 2008 [10]

Figure 2.24 displays energy consumption of Turkey on the basis of primary energy sources. As can be seen from the figure the country mainly utilizes oil and gas both of them are being imported energy sources. In spite of the fact that Turkey is in rich in terms of coal reserves, utilization of most of those reserves are problematic due to their high ash, sulfur content. Hard coal, which is considered to be good in quality, is only found in north coast of Turkey. Thus, Turkey is confronted with environmental problems due to the utilization of almost all types of lignite coals. In Figure 2.25 reserve and locations of domestic coals is demonstrated.

As stated above Turkey's energy production is almost 80% relied on imported sources. Below, figures related to Turkey's electricity production according to energy sources are presented.

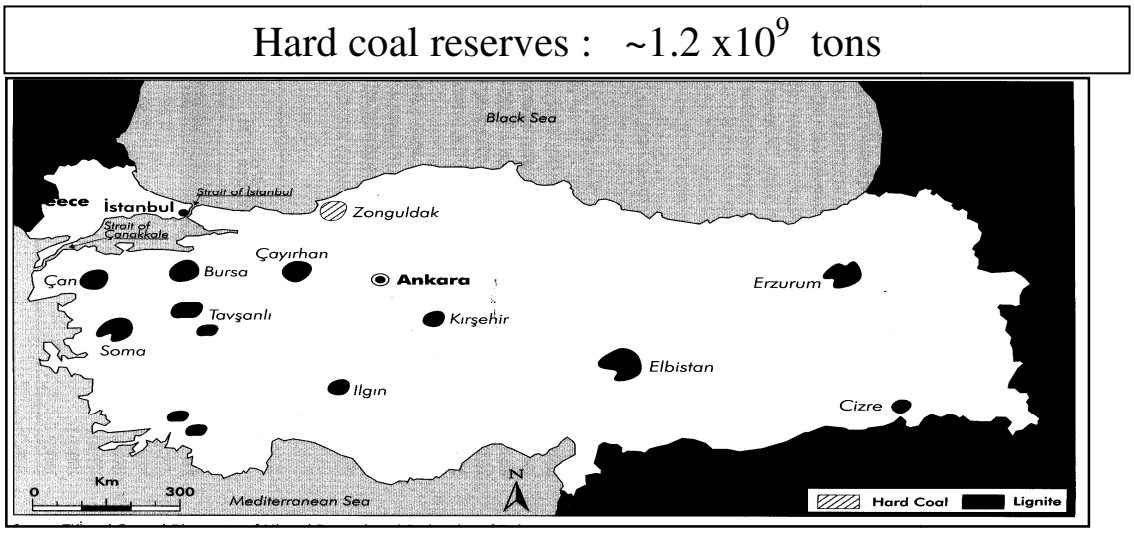

Figure 2.25: Reserves and location of hard coals&lignites [16]

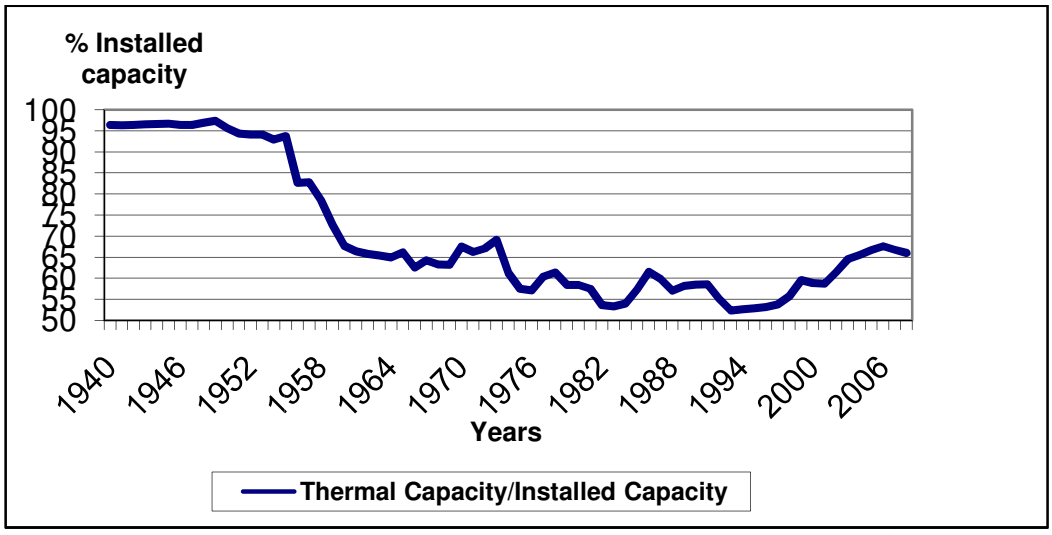

Figure 2.26: Ratio of installed thermal capacity [17]

In Figure 2.26, Turkey's dependence on thermal power that has been underlined in the introduction part of the subsection could be clearly seen. In order to gain knowledge about the thermal power capacity trend another figure demonstrating the annual based thermal capacity is displayed below.

Figure 2.27 coupled with 2.26 reveal the main source used in Turkey for meeting energy demand of the country. From the beginning of 1900s coming up to 2009, the main sources have been the thermal and hydro power for Turkey. Throughout the years, proportion of energy produced from these two sources had shown variation and this is displayed in Figure 2.27.

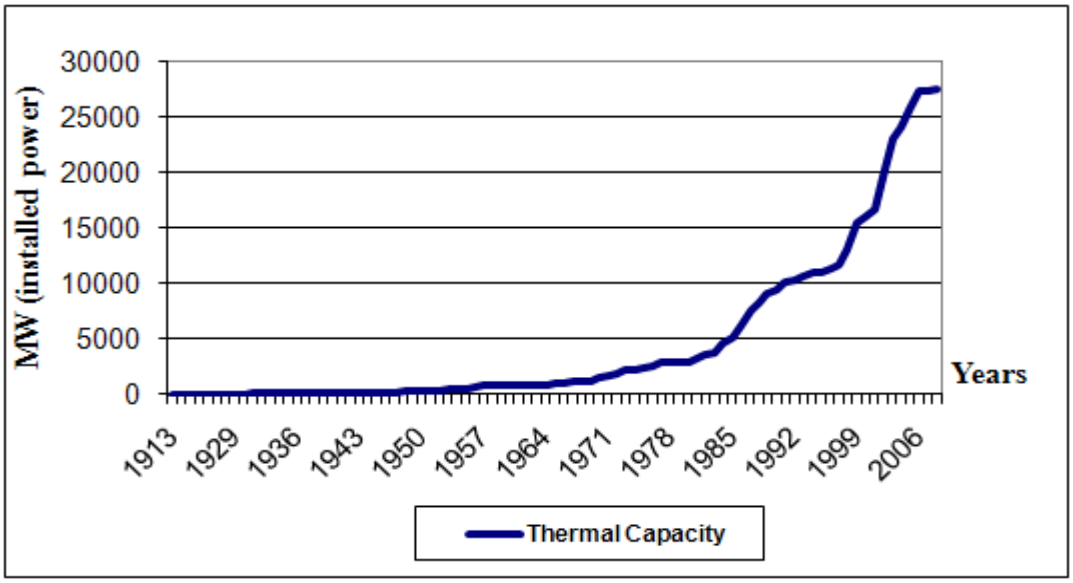

Figure 2.27: Yearly thermal power capacity in Turkey [17]

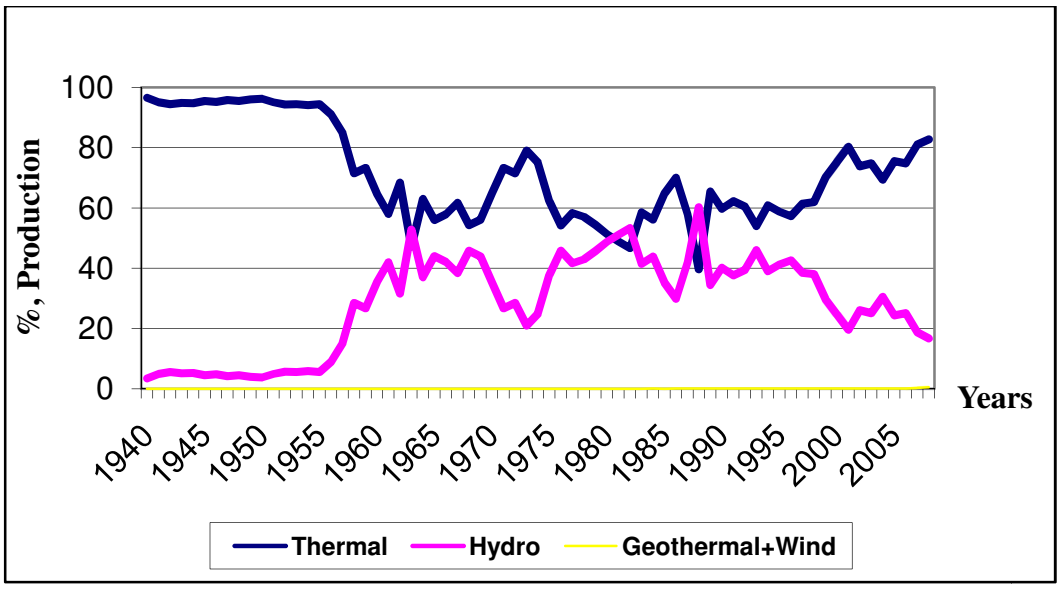

Figure 2.28: Electricity production based on primary energy sources [17]

As can be seen in Figure 2.28, the hydro power share has been decreasing since 1990s, and as this trend carried on Turkey's dependence on thermal power plants increased in order to supply energy. The CO_2 emission problem, vulnerability of natural gas fired power plants regarding the price variability (the price of natural gas has shown a dramatic increase over the last 5 years) coupled with the fact that relying on mainly imported fuels in such a global financial crisis might lead the stoppage of energy investments the country is faced with an ultimate challenge [18]. There has to be a way of producing local, clean and sustainable energy. In contrast to this fact, it could easily be verified by examining the above figures shown in this sub section that Turkey has focused on producing its energy from fosil fuels. The coming figures 2.29 reflects this dramatic fact very well.

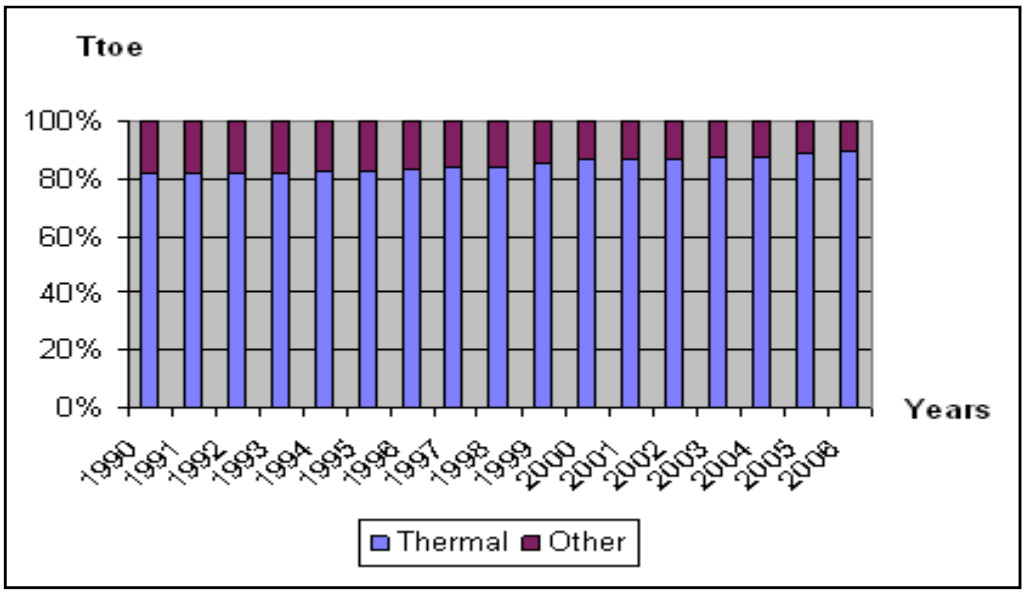

Figure 2.29: Total primary energy consumption between 1990-2006 [19]

3.BIOMASS

Biomass is a renewable energy source that is believed to be alternative to the conventional fuels such as coal, oil, natural gas in today's world. It is the third largest primary energy source after coal and oil [20]. "Biomass is an organic material that has stored sunlight in the form of chemical energy. All biomass is produced by green plants converting sunlight into plant material through photosynthesis. The use of biomass as a fuel is a carbon neutral process since the carbon dioxide captured during photosynthesis is released during its combustion. Biomass includes agricultural and forestry residues, wood, byproducts from processing of biological materials, and organic parts of municipal and sludge wastes. Photosynthesis by plants captures around 4,000 EJ/year in the form of energy in biomass and food. The schematic of the carbon cycle regarding biomass utilization is given in Figure 3.1.

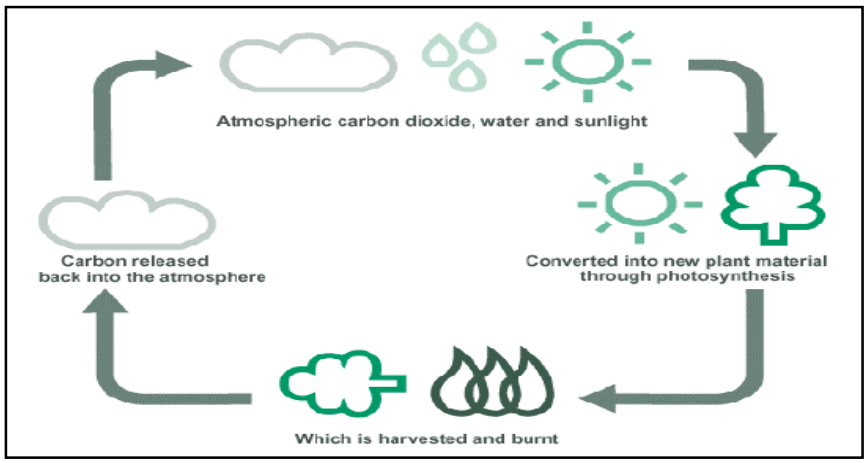

Figure 3.1: Life cycle of biomass [20]

The estimates of global biomass energy potential vary widely in literature. The variability arises from the different sources of biomass and the different methods of determining estimates for those biomasses. Fischer and Schrattenholzer estimated the global biomass potential to be 91 to 675 EJ/year for the years 1990 to 2060. Their biomass included crop and forestry residues, energy crops, and animal and municipal wastes. Hoogwijk estimated these to be 33 to 1135 EJ/year. Biomass included energy crops on marginal and degraded lands, agricultural and forestry residues, animal manure and organic wastes. Parikka estimated the total worldwide energy potential

from biomass on a sustainable basis to be 104 EJ/year, of which woody biomass, energy crops and straw constituted 40.1%, 36% and 16.6%, respectively. Only about 40% of potential biomass energy is currently utilized. Only in Asia, does the current biomass usage slightly exceed the sustainable biomass potential. Currently, the total global energy demand is about 470 EJ/year. Perlack estimated that, in the United States, without many changes in land use and without interfering with the production of food grains, 1.3 billion tons of biomass can be harvested each year on a sustainable basis for biofuel production. 1.3 billion tons of biomass is equivalent to 3.8 billion barrels of oil in energy content. US equivalent energy consumption is about 7 billion barrels per year. However, harvesting, collecting and storage of biomass adds another dimension of technical challenges to the use of biomass for production of fuels, chemicals and biopower [21,22]."

Biomass has considerable advantages over fosil fuels especially from the environment point of view. Biomass utilization is considered to be CO_2 neutral, thus usage of biomass in industrial processes does not contribute to global warming whereas; coal, oil and natural gas combustion results in vast amounts of CO_2 emissons to the atmosphere. Furthermore, biomass utilization provides a decrease in SO_2 and NO_x emissions compared to fosil fuels. In addition to that utilization of biomass decreases the dependency on imported fosil fuel. Besides this, disposal of wastes could be achieved by utilizing the biomass residue as energy source thus resulting in a decrease in disposal cost. As the above information is kept in mind, it is obvious that Turkey, due to its advantageous geographical location, has an important biomass potential and in case of utilizing its potential in an efficient way, Turkey would have a chance going into a reduction in CO_2 emissions as well as the negative impacts of fosil fuels. Turkey's biomass potential is given in the following figures.

The biomass inventory of Turkey has been reviewed by several authors and it has been revealed that, biomass utilization for energy production purposes would be beneficial for Turkey both in terms of environmental (disposal of waste, reduction in CO_2 emissions) and cost effectiveness reasons. Utilization of biomass for energy production provides sustainable growth.

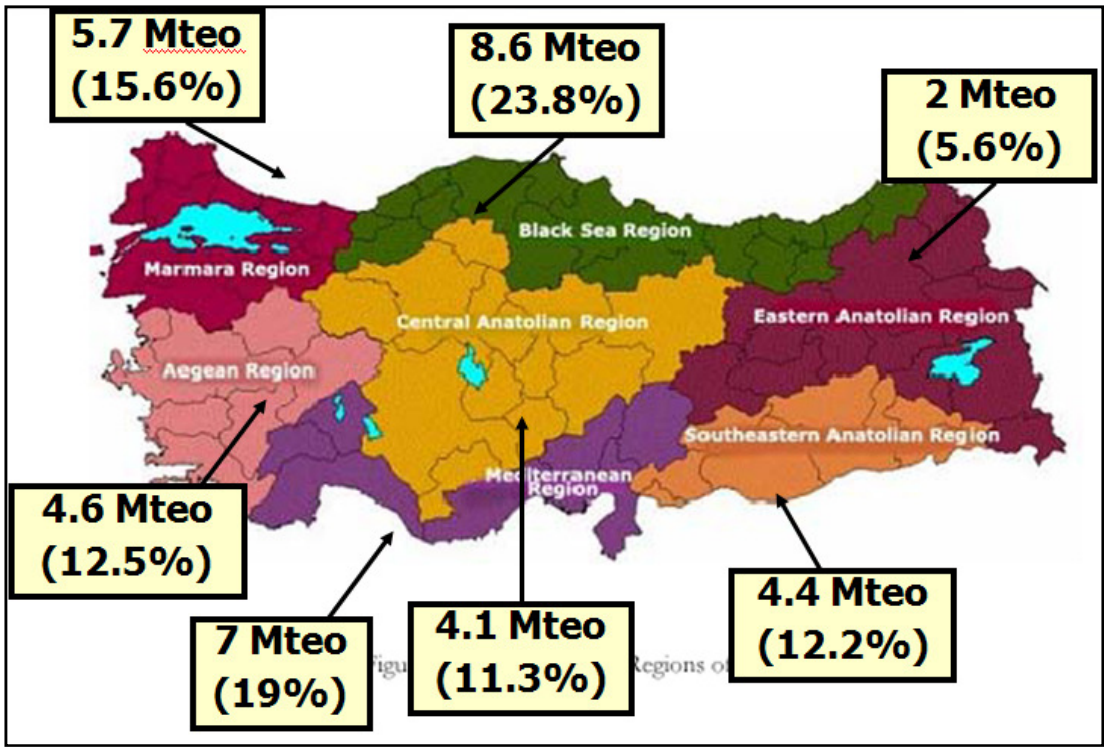

Figure 3.2: Regional biomass potential in Turkey [23]

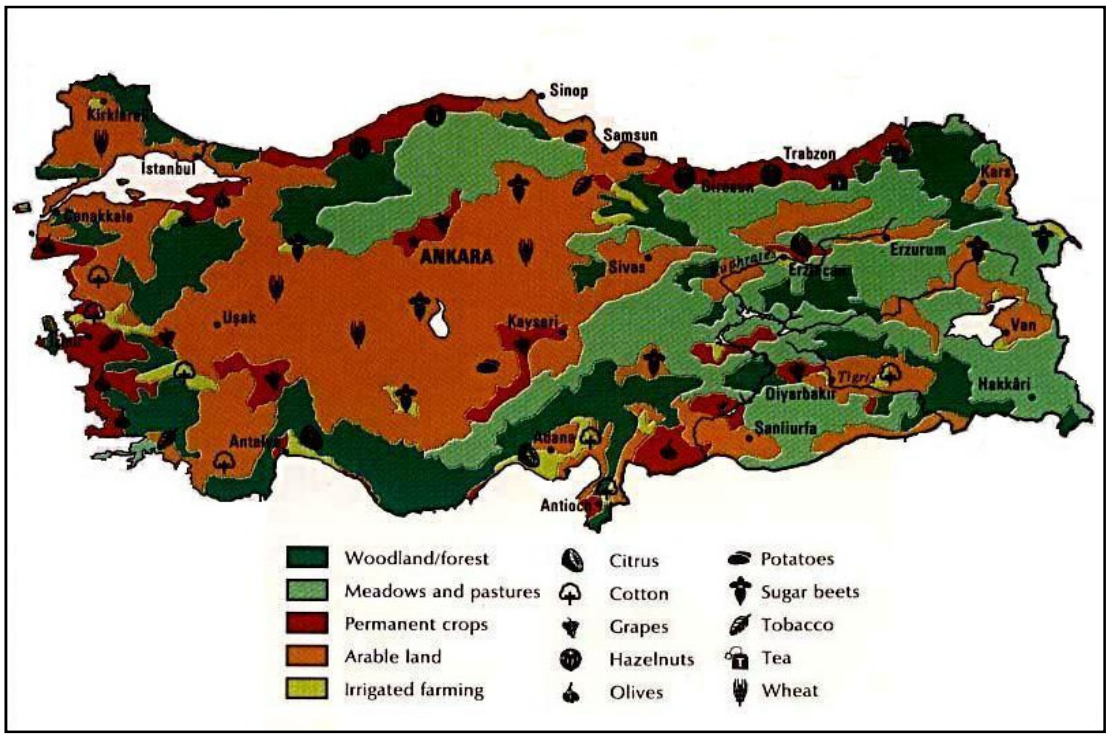

Figure 3.3: Geographical distribution of biomass and land use in Turkey [23]

Renewable energy sources is the key factor for sustainable energy production for Turkey, and as can be seen in Figures 3.2, 3.3 and Table 3.1 there exists a vast potential which needs to be handled via realistic policies.

Table 3.1: Annual biomass potential of Turkey [23]

Biomass	Annual potential (mtons)	Energy value (mtoe)
Annual crops	54.4	15.5
Perennial crops	16.0	4.1
Forest residues	18.0	5.4
Residues from agro-industry	10.0	3.0
Residues from wood industry	6.0	1.8
Animal wastes	7.0	1.5
Other	5.0	1.3
Total	116.4	32.6

3.1 Biomass Types

Although a strict classification of biomass types does not exist, a common belief is that biomass could be grouped into eight categories [24]:

- Woody and forest biomass
- Energy plantation
- Conventional agricultural biomass
- Animal residues
- Landfill gas
- Organic municipality wastes
- Industrial wastes
- Tyres

3.2 Biomass Conversion Processes

The energy content of the biomass is withdrawn via three methods. Those are namely thermochemical, physical and biological processes. The selection criteria among these three methods depend on several factors such as the type and quantity of biomass, end-use requirements, environmental issues, economic factors. A brief description and final products obtained at the end of the processes is given below.

3.2.1 Thermochemical Conversion

Process is based on addition of oxygen and heat in order to produce gaseous products. There are five subtitles two of them being lesser used and those methods are displayed in Figure 3.4.

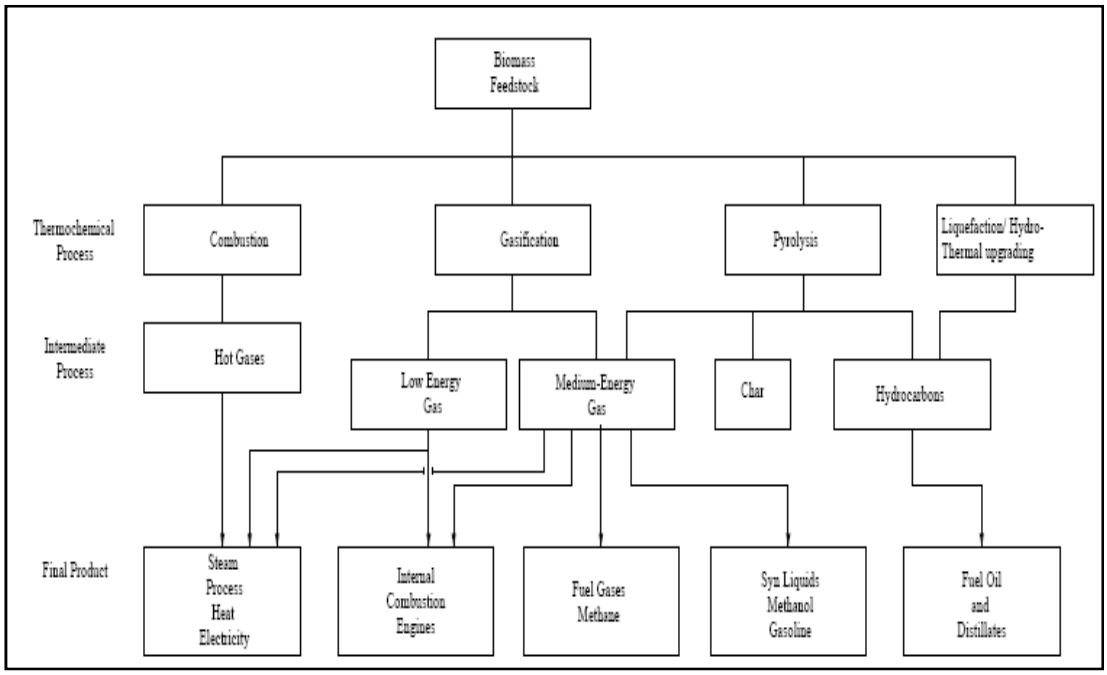

Figure 3.4: The main processes and the related products [25]

3.2.1.1 Combustion

Combustion is very widely used technique to convert the chemical energy stored in biomass into heat, electricity, or mechanical power. The output of the process is generally high temperature (1073-1173 K) gases. Combustion is achieved in excess O_2 medium.

3.2.1.2 Gasification

Gasification is the conversion of biomass into combustible gas mixture by partial oxidation at temperatures around 1073-1173 K. The product is named as syngas, a mixture of CO-H_2. Oxygen fed to the system is less than the theoretical oxygen amount required for complete burning. The lambda is always less than 1 for gasification process. Details about gasification is given in section 4.

3.2.1.3 Pyrolysis

Decomposition of the organic materials contained in biomass in the absence of air to yield liquid, solid and gaseous by heating to around 773 K is named as pyrolysis.

Pyrolysis could be achieved via two methods: Slow and fast pyrolysis that lead different product fractions. The conventional slow pyrolysis process is carried out in the batch mode over long time periods whereas; the fast pyrolyis lasts about a few seconds. In the former one, the reactions are generally characterized by rapid heating rates and the process could be classified as continuous. At the end of the process bio-oil is formed as the main product while, in slow pyrolysis the products formed are charcoal, pyroligneous oil and gases. The fraction of the products depend on the heating rate, pyrolysis temperature and type of feedstock [25,26].

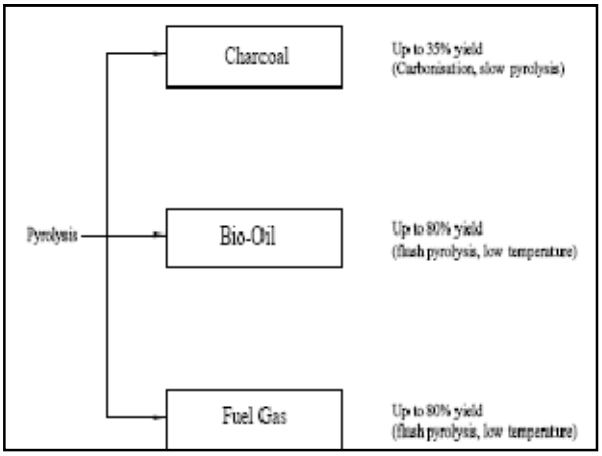

Figure 3.5: Pyrolysis products [25]

3.2.1.4 Liquefaction and HTU

Liquefaction is a low temperature high pressure catalyst requiring process that produces liquid product. In HTU, biomass is partly oxygenated into hydrocarbons in a high pressure medium. Both of the processes require high pressure and wet environment. HTU is believed to be at pilot stage, and liquefaction is considered to be non economical due to the complexity of the process [25].

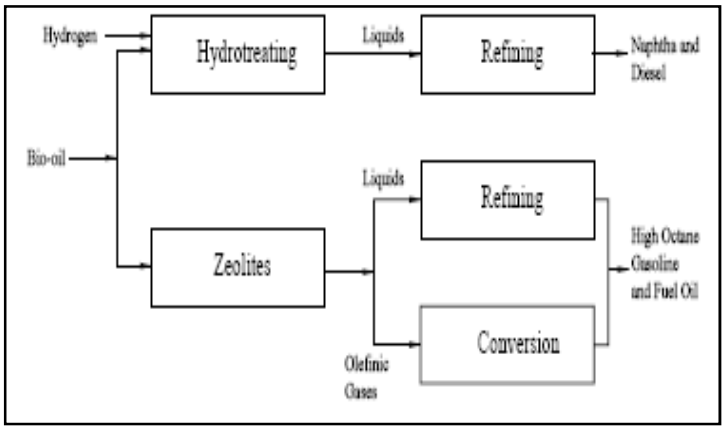

Figure 3.6: Upgrading of bio-oils [25]

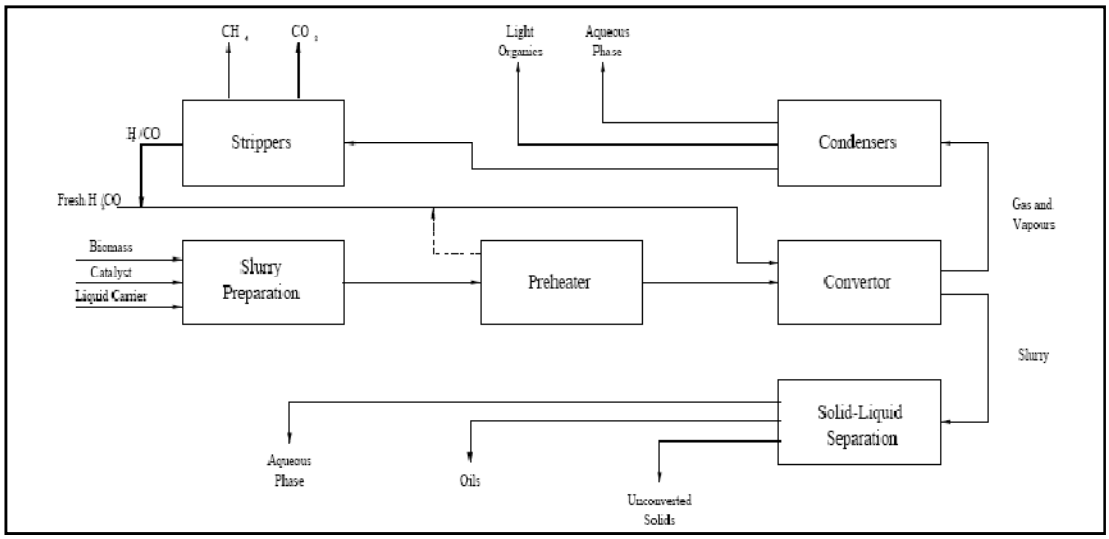

Figure 3.7: Flowsheet of liquefaction [25]

3.2.2 Physical Processes

There are mainly two physical conversion methods which are namely densification and drying. In densification the dry biomass is exposed to high pressure followed by immediate cooling and the process results in formation of logs, briquettes and pellets. Thus, very stable products are formed.

Logs are generally sold in residental markets for fireplace or fuel applications while pellets are convenient for large scale industrial applications, especially as feedstock for burners. Briquettes on the other hand is not as common as pellets but its utilization has displayed an increase in developed countries [27]. Flow diagram for the densification process is given in Figure 3.8.

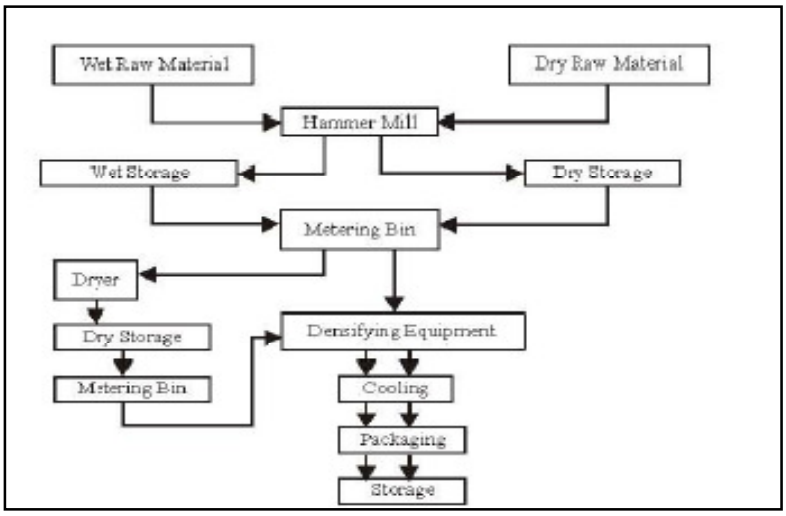

Figure 3.8: Flow diagram of wet and dry biomass during densification [27]

3.2.3 Biological Processes

In biologial treatment there are three methods two of them being more commonly used: Fermentation, anaerobic digestion and mechanical extraction, the latter one being a lesser used process. Fermentation is mainly the conversion of sugars to ethanol. “There are two basic ways of attacking the lignocellulosic structure of the biomass to end up with ethanol. The first one is the acid hydrolysis with a variety of low acid high temperature or high acid low temperature being suitable to both break down the structure of biomass and release free sugars whereas; the second one is the enzymatic hydrolysis after some sort of pretreatment which allows enzymatic attack of the polymers [27]”. Anaerobic digestion is the conversion of biomass into mainly a mixture of CO_2 and CH_4 which is a combustible gas mixture. This is especailly obtained from the animal wastes and the product gas is fed to a gas motor org as turbine to produce electricity. There exists a sample flowsheet for anaerobic digestion process.

“Mechanical extraction is the mechanical process to produce oil from the seeds of various biomass sources” [25]. At the end of the process “cake” is formed in addition to oil and this is further reacted with alcohol to give RME which is used as a supplementary transport fuel. The flowsheet describing the process is displayed below.

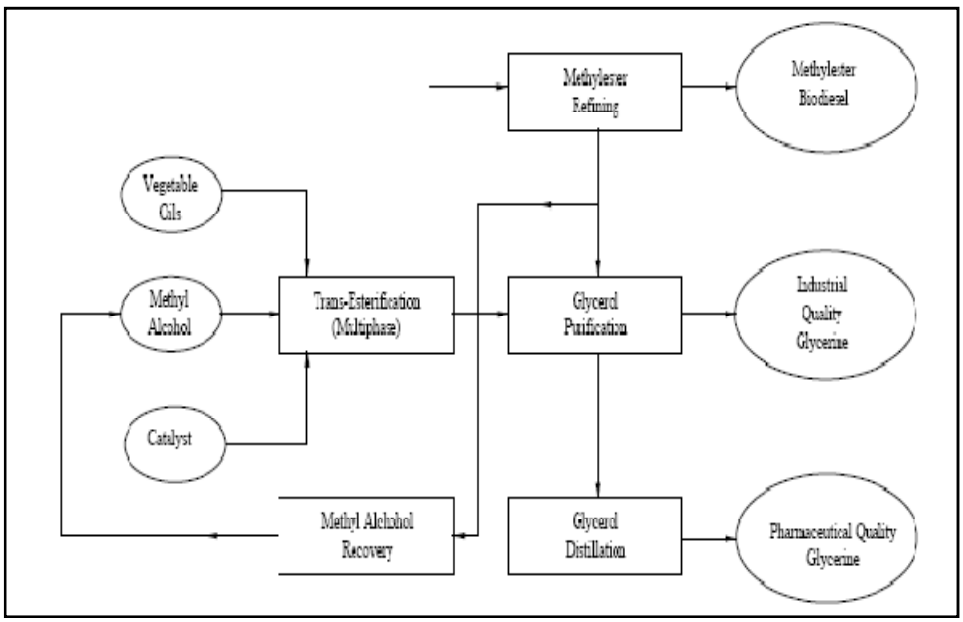

Figure 3.9: Flowsheet of RME production [25]

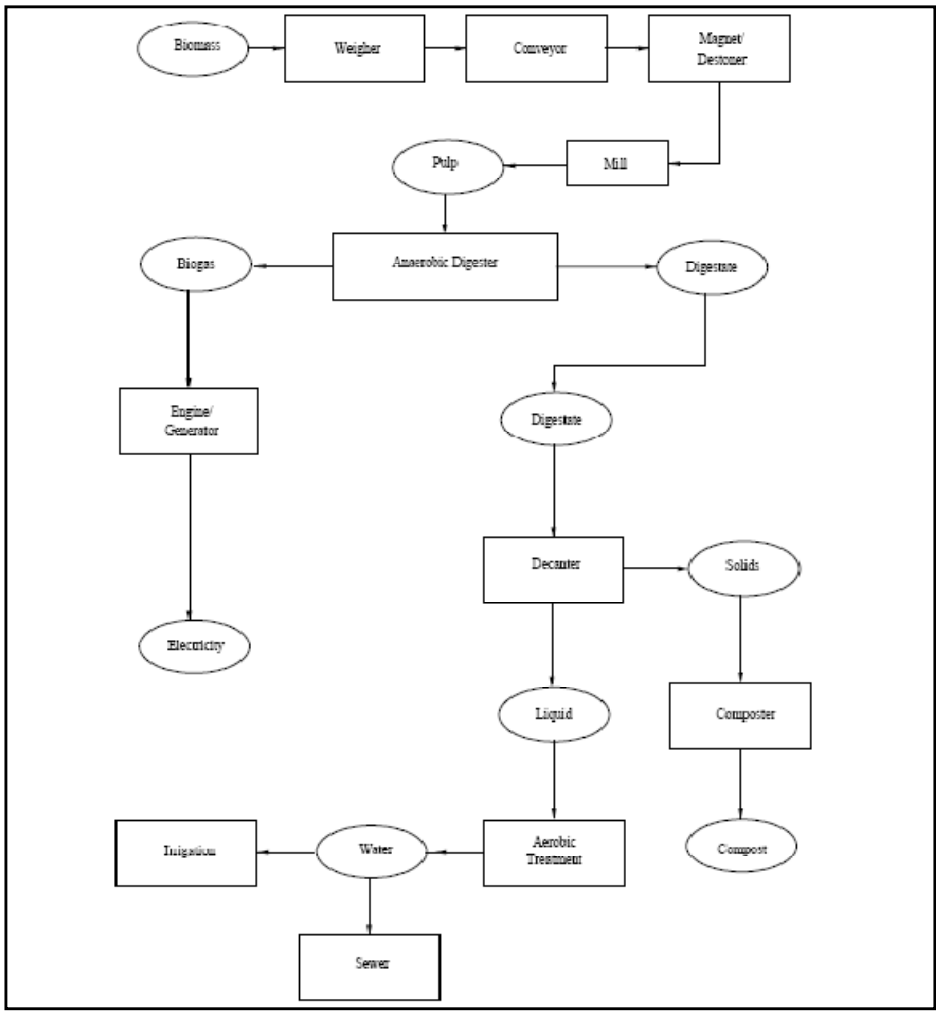

Figure 3.10: Flowsheet of anaerobic digestion [25]

3.3 Comparison of Combustion & Gasification

There are various advantages of this technology over combustion from the environmental, economic point of view.

- NO_x and SO_2 emissions are very low in case of gasification compared to combustion. Infact NO_x and SO_2 is not observed in gasification where N_2 and H_2S are the resulting flue gases. Since N_2 is already present in air it is obvious that there is no harm coming from N_2 while H_2S is much more easily captured compared to SO_2 which is produced at the end of combustion. This is valid for coal gasification, if biomass gasification is concerned there is almost no H_2S emission since sulfur content of biomass is negligibly small. In addition to that CO_2 capture is more economical in a gasification based plant.

- The process enables to convert low value materials such as municipal wastes, pet coke into high value products. Besides this, chemicals, fertilizers, liquid fuels and electricity could be produced by using syngas as the raw material. In Table 3.2 a comparison of the product gas at the end of the combustion and gasification proceses could be seen.

- Gasification process has product and raw material flexibility. In order to be more specific, the type of fuels range that can be used as the feedstock is very wide as well as the utilization field of the products.

- Gasification requires approximately 14-24% less water consumption for electricity production and when it comes to losses during the operation gasification provides ~34% saving compared to coal based Technologies [28].

Table 3.2: Comparison of gasification and combustion products [28]

Constituents of Coal	Gasification	Combustion
Carbon	CO	CO_2
Nitrogen	N_2	NO_x
Hydrogen	H_2	H_2O
Sulfur	H_2S	SO_2
Oxygen	-	O_2

Syngas could be used in several industrial processes as the feedstock and those are displayed in Figure 3.11.

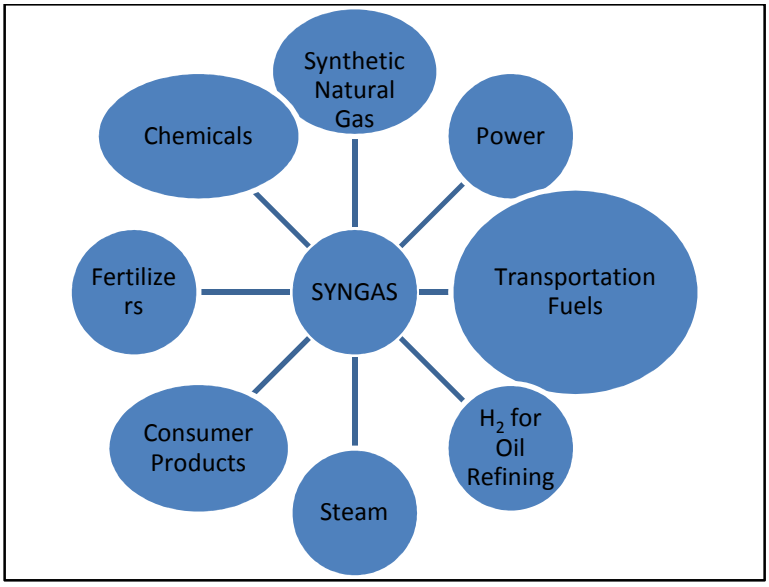

Figure 3.11: Gasification products [28]

Up to this point combustion and gasification have been briefly reviewed. A comparison between the two thermochemical conversion methods is given in Table 3.3.

Table 3.3: Strength and weaknesses of conversion technologies [29]

Flow Regime	Moving (or fixed) Bed	Fluidized Bed	Entrained Bed
Combustion Analogy	Grate fired combustors	Fluidized bed combustors	Pulverized bed combustors
Fuel Type	Solids	Solids	Solids or liquid
Fuel Size	5-50 mm	0.5-5 mm	≤500 µm
Residence Time	15-30 minutes	5-50 seconds	1-10 seconds
Oxidant	Air or O_2 blown	Air or O_2 blown	Almost O_2 blown
Gas Outlet Temperature	673-773 K	973-1173 K	1173-1673 K
Ash Handling	Slagging and non-slagging	Non-slagging	Always slagging
Commercial Examples	Lurgi Dry Ash (non-slagging) BGL (slagging)	GTI U-Gas HT Winkler KRW	GE Shell ConocoPhillips Noell Prenflo
Comments	Moving beds are mechanically stirred, fixed beds are not Gas and solid flow are always countercurrent in moving bed gasifiers	Bed temperature below ash fusion point to prevent agglomeration Preferred for high ash feedstocks and waste fuels	Not preferred for high-ash fuels due to energy penalty of ash melting Unsuitable for fuels that are hard to atomize or pulverize

4. GASIFICATION

Gasification is the thermochemical conversion process that converts carbonaceous material into combustible gas. It is a proven process to produce various products such as electricity, ammonia, methanol, fertilizers, substitute natural gas, steam, transportation fuel.

As introduced in this text in advance, utilization of coal via gasification provides environmentally acceptable solution in today's world. In the introduction and energy review parts, the future projections related to energy demand of some independent international agencies and company's has been presented. Therefore, it is assumed that importance of gasification as a powerful tool for providing clean, affordable and sustainable energy has been understood.

4.1 History of Gasification

Starting from the first century of industrial development gasification has played vital role in gas production. Especially, town gas production from coke took great attention throughout those years. Town gas, being a gaseous product had been served for heating and illumination purposes in Europe and America. Illumination was the first application of utilization of gas product which was followed by heating and a raw material for chemical industry. The industrial application of coal gasification started in England in 1860, which is designed by K.W Siemens.

Afterwards, water gas production evolved in 1870s and this was followed by modern gasification processes namely Winkler Fluid Bed (1926), Lurgi Moving Bed Pressurized Gasification Process (1931) and Koppers Totzek Entrained Flow Process (1940s). After 1950s, the collaboration of designed systems and firms like Texaco, Shell, BGL ended up with developed gasification processes and gasifiers. Nowadays worldwide gasification capacity is increasing based on those modified versions of gasification processes for power, fertilizer, hydrogen and ammonia production [29-31].

Gasification played an important role as the strategic energy supplying technology in World War II in converting coal int transportation fuels via Fischer-Tropsch [29].

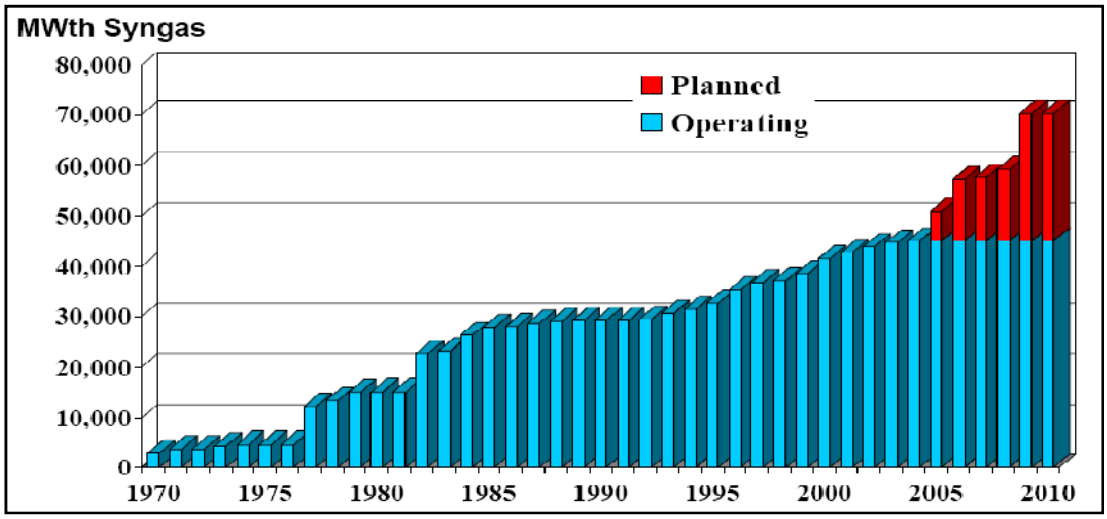

Figure 4.1: Worldwide gasification capacity and growth [29]

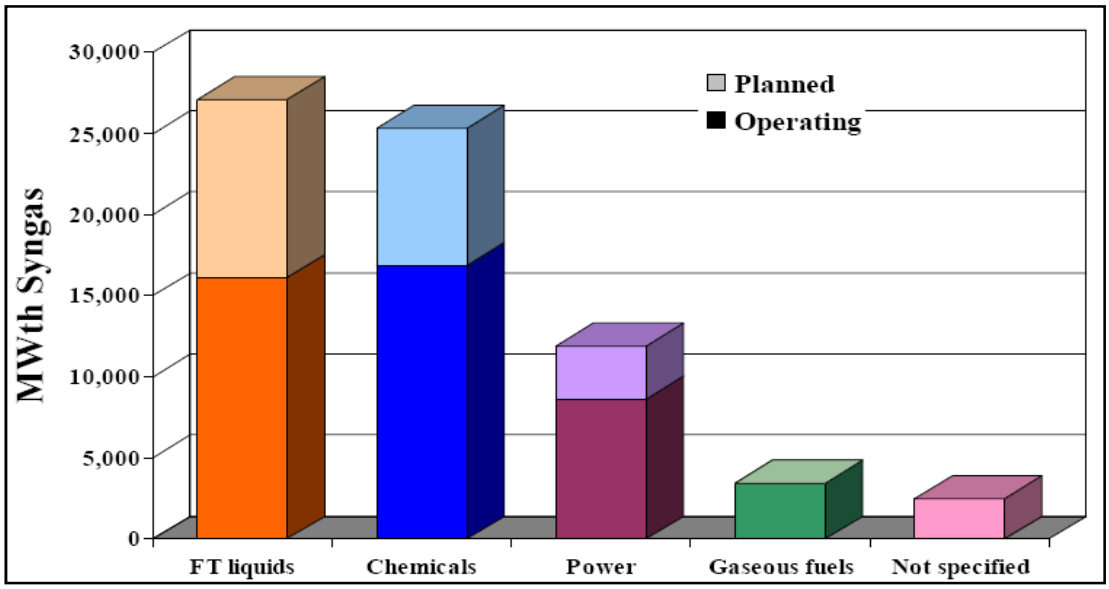

Figure 4.2: Gasification products in year 2005 [29]

4.2 Chemistry of Gasification

The gasification reactions are very complex and the composition of the product gas is a strong function of process conditions, namely temperature and pressure inside the reactor. In this sub chapter, general equations and thermodynamical facts regarding the gasification theory is presented just to give a brief insight.

The gasification takes place at temperatures between 1073 K and 2073 K. The temperature inside the reactor depends on the feedstock character, but generally the

commercial reactors are designed on the basis of thermodynamic equilibrium equations [30].

Combustion reactions,

$C+½\ O_2 = CO$ -111 MJ/kmol **(4.1)**

$CO+½\ O_2 = CO_2$ -283 MJ/kmol **(4.2)**

$H_2 +½\ O_2 = H_2O$ -242 MJ/kmol **(4.3)**

the Boudouard reaction,

$C+CO_2 = CO$ +172 MJ/kmol **(4.4)**

the water gas reaction,

$C+H_2O = CO+H_2$ +131 MJ/kmol **(4.5)**

and the methanation reaction,

$C+2\ H_2 = CH_4$ -75 MJ/kmol **(4.6)**

There is a balance between the above equations and the gasifier should be designed according to the desired product. Indeed many reactions occur simultaneously, howewer by selecting temperature pressure, recycle rate of product etc. the syngas composition could be adjusted [26]. The effect of temperature, pressure and feedstock characteristics had been presented in the literature, and some of them are displayed in the below graphs.

"Reactions 4.1, 4.4, 4.5, and 4.6 describe the four ways in which a carbonaceous or hydrocarbon fuel can be gasified. Reaction .-4 plays a role in the production of pure CO when gasifying pure carbon with an oxygen/CO_2 mixture. Reaction 4.5 takes a predominant role in the water gas process. Reaction 4.6 is the basis of all hydrogenating gasification processes. But most gasification processes rely on a balance between reactions 4.1 (partial oxidation) and 4.5 (water gas reaction).

For real fuels (including coal, which also contains hydrogen) the overall reaction can be written as,

$C_nH_m + n/2\ O_2 = n\ CO + m/2\ H_2$ **(4.7)**

where for gas, as pure methane, m= 4 and n = 1, hence m/n = 4, and

for oil, m/n ≈ 2, hence m = 2 and n = 1, and

for coal, m/n ≈ 1, hence m = 1 and n = 1." [30]

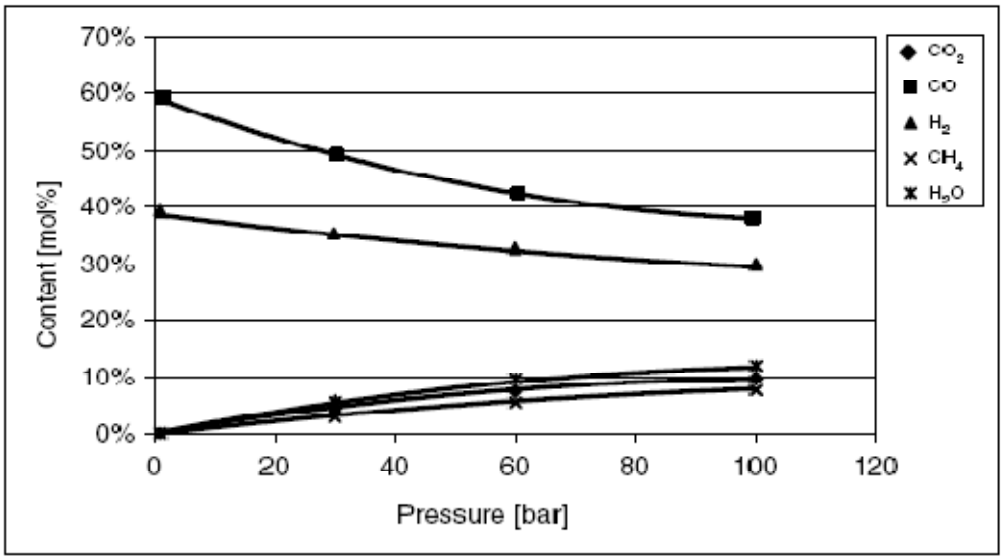

Figure 4.3: Variation of syngas composition with pressure at 1273 K [30]

As could be seen from Figure 4.3 operating pressure is very important for gasifier, and most modern processes (especially power and ammonia production) utilize high pressure gasifiers and the reason for that is shown in Table 3.3. The effect of feedstock characteristics is generally related with softening point of the fuel ash.

Table 4.1: Comparison of compression energy requirements for low and high pressure gasification [30]

		5 Bar Gasification	50 Bar Gasification
Feed pumping energy	35,450 kg/h	0.03 MW	0.09 MW
Oxygen compression	21,120 Nm^3/h	2.85 MW	4.97 MW
Syngas compression	100,000 Nm^3/h	19.70 MW	0.00 MW
Total		22.58 MW	5.05 MW

Operating temperature should be selected based on this information in order not to damage the gasifier. In addition to that, a sample calculation is given below for woody biomass in order to indicate how the feedstock characteristics can alter the product quality in a dramatic fashion.

Table 4.2: Effect of moisture content of poplar wood chips on product yield, gas composition and thermal efficiency in a fixed be dair blown downdraft gasifier [26]

	Wood Moisture Content		
Parameter	13 wt %	24 wt %	34 wt %
Input, kg/h	24	25.1	25.2
Dry wood equialent, wt %	40	36	31
Moisture in wood, wt %	6	12	16
Dry air, wt %	54	52	53
Product distribution, wt %			
Dry gas	87	82	76
Tars	3	6	7
Solids	5	3	3
Aqueous condensate	5	9	14
Gas analysis, mol %			
H_2	17.5	16.7	15.1
CO	19.7	16	11.9
CO_2	12.7	15.8	17.7
CH_4	3.5	3.2	2.1
C_2H_2	0.3	0	0.1
C_2H_4	1.5	1.4	1.1
C_2H_6	0.1	0.2	0.1
C_3H_8	0.2	0.3	0.2
O_2	1.9	0.9	0.9
N_2	42.7	45.5	50.9
Gas HHV, MJ/m^3	7.50	6.67	5.22
Thermal efficiency	74	68	55

Another graph indicating the temperature effect on the product yield and composition is shown below.

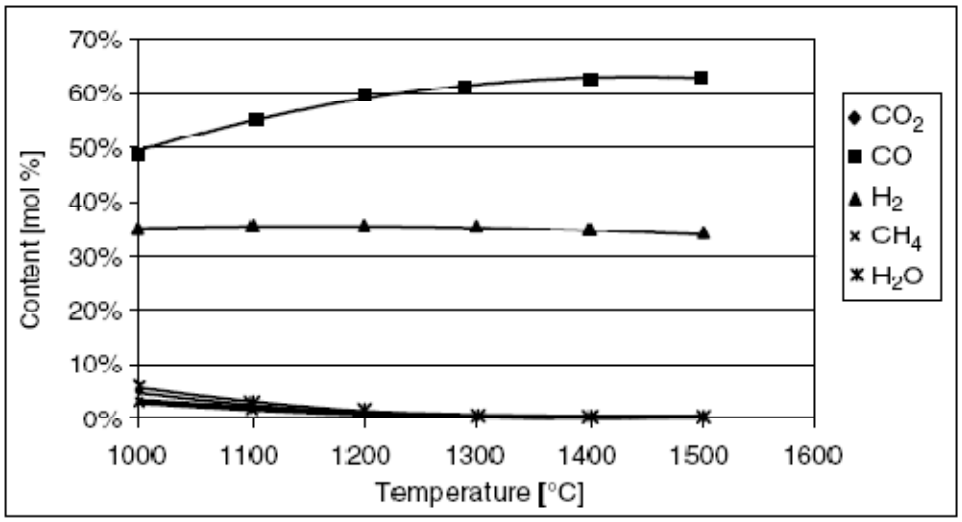

Figure 4.4: Effect of temperature on product composition at 30 bar [30]

4.3 Types of Gasifiers

Gasifiers are classified according to flow regimes, oxidant medium, type of the fuel and particle size of fuel [31].

4.3.1 Moving Bed Gasifier

Moving bed gasifier is a countercurrent reactor in which fuel is fed from top whereas; oxidant is fed form the bottom. Due to the countercurrent arrangement, heat of reaction coming from gasification is utilized in preheating the fuel in the upper parts of the reactor. The moving bed gasifier could be either downdraft or updraft. The schematic of the gasifier is given in Figure 4.5.

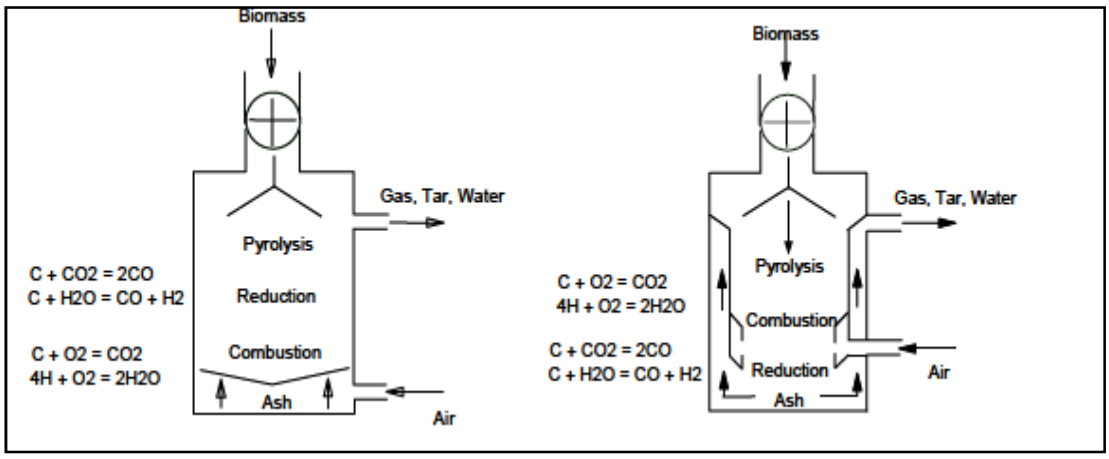

Figure 4.5: Updraft and downdraft gasifiers [33]

The characteristics of moving bed gasifier is listed below.

Low oxidant requirements;

- Relatively high methane content in the produced gas;
- Production of hydrocarbon liquids, such as tars an oils;
- High "cold gas" thermal efficiency when the heating value of the hydrocarbon liquids are included;
- Limited ability to handle fines; and
- Special requirements for handling caking coal [32]

4.3.2 Fluidized Bed Gasifier

Fludized bed gasifier is a well mixed reactor providing good mixing of fuel and oxidant where both fuel and oxidant (steam, air, O_2) are fed from the bottom. The oxidant fed from the bottom has to fluidize the particles, therefore the oxidant flow rate is important process parameter. For a specific particle diameter the minimum fluidization velocity has to be provided and sustained throughout the operation. Due to well mixing, high turbulence and fuel flexibility fluidized bed systems are advantegous.

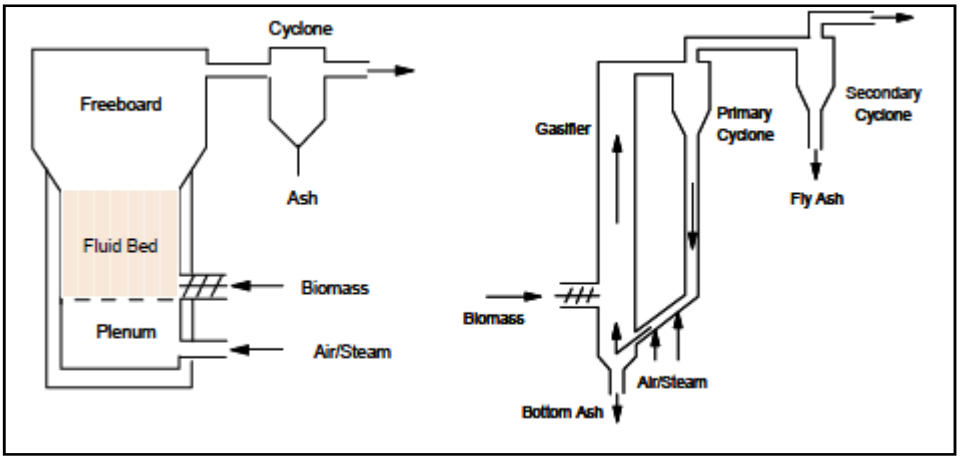

Figure 4.6: Fluidized bed gasifier [32]

The characteristics of fluidized bed gasifier is listed below.

- Extensive solids recycling;
- Uniform and moderate temperature; and
- Moderate oxygen and steam requirements.

4.3.3 Entrained Flow Gasifier

Entrained flow gasifiers are designed to handle very fine fuel particles. Fuel and oxidant are fed co-currently to the gasifier and the solid residence time is very short. Due to that reason, high temperatures like ~1473 K are preferred as the operation temperature. Generally pure oxygen is fed to the system in order to provide high carbon conversion.

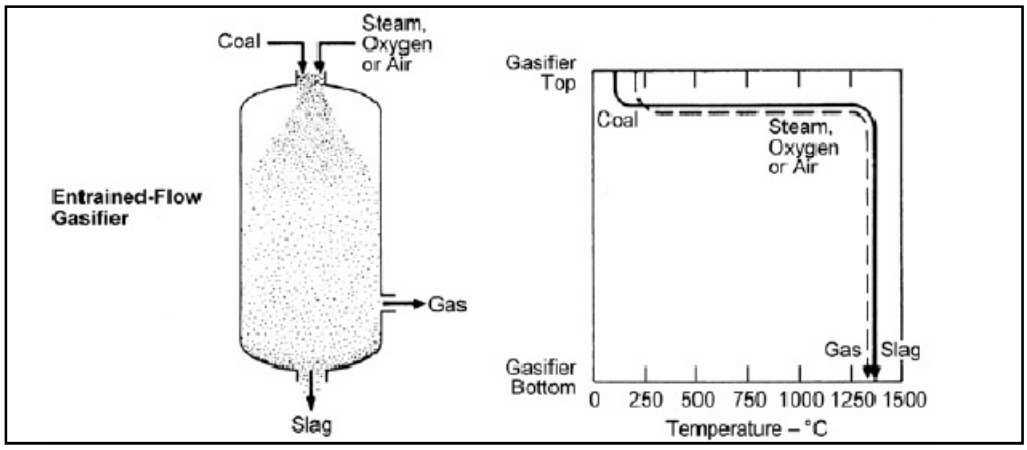

Figure 4.7: Entrained flow gasifier [32]

The characteristics of entrained flow gasifier is listed below.

- High-temperature slagging operation;
- Entrainment of some molten slag in the raw syngas;
- Relatively large oxidant requirements;
- Large amount of sensible heat in the raw syngas; and
- Ability to gasify all coal regardless of rank, caking characteristics or amount of fines.

Table 4.3: Comparison of gasifiers [33]

Gasifier	Advantages	Disadvantages
Updraft	Mature for heat	Feed size limits
	Small scale applications	High tar yields
	Can handle high moisture	Scale limitations
	No carbon in ash	Producer gas
		Slagging potential
Downdraft	Small scale applications	Feed size limits
	Low particulates	Scale limitations
	Low tar	Producer gas
		Moisture sensitive
Fluid Bed	Large scale applications	Medium tar yield
	Feed characteristics	Higher particle loading
	Direct/Indirect heating	
	Can produce syngas	
Circulating Fluid Bed	Large scale applications	Medium tar yield
	Feed characteristics	Higher particle loading
	Can produce syngas	
Entrained Flow	Can be scaled	Large amount of carrier gas
	Potential for low tar	
	Potential for low CH_4	Higher particle loading
	Can produce syngas	Potentially high S/C
		Particle size limits

In Table 3.3 while expressing the benefits of gasification, lower emission and higher power generation efficiency has been mentioned. In order to have a solid understanding about those points, Figures 4.8, 4.9 and 4.10 are presented below.

Table 4.4: Classification of gasifiers based on flow regimes, and commercial applications [29]

Flow Regime	Moving or Fixed Bed	Fluidized Bed	Entrained Bed
Combustion Analogy	Grate fired combustors	Fluidized bed combustors	Pulverized coal combustors
Fuel Type	Solids	Solids	Solids or liquid
Fuel Size	5-50 mm	0.5-5 mm	≤500 microns
Residence Time	15-30 minutes	5-50 seconds	1-10 seconds
Oxidant	Air or O_2	Air or O_2	Almost always O_2
Gas Outlet Temperature	673-773 K	973-1173 K	1173-1673 K
Ash Handling	Slagging and non slagging	Non slagging	Always slagging
Commercial Examples	Lurgi Dry Ash (non slagging) BGL (slagging)	GTI U-Gas, HT Winkler, KRW	GE Energy, Shell, Conocophillips, Noell
Comments	Moving beds are mechanically stirred. Fixed beds are not. Gas and solid flows are always countercurrent in moving bed gasifiers.	Bed temperature below ash fusion point to prevent agglomeration. Preferred for high ash feedstock and waste fuels.	Not preferred for high ash fuels due to energy penalty of ash-melting. Unsuitable for fuels that are hard to atomize or pulverize.

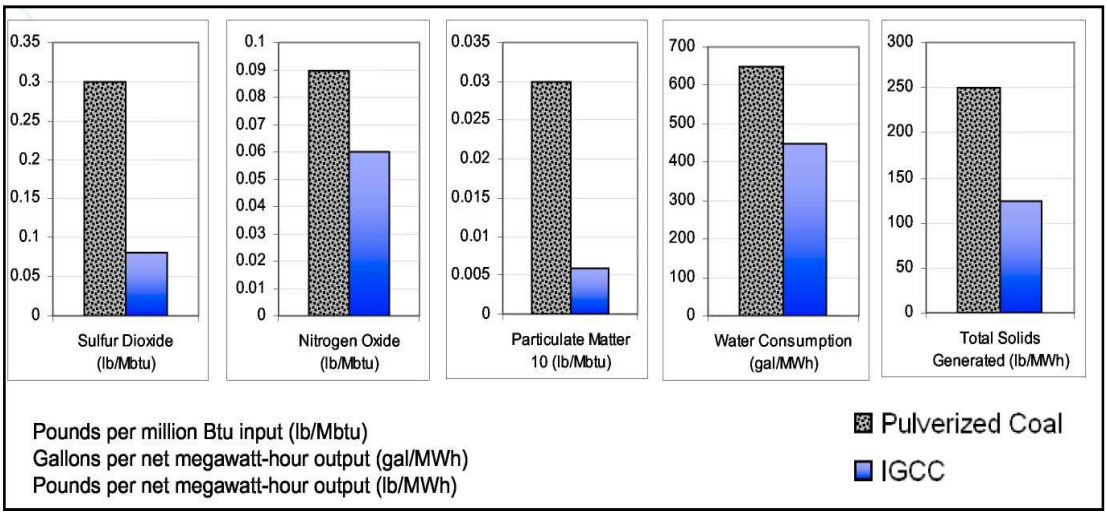

Figure 4.8: Environmental performance of IGCC, PC thermal power plants [34]

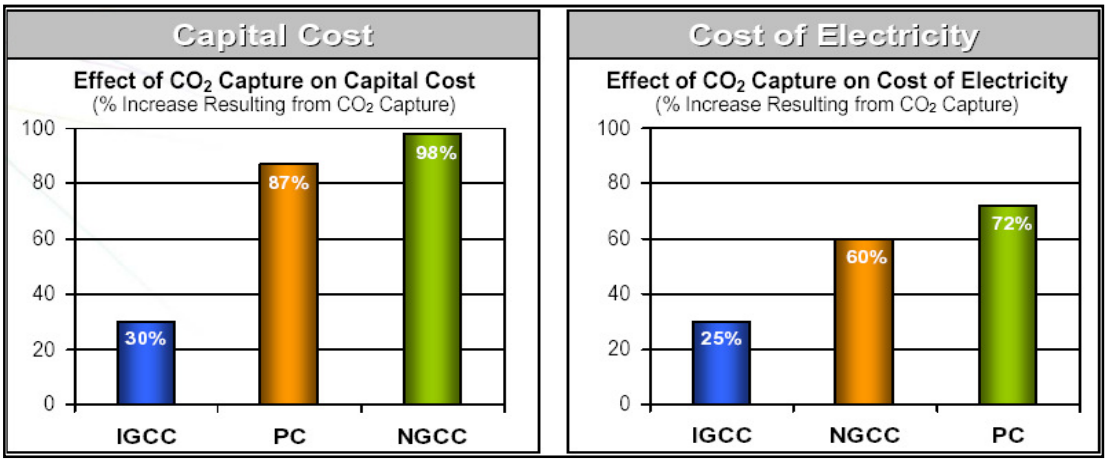

Figure 4.9: Comparison of potential CO_2 capture costs associated with IGCC, PC thermal power plants [34]

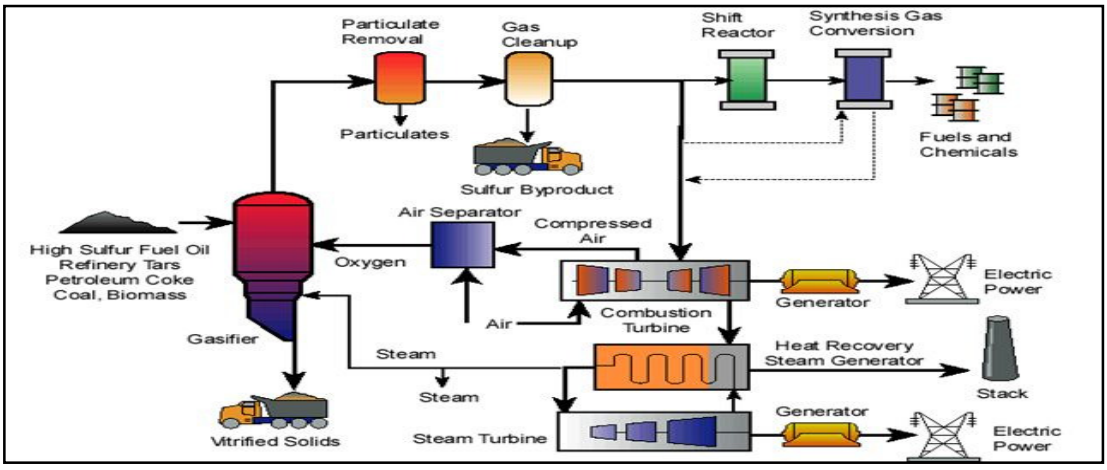

Figure 4.10: Typical flowsheet of IGCC plant [34]

5. THERMAL DECOMPOSITION REACTIONS KINETIC OF BIOMASS

Biomass has been used as an energy source since centuries and far more efficient and environmental usage of this fuel, new designs have been made in the configuration of gasification systems. Kinetic data is necessary for the design of processes by which productions of fuel gases, chemicals and energy, charcoal and activated carbon are carried out. Similarly, thermal decomposition reactions kinetic of biomass should be well known for the development of gasification systems. This kinetic data is usually obtained using thermal analysis methods (thermogravimetric analysis).

The kinetics of thermal decomposition reactions of carbonaceous materials is complicated as these materials involves a large number of reactions in parallel and series. Although thermogravimetric analysis provides general information on the overall reaction kinetics, rather than individual reactions, it could be used as a tool for providing comparison of the kinetic data which are under the effect of various reaction parameters such as temperature and heating rate.

5.1 Thermal Analysis Methods

Thermal analysis methods having wide range of applications since 1960s, is defined as follows by the International Confederation for Thermal Analysis and Calorimetry (ICTAC):" A group of techniques in which a property of the sample is monitored against time or temperature while the temperature of the sample, in a specified atmosphere, is programmed" [35].

There are various thermal analysis methods and those are classified according to the type of a sample's properties that are detected. The abbreviations and the accepted names for different thermal analysis methods are tabulated in Table 5.1.

The development of thermal analysis methods dates back to over 100 years. The first efforts were made by Le Chatelier in 1887 in thermal analysis experiment that related the heating curve for clay minerals. Roberts-Austen was the first to develop DTA in 1899 and this was followed by development of the first thermobalance by Honda in 1915. In 1925, the first TG data was first analyzed by Kujira and Akahira for kinetic

purposes where the aim of the experiment was to predict the thermal life of insulating materials. Just before the second world war, thermo-dilatometry became the third thermal analysis method to be developed.

The techniques mentioned above were mainly applied to minerals, metals, inorganic substances, ceramics and refractory materials [36,37]. After the second world war the technology of automation and recording had been developed that led to the production of fully automation apparatus. The fully automated devices became commercially available at the end of fifties. Another important development that is worthy of note that, is the formulation of the parts of the thermal analysis assembly. The assembly was consisted of a furnace, a temperature controller, a transducer to measure the sample physical property and a recorder, which records the transducer output signal as a function of the temperature or time. In most cases, the temperature was controlled at a constant rate of heating or cooling.

DSC, which is a dynamic operation of a conduction calorimeter was developed as a modified version of DTA that provided the measurement of heat flux. In the 1960s, with the applications to polymers for the purpose of melting behavior observation, thermal analysis showed an increase especially by the contribution of DSC.

After DTA, TG, thermo-dilatometry and DSC many other new techniques have been coined. One of the notable thermal analysis techniques is the `three-dimensional thermal analysis' that gave chance to mankind for the investigation of microscopic properties such as chemical and crystal structures. Three dimensional techniques provided more information about the structure of the sample that is under investigation. EGA by mass spectrometry, thermo-photometry, thermoanalytical X-ray diffraction and thermal analysis by FT-NMR fall within this category [37].

5.2 Thermogravimetric Analysis (TGA)

Thermogravimetric analysis is the most widely used thermal analysis method which is based on mass loss of the material that is under inverstigation as a function of temperature. In thermogravimetry mass change of a substance is continuously monitored against temperature, where it is heated at a constant rate or kept at constant temperature. As agreed conventionally, mass loss is plotted on the y-axis whereas; temperature is located on the x-axis [37,38]. “There are three modes of

thermogravimetry that may be mentioned: (a) isothermal or static thermogravimetry, in which the sample is recorded as a function of time at constant temperature; (b) quasistatic thermogravimetry, in which the sample is heated to constant meass at each of a series of increasing temperatures; and (c) dynamic thermogravimetry, in which the sample is heated in an environment whose temperature is changing in a predetermined manner, preferably at a linear rate."

In Figure 5.1 a characteristic single stage reaction TG curve is displayed. There exist two important temperatures that could be taken as characteristics of any single stage nonisothermal reaction. T_i, the lowest temperature at which mass change could be detected by the thermobalance is named as the initial temperature and T_f, the temperature at which decomposition of the sample is nearly complete is named as the final temperature [37,38].

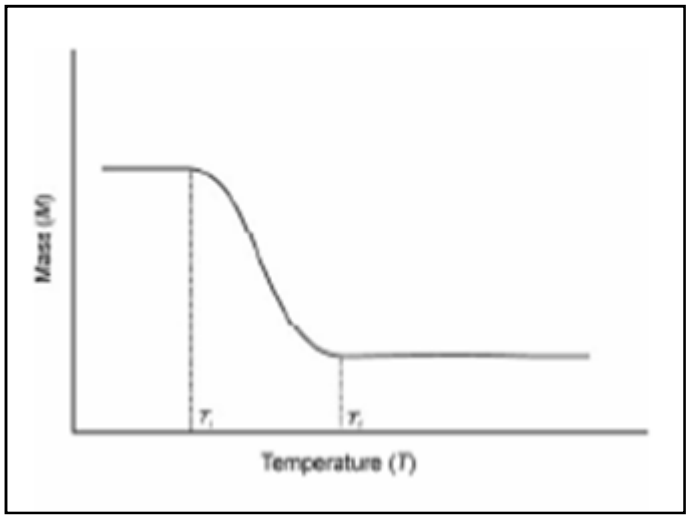

Figure 5.1: A typical TG curve [38]

There are wide range of properties that could be investigated via TG, and those are listed below [39].

a) specific heat

b) thermal expansion

c) weight

d) flow stress

e) viscosity

f) elastic modulus and damping

g) evolved gases

h) phase changes and lattice parameter

Table 5.1: Recommended terminology for thermal analysis method [36]

Acceptable Name	Acceptable Abbreviation	Rejected name(s)
A. General		
Thermal analysis		Thermography Thermoanalysis
B. Methods associated with weight change		
1. Static		
Isobaric weight change determination		
Isothermal weight change determination		Isothermal thermogravimetric analysis
2. Dynamic		
Thermogravimetry	TG	Thermogravimetric analysis Dynamic thermogravimetric analysis
Derivative thermogravimetry	DTG	Differential thermogravimetry Differential thermogravimetric analysis Derivative thermogravimetric analysis
C. Method associated with energy change		
Heating curves[b]		Thermal analysis
Heating-rate curves[b]		Derivative thermal analysis
Inverse heating-rate curves[b]		
Differential thermal analysis	DTA	Dynamic differential calorimetry
Derivative differential thermal analysis		
Differential scanning calorimetry	DSC	
D. Methods associated with evolved volatiles		
Evolved gas detection	EGD	Effluent gas detection
Evolved gas analysis	EGA	Effluent gas analysis Thermovaporimetric analysis
E. Methods associated with dimensional change		
Dilatometry		
Derivative dilatometry		
Differential dilatometry		
F. Multiple techniques		DATA (Differential and thermogravimetric analysis)
Simultaneous TG and DTA etc.		Derivatography Derivatographic analysis

5.3. Calculation of Kinetic Parameters From Thermogravimetric Data

Thermogravimetric analysis is one of the most extensive techniques to study the thermal decomposition reaction kinetics of a fuel because of its simplicity and the information afforded by a single thermogram. Most kinetic studies use simple reaction models in different temperature range.

Thermogravimetric analysis data is useful for determining the decomposition temperatures and rates of solid materials. Reaction rate parameters such as activation energy E_a and frequency factor (A) can be determined from constant heating rate data using a simplified Arrhenius equation.

Some methods to evaluate the kinetic coefficients using the non-isothermal thermogravimetric curves are as follows [40].

- Integral methods where the change of mass with temperature is used
- Differential methods where the rate of the mass change is used
- Difference differential methods where the secondary differnces in the rate of the mass change are considered
- Spesific methods that could be applied to first rates
- Methods where non-linear heating rates are used

These methods are based on the combined usage of these equations:

$$\frac{d\alpha}{dt} = k \cdot f(\alpha) \qquad \textbf{(5.1)}$$

$$k = A \cdot \exp\left(\frac{-E}{R \cdot T}\right) \qquad \textbf{(5.2)}$$

$$T = T_0 + b \cdot t \qquad \textbf{(5.3)}$$

Where;

f(α) = Differential form of the kinetic model

k = Reaction rate constant (s^{-1})

A = Frequency factor (s^{-1})

E = Activation energy (kcal.mol^{-1} or kJ.mol^{-1})

R = Gas constant (kcal.mol^{-1}.K^{-1} or kJ.mol^{-1}.K^{-1})

b = Constant heating rate (K. s^{-1})

T_o = Initial temperature (K)

α = Conversion

T = Temperature at time (K)

Conversion is evaluated with the following equation:

$$\alpha = \frac{W_0 - W_t}{W_0 - W_\infty} \quad \textbf{(5.4)}$$

W_0 = Initial weight of the sample

W_t = Weight of the sample at time, t

W_∞ = Weigt of the sample at the end of the reaction

When equations 5.1, 5.2 and 5.3 are combined:

$$\frac{d\alpha / dt}{f(\alpha)} = \left[\frac{A}{b}\right] - \exp\left[\frac{-E}{R \cdot T}\right] \quad \textbf{(5.5)}$$

This equation is linearized taking the logarithm of both sides:

$$\ln\frac{d\alpha / dt}{f(\alpha)} = \ln\left[\frac{A}{b}\right] - \left[\frac{E}{R \cdot T}\right] \quad \textbf{(5.6)}$$

In order to determine the kinetic constants, the linearized equation has been solved with many different f(α) assumptions. When the left side of the equation is sketched versus 1/T, the shift of the resulting line gives the ln[A/b] value and the slope gives [-E/R] value. f(α) is the most suitable function that represents the degredation reaction.

The most suitable method to determine the kinetic parameters of biomass using the thermogravimetric curves is the Coats-Redfern method [41] .Assume the degradation reaction:

$$a.A(k) \leftrightarrow b.B(k) + c.C(g) \quad \textbf{(5.7)}$$

This integral method expresses the disappearance rate of A with equation (5.7), assuming:

$$\frac{d\alpha}{dt} = k.(1-\alpha)^n \quad \textbf{(5.8)}$$

$$f(\alpha) = (1-\alpha)^n \quad \textbf{(5.9)}$$

The integral of equation (5.9) is taken and linearized in order to find equations to evaluate kinetic variables. These are:

For n≠1;

$$\log\left[\frac{1-(1-\alpha)^{1-n}}{(1-n).T^2}\right] = \log\left[\frac{A.R}{b.E}\right] - \left[\frac{E}{2.303.R.T}\right] \quad \textbf{(5.10)}$$

The appropriate n value is selected and the plot of 1/T versus $\log\left[\frac{1-(1-\alpha)^{1-n}}{(1-n).T^2}\right]$ is sketched and the slope of the resulting line gives E value and the shift gives A value.

For n=1;

$$\log\left[-\log\frac{(1-\alpha)}{T^2}\right] = \log\left[\frac{A.R}{b.E}\right] - \left[\frac{E}{2.303.R.T}\right] \quad \textbf{(5.11)}$$

The plot of 1/T versus $\log\left[-\log\frac{(1-\alpha)}{T^2}\right]$ is sketched and the slope of the resulting line gives $\left[-\frac{E}{2.303.R.T}\right]$ value and the shift gives $\log\left[\frac{A.R}{b.E}\right]$ value.

5.4. Literature Survey

The pyrolytic decomposition of olive residue/plastic under N_2 atmosphere between 300 and 1273 K at four heating rates have been investigated; 2, 10, 20 and 50 K/min. The N_2 flow rate was determined to be 60 ml/min and the sample amount used in TG was around 20 mg for both olive residue and plastic. According to the study, the decomposition of the mixure has been accomplished in three stages. The first two was linked to the hemicellulose and cellulose decomposition of olive residue whereas; the last stage was attributed to the decomposition of lignin and plastic in the mixture. For olive residue/plastic mixtures, in the three stages of the pyrolysis

process, activation energies 155–165 kJ/mol for the first stage, 205–212 kJ/mol for the second one, and 172–221 kJ/mol for the third one [42].

Experimental thermal decomposition study of four biomass sample pyrolysis has been carried out. Wheat, winter barley, oat, and B. carinata straws from Spain and Denmark were studied since these biomasses were key samples in an EU project aiming at the reduction of the cost and emission in the combustion of high alkali biofuels A distributed activation energy model (DAEM) was used due to the complexity of the biomass samples of agricultural origin. Method of least squares were utilized for decomposition kinetics determination. The evaluation was both carried out on DTG and TGA data, and it is advised that in case of good description of the high reaction rate regions of the process is required DTG data should be preferred [43].

Thermal decomposition of coal and biomass samples by using distributed activation energy model (DAEM) has been studied. The samples utilized in experiments were Datong bituminous coal, Jindongnan lean coal and corn-skin stalks. The thermogravimetric experiments were carried out for all samples in the decomposition range of 313 K to about 1173 K for corn-stalk skins and 313 K to about 1473 K for the coals. The experiments showed that three fuels have approximate Gaussian distribution curves. ln k_o is linear with activation energy (E) for three of them and the activation energy for corn-skin stalk is smaller than that of Jindongnan lean coal and Datong bituminous coal [44].

Thermochemical properties of four different biomass samples namely, corn stalk, shea meal, sugarcane bagasse 1 and sugarcane bagasse 2 have been evaluated under oxidizing and inert atmospheres. 5-7 mg of the biomass samples were tested with a heating rate of 10 K/min from room temperature to 378 K and 20 K/min from 378 K to 1223 K. It was observed that the rate of weight loss for all the biomasses in an inert atmosphere were slower than when oxidised. The activation energies under inert and oxidizing atmospheres were found to be 77, 58, 71, 67 kJ/mol and 113, 75, 116, 108 kJ/mol for CS, SB1, SB2 and SM, respectively. At the end of the studt it has been revealed that CS was found to be the most reactive in both inert and oxidative environments. SB2 and SB1 exhibited a similar behaviour but with different values of reactivity and activation energy [45].

Gasification kinetics of pine and birch charcoals was studied by thermogravimetric analysis (TGA) at CO_2 partial pressures of 51 and 101 kPa. The study differs from isothermal studies via the fact that one has to wait for the stabilization of the experimental conditions, since the whole gasification process has been studied. For that reason, low sample masses (1-2 mg) and relatively slow heating rates (5-20 K/min) were employed in order to guarantee a true kinetic control. The results showed that the activation energy of the gasification step was 262 kJ/mol while the reaction order of CO_2 was turned out to be 0.40 [46].

The chemical and physical properties of corn stover related to thermochemical conversion have been investigated under both inert (N_2) and oxidizing atmospheres . Approximately 5–10 mg of the corn stover samples was placed in the pan of the TGA and the heating rates utilized were 10, 30 and 50 K/min. The weight loss of corn stover has been found to occur in three stages [47].

The pyrolysis of bamboo has been studied in order to understand, model and control the process. Bamboo samples were obtained Hong Kong and TG experiments were carried out in the presence of N_2. Approximately 10-15 mg of samples were heated to 773 K at the heating rate of 1 to 20 K/min and then held isothermal for 10 minutes. Runge-Kutta algorithm was adopted to estimate the kinetic parameters for bamboo pyrolysis. Furthermore, the number of reaction order was assumed to be 1. Different solution assumptions were adopted since, the evolution of intermediates and the possible secondary reaction formation could contribute to the overall weight loss. At the end of the study it has been revealed that Further study on the intermediate reactions as well as secondary subcomponents is necessary for beter understanding of bamboo pyrolysis process [48].

A TGA study proposing a method for the purpose of characterizing biomass material to be utilized with coal for energy production has been studied. The proposed TGA method uses a heating rate of 5 K/min from ambient to 1173 K in nitrogen at a flow rate of 30 ml/min with four diffetent biomass materials, palm kernel expeller, cereal co-product, sawdust and olive cake. All of the four biomass types were blended with high volatile UK coal in proportions of 5%, 10%, 15%, and 20% (wt/wt% basis) with a particle size of 106–150 mm. It is emphasized that, more study is required for the characterization of many other coals and biomass types [49].

The structural properties and the reactivity of pine seed shells, olive husk and wood chips upon pyrolysis, combustion and gasification (with CO_2 and H_2O). Several isothermal and non-isothermal thermogravimetric tests were carried out in order to assess the reactivity of the fuels and determine the kinetic parameters for pyrolysis, combustion and gasification processes. "Five sets of thermogravimetric experiments have been carried out. Non-isothermal pyrolysis under inert conditions, non-isothermal pyrolysis under oxidative conditions, isothermal combustion of char, isothermal gasification of char with carbon dioxide, isothermal gasification of char with water vapor. In non-isothermal experiments samples were dehumidified in the TG for 5 min at 373 K in an upward flow of 50 ml/min. The temperature was then raised from 373 K to 1073 K at a constant heating rate. In experiments of char gasification with carbon dioxide the reaction temperature TR was comprised between 1023 and 1183 K and CO_2–N_2 mixtures were used with carbon dioxide partial pressure in the range 0.05–1 bar. Char gasification with water vapour was carried out at 1103 K with 30% H_2O(v) in N_2". The experiments showed that olive husk is the most reactive biomass upon pyroylsis, combustion and gasification. The kinetic analysis were made bu using the methods offered by Kissinger and Friedman. The reaction order, activation energy, preexponential factor and the conversion rate could be found in the article [50].

The pyrolysis characteristics of hemicellulose, cellulose and lignin which are being the main structural components of biomass using TGA with differential scanning calorimetry detector and a pack bed has been searced. The study has revealed that hemicellulose and cellulose decomposes around 493-588 K and 588-673 K respectively. On the contrary lignin decomposition has occurred in a wider range (433 K-1173 K) compared to that of hemicellulose and cellulose. 10 mg sample was used in the experiments, N_2 as the carrier gas with 120 ml/min. The sample was heated at a heating rate of 10 K/min. At the end of the study, the following results were drawn: "The pyrolysis of cellulose was mainly happened at 588-673 K, while that of lignin covered a whole temperature range 423-1173 K. At low temperatures (<773 K), the pyrolysis of hemicellulose and lignin involved exothermic reactions while those of cellulose were endothermic. However, at high temperatures (>773 K), the situation just changed inversely. CO_2 releasing was mainly caused by the primary pyrolysis, while secondary pyrolysis was the main source for releasing of CO and

CH_4. Hemicellulose showed higher CO and CO_2 yield, while lignin displayed higher CH_4 releasing. Organics compounds (C=O, C–O–C, etc.) were mainly released out at low temperatures, i.e., 473-673 K and 573-723 K from hemicellulose and cellulose, respectively. Nevertheless, almost no organics compound was detected from lignin pyrolysis [51].

Two types of olive oil residue (non-leached and water-leached olive-oil residue) at three heating rates (10, 20 and 50 K/min) under air atmosphere has been studied. Olive-oil residue samples of 10 mg were subjected to thermogravimetric analysis in a dry air atmosphere (21% oxygen and 79% nitrogen) at three heating rates (10, 20 and 50 K/min) from ambient temperature to 973 K. The thermal degradation rate in active and passive zones, the initial degradation temperature, and the residual weight at 973 K were determined. It has been pointed out that increasing the heating rate increased the thermal degradation rate, the residual weight at 973 K, and the initial degradation temperature. At the end of the experiments following outcomes has been revealed: "The thermal behaviour of olive-oil residue depends on the chemical composition, inorganic substances–i.e. ash content– and rate of heating, the higher the cellulosic content of the sample, the higher is its thermal degradation rate, From the obtained results it can be concluded that the waterleached olive-oil residue sample (WL-OR) is more degradable through thermochemical conversion processes in comparison with non-leached olive-oil residue sample (NL-OR)" [52].

The gasification kinetics of chars from different biomass species within the temperature range 1073-1223 K, CO_2 concentrations of 10 to 100 v/v, and pressures between 1 and 20 bar using thermogravimetric analysis (TGA) have been investigated. For the biomass sample radiata pine *(Pinus radiata),* spotted gum *{Eucalyptus maeutata),* and sugarcane bagasse were used with the particle size 120 and l80 μm. Global char reactivity decreased by increasing pyrolysis pressure. The gasification reaction of biomass was found to be chemically controlled up to 1173 K. The Langmuir-Hinshelwood rate equation represented the pressurized radiata pine ehar gasification kinetics well. The total pressure had little effect on reactivity, indicating that both external and internal gas diffusion processes did not influence the reaction for temperatures and pressures up to 1173 K and 20 bar, respectively [53].

An experiment on five different chestnut woods grown in France, Italy, Russia has been carried out in order to gain deeper understanding of the effect of sample origin, extraction and hot water washing on devolatilization kinetics. Following the execution of appropriate pretreatment techniques, chestnut samples have been employed for TG tests. High-purity nitrogen has been used for the tests at a flow rate of 150 mL/min, and the heating rate is adjusted to 5 K/min in order to minimize heat and mass transfer with a sample mass of 5 mg. The following results are derived: The thermogravimetric curves, measured for a heating rate of 5 K/min, show a significant influence of the origin though extraction and hot-water washing act to reduce differences, peculiarities due to species (chestnut versus beech) and sample origin are preserved. Compared with hot-water washing, extraction is less effective for the modification of the characteristic reaction temperatures, most likely as a consequence of the very slow and flat degradation rates attained by extractives over the entire temperature range examined. The char yield is always significantly reduced by the two pretreatments [54].

The gasification kinetics of WPOS (wood matter from pressed oil-stone, which is composed of a granular solid made up of irregular and heterogeneous agglomerates of small particles of pit and pulp) via TGA at various temperatures (1073–1123–1148–1173–1198 K), CO_2 partial pressures (0.20–0.35–0.50 bar) and CO partial pressures (0.0–0.20 bar) has been studied. N_2 is used as the inert atmosphere and the sample was heated to 378 K, kept for 5 minutes in order to lose its moisture and then heated to 1273 K by 30 K/min at constant heating rate throughout the process. The following results have been achieved:

· The external diffusion resistance may limit the measured reactivities, especially at low CO_2 partial pressures ($p_{CO2} \leq 0.2$ bar) and high temperatures ($T \geq 1173$ K).

· According to the nth model the activation energy is 133 kJ/mol, the reaction order is 0.43 and the frequency factor is $1.01*10^{-4}$/min $bar^{-0.43}$ for the CO_2 gasification experiments.

· The activation energy of the WPOS char gasification is significantly lower than other biomass chars, probably due to a catalytic effect associated to a high alkali content.

· The product of the gasification reaction (CO) has a significant inhibition effect.

· Both the n^{th} and the L–H models fit very well with the reactivity data for those cases without CO inhibition. The L–H model seems to be more robust and works very well in presence of CO [55].

The thermogravimetric behavior of four types of rice husks at three heating rates 10, 20 and 50 K/min in air, oxygen ad nitrogen atmospheres have been examined. The samples used in experiments were ~ 80 mg. The thermal degredation in active and passive zones, degredation temperature, and the residual weight at 973 K were determined. As the heating rate increased thermal degredation rate and the residual weight at 973 K increased whereas; on the contrary the initial degredation temperature decreased. Higher cellulose content of the rice husk results in higher initial degredation tempereature and higher degredation rate [56].

A Study investigating the pyrolysis process of switchgrass under N_2 atmosphere at 10, 20, 30, 40 K/min has been conducted. Thermal decomposition of switchgrass occurred between 423 K and 823 K. The kinetics of biomass pyrolysis has been assumed to consist of three paralel independendent reactions. It is found that for all the heating rates, cellulose and lignin had the highest and lowest activation energies respectively. The values of R^2 indicated that, the pyrolysis of switchgrass is described by the three paralel independent nth order reactions model [57].

The pyrolysis kinetics of six different Chinese biomasses via two pseudo-component models have been investigated. The analysis revealed that the three pseudo component model with n-order kinetics is more accurate than the model with first order kinetics. For cellulose, a reaction order of one gave good results while the reaction order of hemicellulose ranged between 1.5 and 4. The maximum pyrolysis rate increases with increased heating rate, and the corresponding peak temperature also increases [58].

A study for determining the thermal characterization of fifteen tropical biomass feedstocks has been carried out. Results of the study showed that the cashew nut shells were the most reactive fuels due to their highest overall mass loss and the highest mass loss rate at the first peak. All the fuels exhibitied the first reaction order, except the sisal bole which was decomposed with the zero reaction order. The calculated activation energies varied between 239 and 542 kJ/mol [59].

The effect of heating rate on the devolatilization of rice husks, olive cake and cacao shells has been investigated. The heating rate was between 5-100 K/min, and pure N_2

was used as the carrier gas. A Variable Activation Energy Model for Biomass Devolatilization (VEB) were developed. Average E_a values for rice husks, olive cake and cacao shells were found to be 135.5, 119.1, 127.7 kJ/mol. Graphical correlations were provided for the T_{onset} and T_m. The trend of E_a is an indication of multi-step nature of biomass devolatilization [60].

Thermal behavior of *Arundo donax* by thermogravimetric analysis under inert atmosphere at heating rates ranging from 5 to 20 K/min has been studied. Gaseous emissions and volatile organic compounds were measured and global kinetic parameters were determined in two main phases, namely active and passive. The hemicellulose and cellulose degradation were characterized in the active zone. It has been found that, mass loss rates, mass losses and emissions were strongly influenced by the variation of the heating rate. It was found that, hemicellulose undergoes a thermal decomposition with a reacion order 0.5 whereas; cellulose decomposes with a reaction order 1. The E_a for hemicellulose decomposition was calculated around ~ 110 kJ/mol, where the E_a for cellulose varied between 160 and 50 kJ/mol as the heating rate was changed [61].

6. MATERIALS AND METHODS

In this study thermal gravimetric analysis was used to determine the thermal decomposition reactions kinetics of several biomass samples under nitrogen atmosphere. The selected biomass samples which are widely available in Turkey were; hazelnutshell, olive cake, corn cob and sugarcane bagasse.

6.1 Thermogravimetric Analyser

The thermogravimetric system (TA Q600 SDT) was used in decomposition experiments. The specifications of the device are given in Table 6.1 and Figure 6.1.

Table 6.1: The specifications of the thermogravimetric system

Specification	Value
System design	Horizontal balance and furnace
Balance design	Dual beam (growth compensated
Sample capacity	200 mg (350 mg including sample holder)
Balance sensitivity	0.1 μg
Furnace type	Bifilar wound
Temperature range	Ambient to 1773 K
Heating rate – Ambient to 1273 K	0.1 to 100 K/minute
Heating rate – Ambient to 1773 K	0.1 to 25 K/minute
Furnace cooling	Forced air 1773 to 50 K in < 30 minutes 1000 to 50 K in < 20 minutes
Thermocouples	Platinum/Platinum-Rhodium (type R)

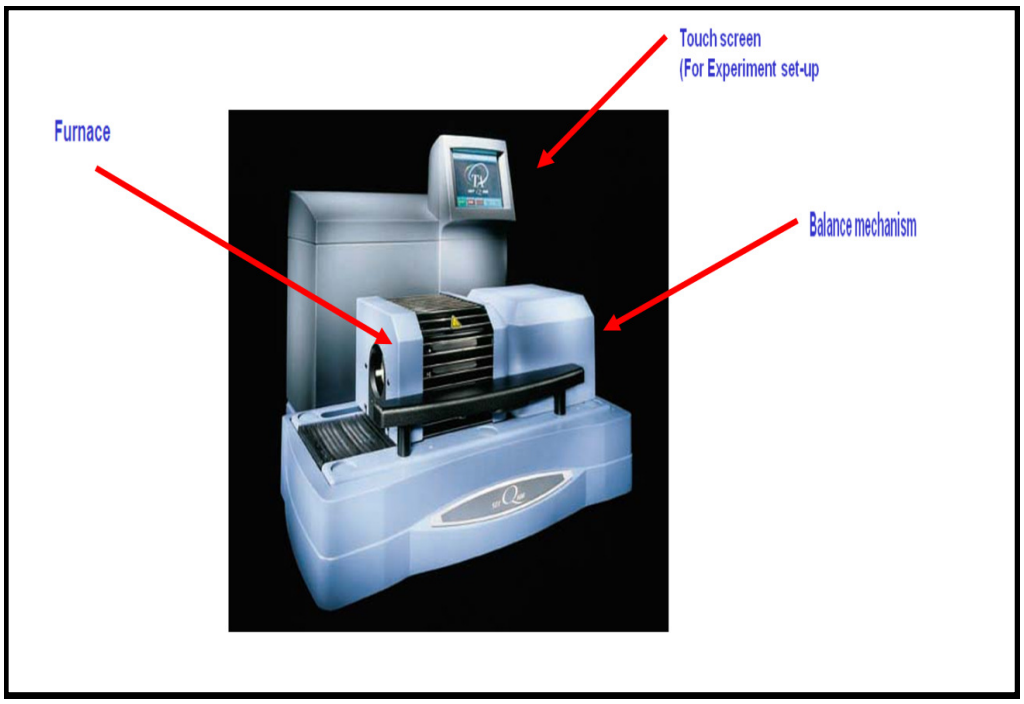

Figure 6.1: Thermogravimetric system

6.2 Experimental Conditions

Thermogravimetric analyses of hazelnutshell, olive cake, corn cob and sugarcane bagasse have been carried out. The desired particle sizes (< 250 μm) of the biomass samples were obtained by grinding and sieving. The weight loss was recorded in the temperature range of 298-1073 K. About 40 mg of sample were heated up to 378 K under nitrogen flowing gas and held at that temperature until the weight loss rate is zero. Then sample was heated up to 1073 K and held at that temperature until weight loss rate is zero (30 min). In order to determine the effects of heating rate and gas flow rate, the experiments were performed in four different heating rates of 5, 20, 50 and 100 K/min and two different nitrogen flow rates (50 and 100 cm^3/min). All experiments were repeated for two times to confirm the repeatability of the experiments and authenticity of the generated data.

The derivative thermogravimetric analysis (DTG) profiles, which show the rate of weight losses from the sample versus temperature, were derived from the TGA curves. Using these profiles, the influences of heating rate and gas flow rate on the weight losses from the samples were examined considering the thermal decomposition temperatures.

6.3 Analysis of the Samples

Proximate analyses (moisture, volatile matter, fixed carbon and ash contents) of the biomass samples were conducted using a thermogravimetric analyser (TA Q600 SDT) and the results on original-base are given in Table 6.2. Proximate TG method involves heating the sample (under N_2) at a rate of 10 K/min to 378 K then holding for 10 min to obtain the weight loss associated with moisture. The temperature is then ramped from 378 K at a rate of 40 K/min to 1223 K (under N_2) and held for 10 min to obtain the weight loss associated with volatiles release. Air is then introduced into the furnace chamber to oxidise the carbon in the char and the weight loss associated with this is the fixed carbon. The remaining material after combustion is the ash.

Structural compositions of the biomass samples were carried out by analytical means to determine the extractives, lignin, holocellulose and α-cellulose contents. Extractives in the sample were determined according to TAPPI T204 om-88 [62]. In this method, the sample is extracted with a mixture of ethanol and benzene, and then washed with alcohol and water. Ethanol–benzene mixture extracts fats, some resigns and wood gums. Hot water extracts tannins, gums, sugars, starches and coloring matter. The sample remaining after alcohol–benzene extraction was used to determine the holocellulose, which consists of celluloses plus hemicelluloses. For this purpose, the sample was heated with the mixtures of water, $NaClO_2$ and acetic acid. Extracted sample was cooled, washed with acetone, dried in the air and then weighed. The lignin content of the sample was determined according to the TAPPI T222 om-88. This method involves the treatment of the extracted sample with sulphuric acid to hydrolyse the cellulose and disperse all non-lignin materials. α-Cellulose content of the sample was determined according to TAPPI T203 om-88 standard by extracting the holocellulose with 17.5 % (v/v) sodium hydroxide solution. The results are tabulated in Table 6.3.

Table 6.2: Proximate analyses of biomass samples

Sample	Moisture (%)	Volatile Matter (%)	Fixed Carbon (%)	Ash (%)
Hazelnutshell	9.23	71.72	17.07	1.98
Olive cake	8.32	74.58	15.32	1.77
Corn cob	7.48	76.49	10.59	5.44
Sugarcane bagasse	9.72	78.39	8.61	3.28

The proximate analyses results indicate that the range of moisture, volatile matter, fixed carbon and ash contents of the samples vary between 7.48-9.72 %, 71.72-78.39 %, 8.61-17.07 % and 1.77-5.44 %, respectively.

Table 6.3: Structural compositions of the biomass samples

Sample	Extractive Matter (%)	Lignin (%)	Hemicellulose (%)	α-Cellulose (%)
Hazelnutshell	12.19	44.40	5.99	75.44
Olive cake	11.16	32.62	3.97	89.31
Corn cob	21.53	4.73	18.45	-
Sugarcane bagasse	13.51	5.57	18.77	75.66

The extractive matter contents of the sample vary between 11.16-21.53 % and the lignin contents vary between 4.73-44.40 %. Sugarcane bagasse has the highest hemicellulose whereas olive cake has the lowest. Olive cake has the highest α-cellulose where hazelnut shell has the lowest.

7. RESULTS AND DISCUSSIONS

The thermal decomposition characteristics of biomass samples (hazelnut shell, olive cake, corn cob and sugarcane bagasse) were investigated through thermogravimetry (TG) at four different heating rates and under two different nitrogen gas atmospheres.

7.1. Hazelnut Shell

Hazelnut has become one of the extremely important crops for social, economic and as well as environmental aspects for many years in Turkey, the most important hazelnut producer and exporter in the world. From social point of view, it is the most important source of income especially for people living in eastern Black Sea region. From economic point of view it has a great deal of employment capacity and supplies about one billion U.S. dollars as foreign exchange income every year. Besides the economic contribution, utilisation of country resources and preventing erosion in unsuitable lands for soil treatment is achieved.

In this study, the thermal decomposition characteristics of hazelnut shell taken from hazelnut production plant in Akçakoca were investigated through thermogravimetry at four different heating rates and two nitrogen gas atmospheres. Figures 7.1-7.3 present the differential thermograms of the hazelnut shell sample. As could be seen from the figures, the thermal decomposition behavior of the samples shows that the thermal decomposition process can be approximately described by moisture and volatile lumps. The temperature range for the volatile evolution is referred to as offering a clue to the key mechanistic steps in the overall hazelnut breakdown process. The DTG curves show three main regions in volatile evaluation. Because the temperature intervals of hemicellulose and cellulose decomposition partially overlap each other, the hemicellulose decomposition (first region) usually appears as a more or less pronounced “shoulder” instead of a well-defined peak. The second region is associated with the attainment of the maximum, mainly because of cellulose decomposition, followed by a rapid decay and a long tail. Lignin decomposes in a

wider range compared to that of hemicellulose and cellulose, for that reason peak does not appear in case of lignin decomposition.

Effect of Heating Rate

The heating rate is one of the most important parameters influencing the thermal decomposition characteristics. In this study, the heating rates were varied as 5, 20, 50 and 100 K/min. The effects of heating rate on thermal decomposition of hazelnut shell were shown in Figure 7.1. It is clear from the DTG profiles obtained from the thermal decomposition that considerable different trends in the rates of weight losses took place when heating rate changed between 5 and 100 K/min. At the lower value of this interval of heating rate, the maximum rate of weight loss was so low that it was only 2.8 %/min for 5 K/min. As the heating rate increased, maximum rates of weight losses also increased so obviously that they were determined as 10.2, 22.3 and 45.6 %/min for the heating rates of 20, 50 and 100 K/min, respectively. The phenomenon related to this important change in the maximum rate of weight losses can be interpreted by the fact that biomass has a heterogeneous structure and possess a number of constituents. These constituents give their characteristic individual decomposition peaks in definite temperature ranges during the thermal decomposition process. For sufficiently low heating rates during thermal decomposition, most of these peaks can be seen as small broken lines or vibrations. However, at higher heating rates separate peaks do not arise due to simultaneous decomposition. Several adjacent peaks are united to form overlapped broader and higher peaks.

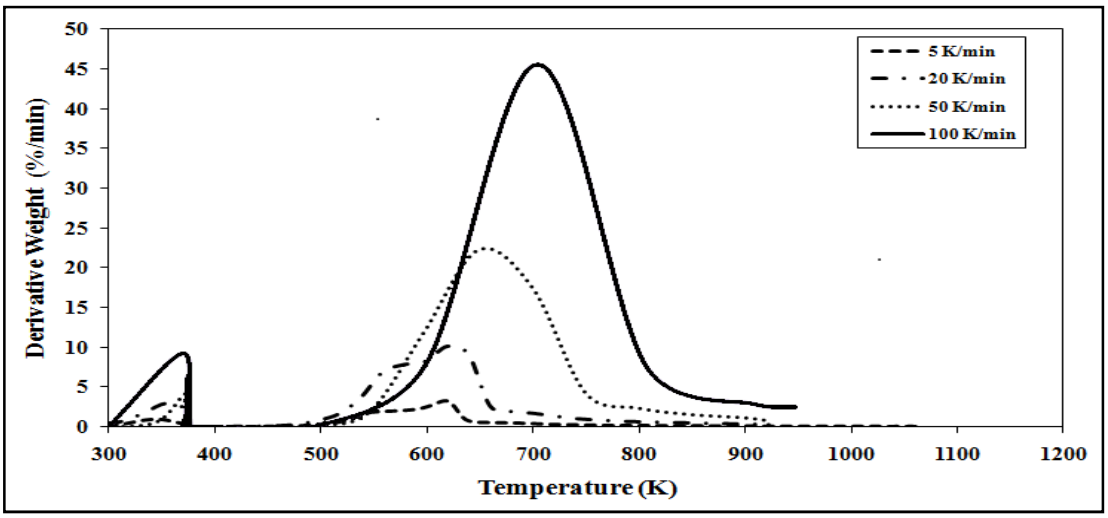

Figure 7.1: The effects of heating rate on thermal decomposition of hazelnutshell (Nitrogen gas flow rate: 100 cm^3/min)

Although, the maximum rate of weight losses are higher at high heating rates, the number of the peaks was relatively lower at these heating rate. For example, at the heating rate of 50 K/min, only one peak appeared. This indicates that an increase in the heating rate from 20 to 50 K/min shifted the main peak to the right and one of the minor peaks at lower temperatures became the major peak at higher heating rates. A similar trend was also observed between the heating rates of 50 and 100 K/min.

Total weight losses from the sample were determined as 75.3, 75, 74.7, and 75.2 % on original basis at the heating rates of 5, 20, 50 and 100 K/min, respectively. The increase in heating rate did not cause an important change in weight loss. However, higher heating rate would translate into a shorter contact time between the char and the N_2 gas during the temperature ramp-up stage. This would imply a shorter dwell time for the char and therefore the decrease the weight loss was not high and the effect of the heating rate was negligible. By the pyrolysis of palm oil waste, Yang et al.[43] indicated that increasing of heating rate from 0.1 K/min to 100 K/min, weight loss decreased. This decrease could be explained by the enlargement of heat transfer rate and the decrease in contact time when heating rate was increased [42]. The temperatures at which volatile evolution reaches a maximum (maximum peak temperature) during thermal decomposition process were also affected from the variation of the heating rate. They were determined as 612, 619, 649 and 705 K for the heating rates of 5, 20, 50 and 100 K/min, respectively. The increase in heating rate from 5 K/min to 100 K/min induced the peak temperatures shifted to higher values.

The effect of heating rate was also investigated for N_2 atmosphere with flow rate of 50 cm^3/min and the data obtained were given in Figure 7.2. It is clear from the DTG profiles obtained from the thermal decomposition that considerable different trends in the rates of weight losses took place when heating rate changed between 5 and 100 K/min. At the lower value of this interval of heating rate, the maximum rate of weight loss was so low that it was only 3.2 %/min for 5 K/min. As the heating rate increased, maximum rates of weight losses also increased so obviously that they were determined as 10.3, 22.6 and 46.4 %/min for the heating rates of 20, 50 and 100 K/min, respectively. As a comparison, the decrease in N_2 flow rate at different heating rates did not cause an important change in the rates of weight losses.

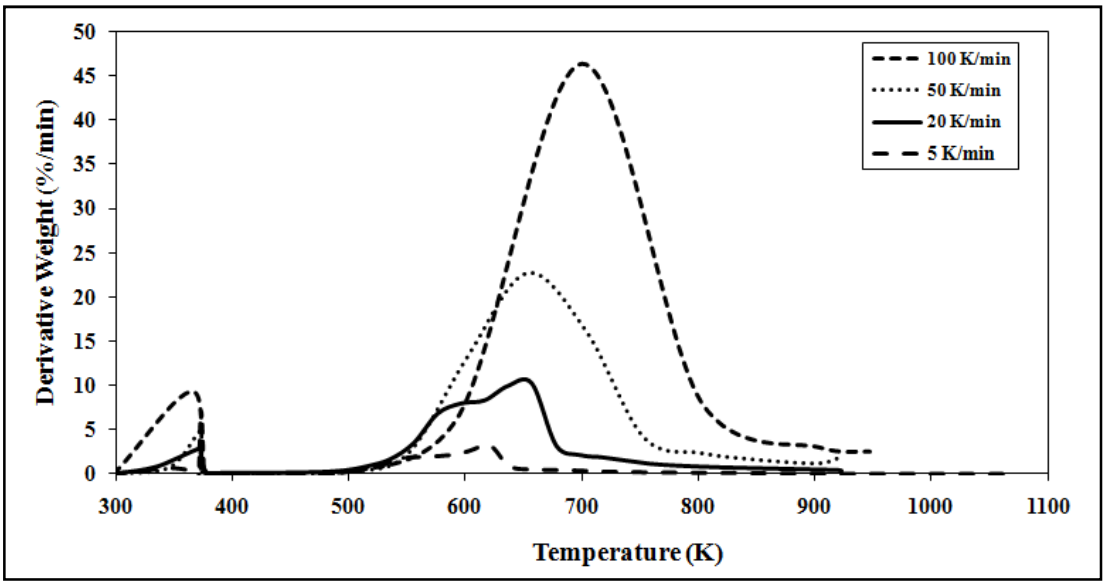

Figure 7.2: The effects of heating rate on thermal decomposition of hazelnut shell (Nitrogen gas flow rate: 50 cm^3/min)

Maximum peak temperatures resulted in N_2 atmosphere with flow rate of 50 cm^3/min were affected from the variation of the heating rate. They were determined as 612, 647, 652 and 701 K for the heating rates of 5, 20, 50 and 100 K/min, respectively. The increase in heating rate from 5 K/min to 100 K/min induced the peak temperatures shifted to higher values.

Total weight losses from the sample were also determined as 74.5, 74.6, 74.2 and 75.5 % on original basis at the heating rates of 5, 20, 50 and 100 K/min, respectively. The increase in heating rate did not cause an important change in weight loss.

Effect of Gas Flow Rate

Effect of gas flow rate on thermal decomposition of hazelnut sample was investigated under two different gas flow rate (50 and 100 cm^3/min) in N_2 atmosphere. The TG and DTG curves of the samples, representing the effect of change of flow rate are plotted in Figure 7.3. Total weight loss was slightly increased by the increase of gas flow rate. For example, weight losses for the thermal decomposition with 50 cm^3/min gas flow rate at the heating rate of 20 and 50 K/min were 74.6 % and 74.2 %, whereas they were obtained to be 75 and 74.7 % in case of the gas flow rate of 100 cm^3/min, respectively. Especially, the increased flow rate enhances the diffusion of the N_2 molecules into the lignocellulosic structure, and causes an increase in weight loss. Flow rates higher than 40 cm^3/min, are enough for initiating the thermal decomposition. Weight loss stays approximately the same.

Similar studies in the literature showed that the weight loss (%) is not affected by the gas flow rate [42]. These differences are negligible, since in termogravimetric analysis where a few amount of sample such as 50 mg is used, varying the flow rate of N_2 from 40 cm^3/min to 120 cm^3/min does not have effect on the shell pyrolysis. The reason for that could be explained as follows: 40 cm^3/min N_2 flow rate is enough to mitigate the potential difference caused by the external heat and mass transfer in the gas phase. Maximum peak temperatures were slightly decreased by an increase in the gas flow rate. Changing the gas flow rate from 50 to 100 cm^3/min at heating rates of 20 and 50 K/min, the maximum peak temperatures shifted from 647 and 652 to 619 and 649 K, respectively.

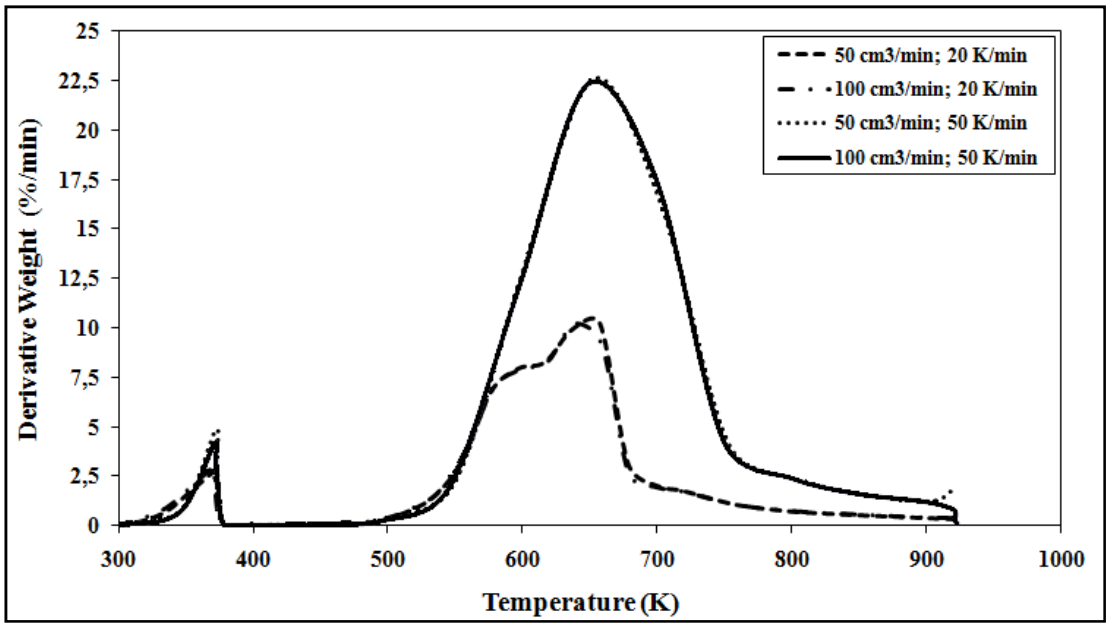

Figure 7.3: The effects of gas flow rate on thermal decomposition of hazelnut shell

7.2. Olive Cake

In the Mediterranean countries, the production of olive and olive oil is abundant. Olive industry in Turkey, with 0.8 milion hectares olive land and having more than 95 millions olive trees, is one of the important sectors in employment, trade, agriculture and industry. Because of the geographical location and having a Mediterranean climate in some parts, Turkey is one of the foremost countries in the production of olive and olive oil together with the Spain, Italy, Greece, and Tunisia.

Olive cake is one important by-product in the production of olive oil. It can be used in different alternative ways such as fertilizer by composting, fuel, etc.

In this study, the thermal decomposition characteristics of olive cake taken from olive oil production plant in Edremit were investigated through thermogravimetry at four different heating rates and two nitrogen gas atmospheres. Figures 7.4-7.6 present the differential thermograms of the olive cake sample. As seen from the figures, the thermal decomposition behavior of the samples shows that the thermal decomposition process can be approximately described by moisture and volatile lumps. The DTG curves show three main regions in volatile evaluation. Because the temperature intervals of hemicellulose and cellulose decomposition partially overlap each other, the hemicellulose decomposition (first region) usually appears as a more or less pronounced "shoulder" instead of a well-defined peak. The second region is associated with the attainment of the maximum, mainly because of cellulose decomposition, followed by a rapid decay and a long tail. The wide range of temperatures, where lignin decomposes (third region), hinders the appearance of a peak attributable to this component.

Effect of Heating Rate

In this study, the heating rates were varied as 5, 20, 50 and 100 K/min and the effects of heating rate on thermal decomposition of olive cake were shown in Figure 7.4. It is clear from the DTG profiles obtained from the thermal decomposition that considerable different trends in the rates of weight losses took place when heating rate changed between 5 and 100 K/min. At the lower value of this interval of heating rate, the maximum rate of weight loss was so low that it was only 3.7 %/min for 5 K/min. As the heating rate increased, maximum rates of weight losses also increased so obviously that they were determined as 13.7, 26.7 and 53.3 %/min for the heating rates of 20, 50 and 100 K/min, respectively. The phenomenon related to this important change in the maximum rate of weight losses can be interpreted by the fact that biomass has a heterogeneous structure and possess a number of constituents. These constituents give their characteristic individual decomposition peaks in definite temperature ranges in the thermal decomposition process. When heating rate is sufficiently low during thermal decomposition, most of these peaks can be seen as small broken lines or vibrations. However, at high heating rates separate peaks do not arise because some of them are decomposed simultaneously, and several adjacent peaks are united to form overlapped broader and higher peaks.

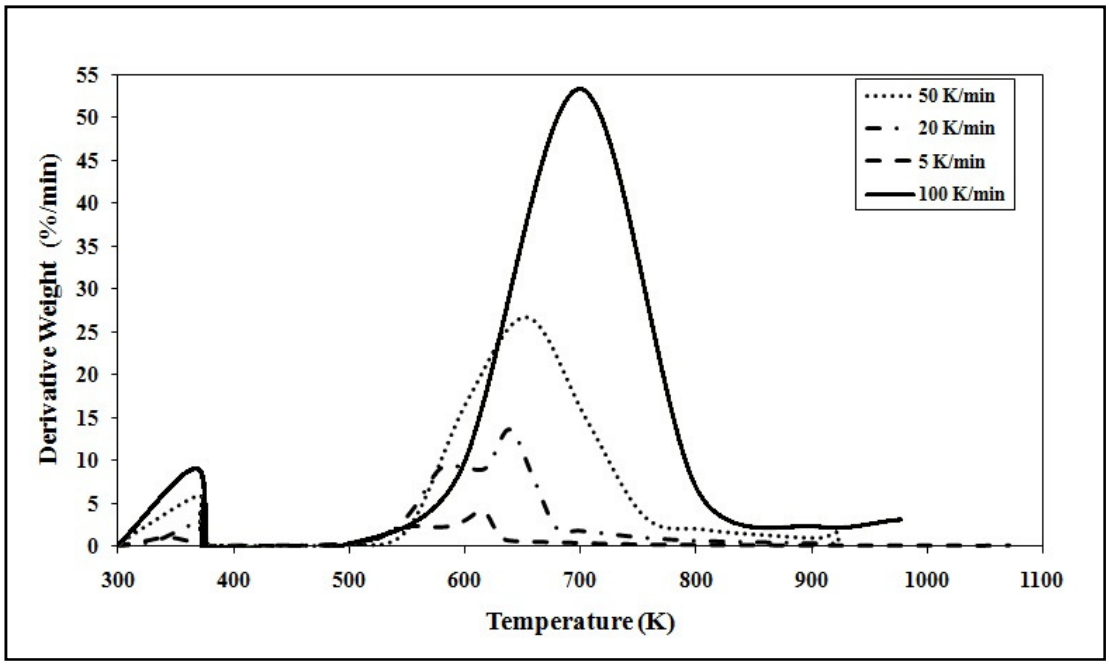

Figure 7.4: The effects of heating rate on thermal decomposition of olive cake (Nitrogen gas flow rate: 100 cm^3/min)

Although, the maximum rate of weight losses are higher at high heating rates, the number of the peaks was relatively lower at these heating rate. For example, at the heating rate of 50 K/min, only one peak appeared. This indicates that an increase in the heating rate from 20 to 50 K/min shifted the main peak to the right and one of the minor peaks at lower temperatures became the major peak at higher heating rates. A similar trend was also observed between the heating rates of 50 and 100 K/min.

Total weight losses from the sample were determined as 78.8, 78.5, 78.9, and 78.3 % on original basis at the heating rates of 5, 20, 50 and 100 K/min, respectively. The increase in heating rate did not cause an important change in weight loss. However, higher heating rate would translate into a shorter contact time between the char and the N_2 gas during the temperature ramp-up stage. This would imply a shorter dwell time for the char and therefore the decrease the weight loss was not high and the effect of the heating rate was negligible.

The temperatures at which volatile evolution reaches a maximum (maximum peak temperature) during thermal decomposition process were also affected from the variation of the heating rate. They were determined as 608, 639, 654 and 700 K for the heating rates of 5, 20, 50 and 100 K/min, respectively. The increase in heating rate from 5 K/min to 100 K/min induced the peak temperatures shifted to higher values.

The effect of heating rate was also investigated for N_2 atmosphere with flow rate of 50 cm^3/min and the data obtained were given in Fig. 7.5. It is clear from the DTG profiles obtained from the thermal decomposition that considerable different trends in the rates of weight losses took place when heating rate changed between 5 and 100 K/min. At the lower value of this interval of heating rate, the maximum rate of weight loss was so low that it was only 2.8 %/min for 5 K/min. As the heating rate increased, maximum rates of weight losses also increased so obviously that they were determined as 9.2, 26.3 and 50.7 %/min for the heating rates of 20, 50 and 100 K/min, respectively. As a comparison, the decrease in N_2 flow rate at different heating rates did not cause an important change in the rates of weight losses.

Maximum peak temperatures resulted in N_2 atmosphere with flow rate of 50 cm^3/min were affected from the variation of the heating rate. They were determined as 610, 620, 650 and 711 K for the heating rates of 5, 20, 50 and 100 K/min, respectively. The increase in heating rate from 5 K/min to 100 K/min induced the peak temperatures shifted to higher values.

Total weight losses from the sample were also determined as 78.8, 79.2, 79,0 and 79.2 % on original basis at the heating rates of 5, 20, 50 and 100 K/min, respectively. The increase in heating rate did not cause an important change in weight loss.

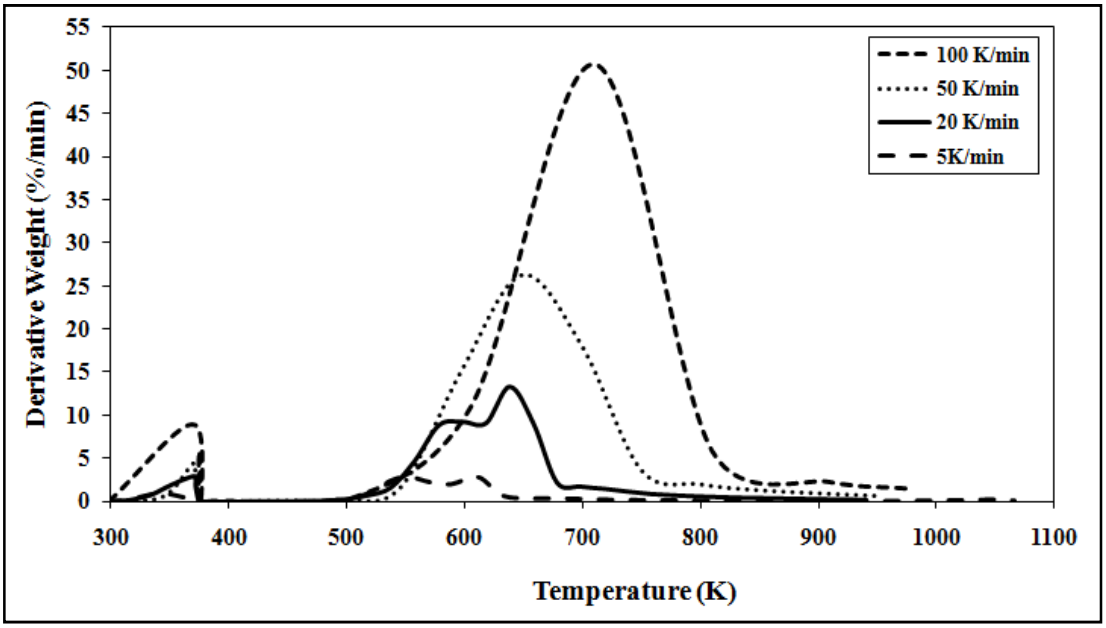

Figure 7.5: The effects of heating rate on thermal decomposition of olive cake (Nitrogen gas flow rate: 50 cm^3/min)

Effect of Gas Flow Rate

Effect of gas flow rate on thermal decomposition of olive cake sample was investigated for two different gas flow rate (50 and 100 cm^3/min) in N_2 atmosphere. The representative TG and DTG curves of the samples, relative to the change of flow rate were plotted in Figure 7.6. Total weight loss was slightly increased by the increase of gas flow rate. For example, weight losses for the thermal decomposition with 50 cm^3/min gas flow rate at the heating rate of 20 and 50 K/min were 79.2% and 79.03 %, whereas they were obtained to be 78.5 and 78.9 % in case of the gas flow rate of 100 cm^3/min, respectively. Especially, the increased flow rate enhances the diffusion of the N_2 molecules into the lignocelulosic structure, and causes an increase of the weight loss. But since 40 cm^3/min and higher flow rates are enough for a thermal decomposition reaction to begin, weight loss stays approximately the same. Maximum peak temperatures were slightly increased by an increase in the gas flow rate. Changing the gas flow rate from 50 to 100 cm^3/min at heating rates of 20 and 50 K/min, the maximum peak temperatures were shifted from 610 and 650 to 639 and 654 K, respectively.

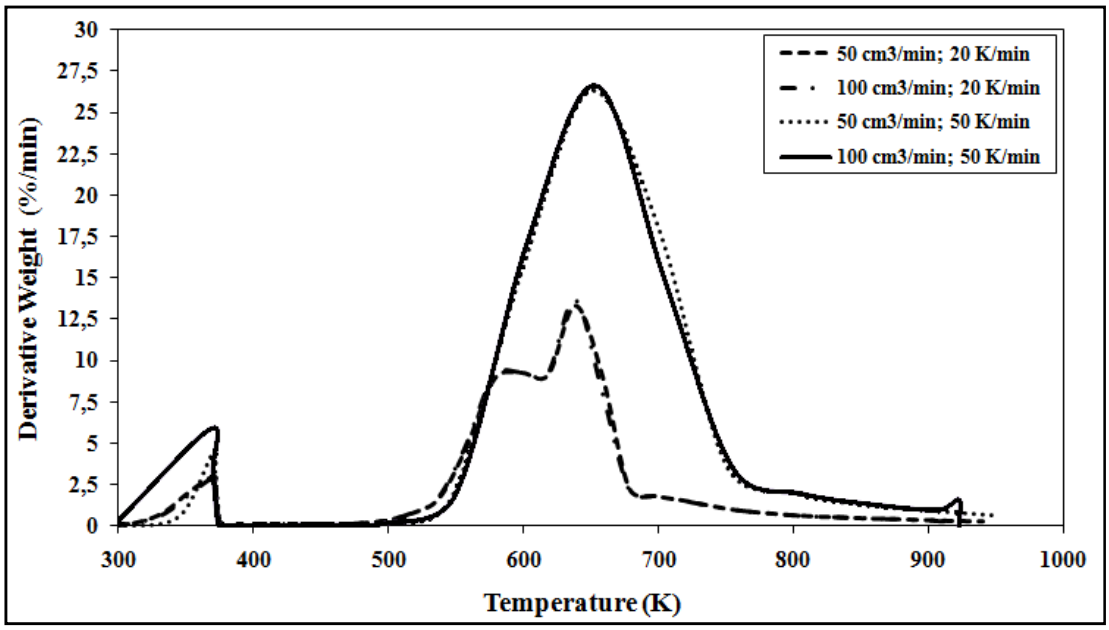

Figure 7.6: The effects of gas flow rate on thermal decomposition of olive cake

7.3. Corn Cob

Corncob is commonly grown in Turkey. The corn production is ranked third in cereal production in Turkey, followed by wheat and barley. An increasing production of

corn has been observed since 1980 in 60 Turkish cities. In Turkey, which is an agricultural country, the corn production is approximately of 2.2 million tons. The available residues represent 2.98 million tons for corn stalks and 1.1 million tons for corncob. In this study, the thermal decomposition characteristics of corn cob were investigated through thermogravimetry at four different heating rates and two nitrogen gas atmospheres. Figures 7.7-7.9 present the differential thermograms of the olive cake sample. As seen from the figures, the thermal decomposition behavior of the samples shows that the thermal decomposition process can be approximately described by moisture and volatile lumps. The DTG curves show three main regions in volatile evaluation. Because the temperature intervals of hemicellulose and cellulose decomposition partially overlap each other, the hemicellulose decomposition (first region) usually appears as a more or less pronounced "shoulder" instead of a well-defined peak. The second region is associated with the attainment of the maximum, mainly because of cellulose decomposition, followed by a rapid decay and a long tail. The wide range of temperatures, where lignin decomposes (third region), hinders the appearance of a peak attributable to this component.

Effect of Heating Rate

In this study, the heating rates were varied as 5, 20, 50 and 100 K/min and the effects of heating rate on thermal decomposition of corn cob were shown in Figure 7.7. It is clear from the DTG profiles obtained from the thermal decomposition that considerable different trends in the rates of weight losses took place when heating rate changed between 5 and 100 K/min. At the lower value of this interval of heating rate, the maximum rate of weight loss was so low that it was only 2.8 %/min for 5 K/min. As the heating rate increased, maximum rates of weight losses also increased so obviously that they were determined as 9.3, 19.2 and 37.5 %/min for the heating rates of 20, 50 and 100 K/min, respectively. The phenomenon related to this important change in the maximum rate of weight losses can be interpreted by the fact that biomass has a heterogeneous structure and possess a number of constituents. These constituents give their characteristic individual decomposition peaks in definite temperature ranges in the thermal decomposition process. When heating rate is sufficiently low during thermal decomposition, most of these peaks can be seen as small broken lines or vibrations. However, at high heating rates separate peaks do not

arise because some of them are decomposed simultaneously, and several adjacent peaks are united to form overlapped broader and higher peaks.

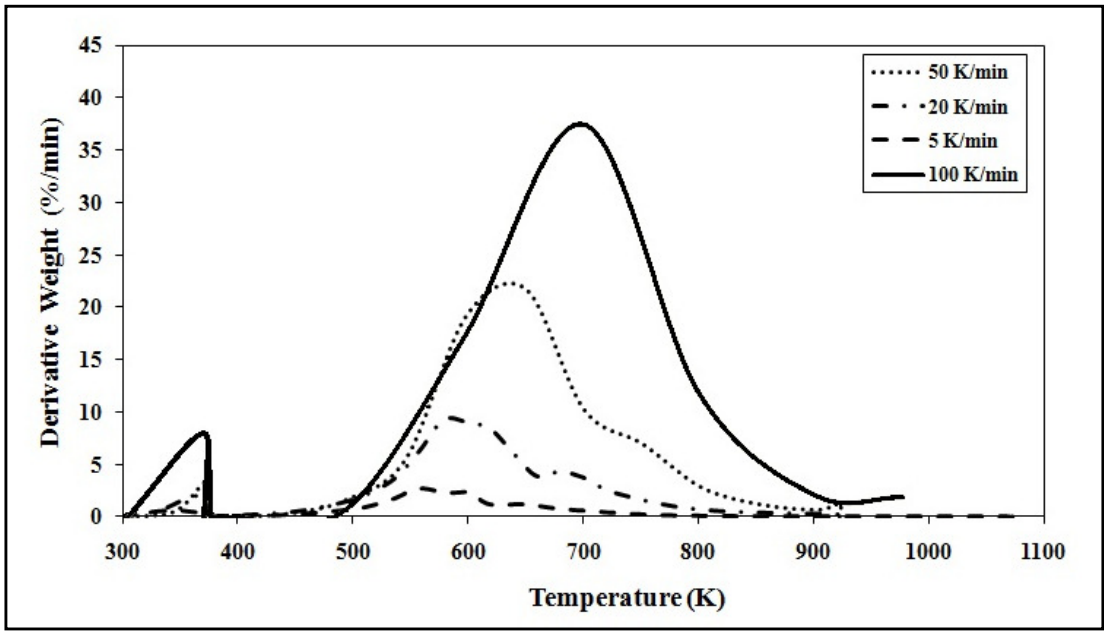

Figure 7.7: The effects of heating rate on thermal decomposition of corn cob (Nitrogen gas flow rate: 100 cm^3/min)

Although, the maximum rate of weight losses are higher at high heating rates, the number of the peaks was relatively lower at these heating rate. For example, at the heating rate of 50 K/min, only one peak appeared. This indicates that an increase in the heating rate from 20 to 50 K/min shifted the main peak to the right and one of the minor peaks at lower temperatures became the major peak at higher heating rates. A similar trend was also observed between the heating rates of 50 and 100 K/min.

Total weight losses from the sample were determined as 78.4, 78.3, 77.9, and 77.6 % on original basis at the heating rates of 5, 20, 50 and 100 K/min, respectively. The increase in heating rate did not cause an important change in weight loss. However, higher heating rate would translate into a shorter contact time between the char and the N_2 gas during the temperature ramp-up stage. This would imply a shorter dwell time for the char and therefore the decrease the weight loss was not high and the effect of the heating rate was negligible.

The temperatures at which volatile evolution reaches a maximum (maximum peak temperature) during thermal decomposition process were also affected from the variation of the heating rate. They were determined as 557, 578, 599 and 701 K for the heating rates of 5, 20, 50 and 100 K/min, respectively. The increase in heating

rate from 5 K/min to 100 K/min induced the peak temperatures shifted to higher values.

The effect of heating rate was also investigated for N_2 atmosphere with flow rate of 50 cm^3/min and the data obtained were given in Fig. 7.8. It is clear from the DTG profiles obtained from the thermal decomposition that considerable different trends in the rates of weight losses took place when heating rate changed between 50 and 100 K/min. At the lower value of this interval of heating rate, the maximum rate of weight loss was 22.0 %/min for 50 K/min. As the heating rate increased, maximum rate of weight loss also increased so obviously that it was determined as 37.8 %/min for the heating rate of 100 K/min. As a comparison, the decrease in N_2 flow rate at different heating rates did not cause an important change in the rates of weight losses.

Maximum peak temperatures resulted in N_2 atmosphere with flow rate of 50 cm^3/min were affected from the variation of the heating rate. They were determined as 598 and 700 K for the heating rates of 50 and 100 K/min, respectively. The increase in heating rate from 50 K/min to 100 K/min induced the peak temperature shifted to higher value.

Total weight losses from the sample were also determined as 75.9 and 76.4 % on original basis at the heating rates of 50 and 100 K/min, respectively. The increase in heating rate did not cause an important change in weight loss.

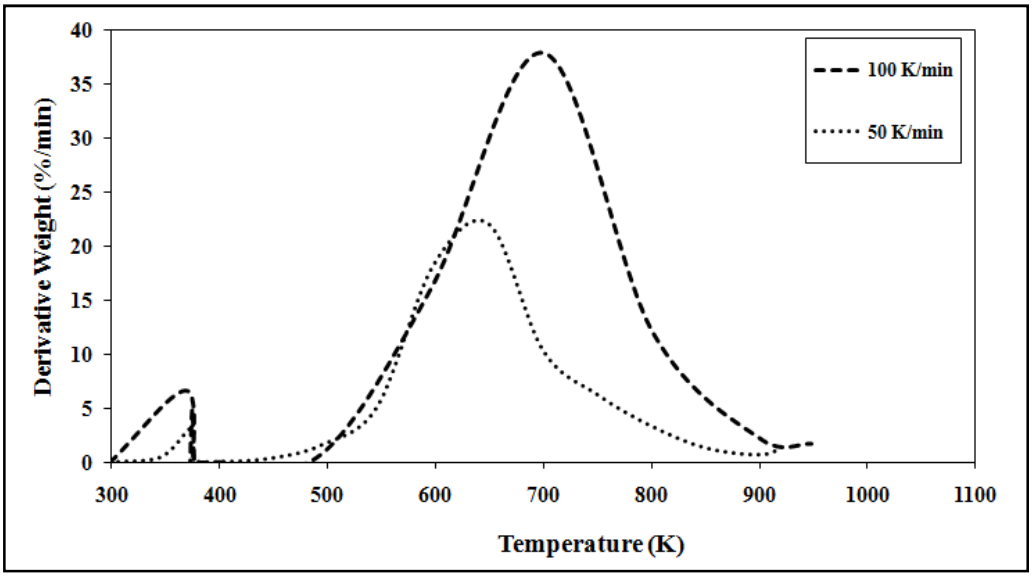

Figure 7.8: The effects of heating rate on thermal decomposition of corn cob (Nitrogen gas flow rate: 50 cm^3/min)

Effect of Gas Flow Rate

Effect of gas flow rate on thermal decomposition of corn cob sample was investigated for two different gas flow rate (50 and 100 cm^3/min) in N_2 atmosphere. The representative TG and DTG curves of the samples, relative to the change of flow rate were plotted in Figure 7.6. Total weight loss was slightly increased by the increase of gas flow rate. For example, weight loss for the thermal decomposition with 50 cm^3/min gas flow rate at the heating rate of 50 K/min was 75.9%, whereas it was obtained to be 78.9 and in case of the gas flow rate of 100 cm^3/min, respectively. Especially, the increased flow rate enhances the diffusion of the N_2 molecules into the lignocelulosic structure, and causes an increase of the weight loss. But since 40 cm^3/min and higher flow rates are enough for a thermal decomposition reaction to begin, weight loss increases very slightly. Maximum peak temperatures were nearly the same by an increase in the gas flow rate.

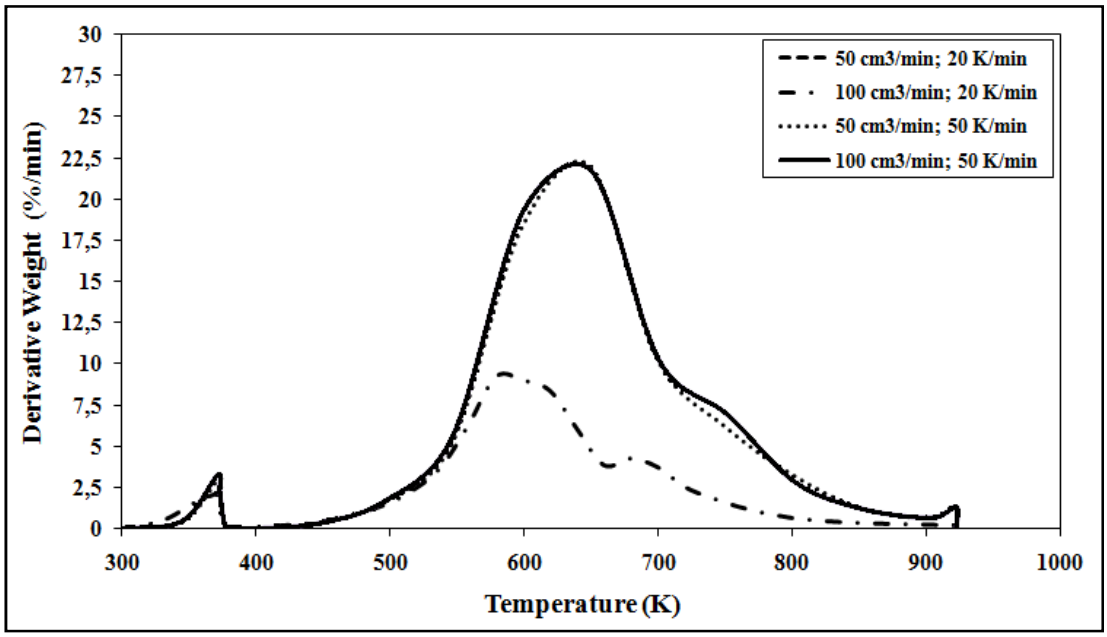

Figure 7.9: The effects of gas flow rate on thermal decomposition of corn cob

7.4. Sugarcane Bagasse

Since bagasse is a by-product of the cane sugar industry, the quantity of production in each country is in line with the quantity of sugarcane produced. In this study, the thermal decomposition characteristics of sugarcane bagasse were investigated through thermogravimetry at four different heating rates and two nitrogen gas atmospheres. Figures 7.10-7.12 present the differential thermograms of the olive

cake sample. As seen from the figures, the thermal decomposition behavior of the samples shows that the thermal decomposition process can be approximately described by moisture and volatile lumps. The DTG curves show three main regions in volatile evaluation. Because the temperature intervals of hemicellulose and cellulose decomposition partially overlap each other, the hemicellulose decomposition (first region) usually appears as a more or less pronounced "shoulder" instead of a well-defined peak. The second region is associated with the attainment of the maximum, mainly because of cellulose decomposition, followed by a rapid decay and a long tail. The wide range of temperatures, where lignin decomposes (third region), hinders the appearance of a peak attributable to this component.

Effect of Heating Rate

In this study, the heating rates were varied as 5, 20, 50 and 100 K/min and the effects of heating rate on thermal decomposition of sugarcane bagasse were shown in Figure 7.10. It is clear from the DTG profiles obtained from the thermal decomposition that considerable different trends in the rates of weight losses took place when heating rate changed between 5 and 100 K/min. At the lower value of this interval of heating rate, the maximum rate of weight loss was so low that it was only 3.1 %/min for 5 K/min. As the heating rate increased, maximum rates of weight losses also increased so obviously that they were determined as 10.6, 21.9 and 35.9 %/min for the heating rates of 20, 50 and 100 K/min, respectively. The phenomenon related to this important change in the maximum rate of weight losses can be interpreted by the fact that biomass has a heterogeneous structure and possess a number of constituents. These constituents give their characteristic individual decomposition peaks in definite temperature ranges in the thermal decomposition process. When heating rate is sufficiently low during thermal decomposition, most of these peaks can be seen as small broken lines or vibrations. However, at high heating rates separate peaks do not arise because some of them are decomposed simultaneously, and several adjacent peaks are united to form overlapped broader and higher peaks. Although, the maximum rate of weight losses are higher at high heating rates, the number of the peaks was relatively lower at these heating rate. For example, at the heating rate of 50 K/min, only one peak appeared. This indicates that an increase in the heating rate from 20 to 50 K/min shifted the main peak to the right and one of the minor peaks at

lower temperatures became the major peak at higher heating rates. A similar trend was also observed between the heating rates of 50 and 100 K/min.

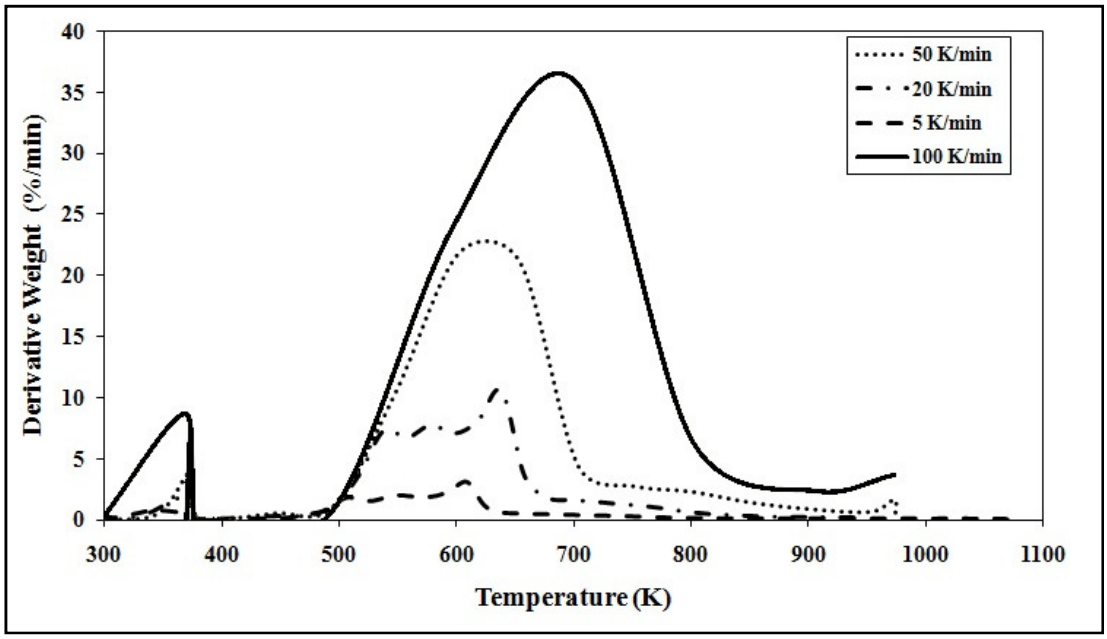

Figure 7.10: The effects of heating rate on thermal decomposition of sugarcane bagasse (Nitrogen gas flow rate: 100 cm^3/min)

Total weight losses from the sample were determined as 79.6, 79.1, 79.3, and 79.6 % on original basis at the heating rates of 5, 20, 50 and 100 K/min, respectively. The increase in heating rate did not cause an important change in weight loss. However, higher heating rate would translate into a shorter contact time between the char and the N_2 gas during the temperature ramp-up stage. This would imply a shorter dwell time for the char and therefore the decrease the weight loss was not high and the effect of the heating rate was negligible.

The temperatures at which volatile evolution reaches a maximum (maximum peak temperature) during thermal decomposition process were also affected from the variation of the heating rate. They were determined as 598, 638, 603 and 701 K for the heating rates of 5, 20, 50 and 100 K/min, respectively. The increase in heating rate from 5 K/min to 100 K/min induced the peak temperatures shifted to higher values.

The effect of heating rate was also investigated for N_2 atmosphere with flow rate of 50 cm^3/min and the data obtained were given in Fig. 7.11. It is clear from the DTG profiles obtained from the thermal decomposition that considerable different trends in the rates of weight losses took place when heating rate changed between 5 and 100

K/min. At the lower value of this interval of heating rate, the maximum rate of weight loss was so low that it was only 2.9 %/min for 5 K/min. As the heating rate increased, maximum rates of weight losses also increased so obviously that they were determined as 10.6, 19.4 and 35.9 %/min for the heating rates of 20, 50 and 100 K/min, respectively. As a comparison, the decrease in N_2 flow rate at different heating rates did not cause an important change in the rates of weight losses.

Maximum peak temperatures resulted in N_2 atmosphere with flow rate of 50 cm^3/min were affected from the variation of the heating rate. They were determined as 603, 639, 603 and 701 K for the heating rates of 5, 20, 50 and 100 K/min, respectively. The increase in heating rate from 5 K/min to 100 K/min induced the peak temperatures shifted to higher values.

Total weight losses from the sample were also determined as 79.4, 79.4, 79,5 and 79.6 % on original basis at the heating rates of 5, 20, 50 and 100 K/min, respectively. The increase in heating rate did not cause an important change in weight loss.

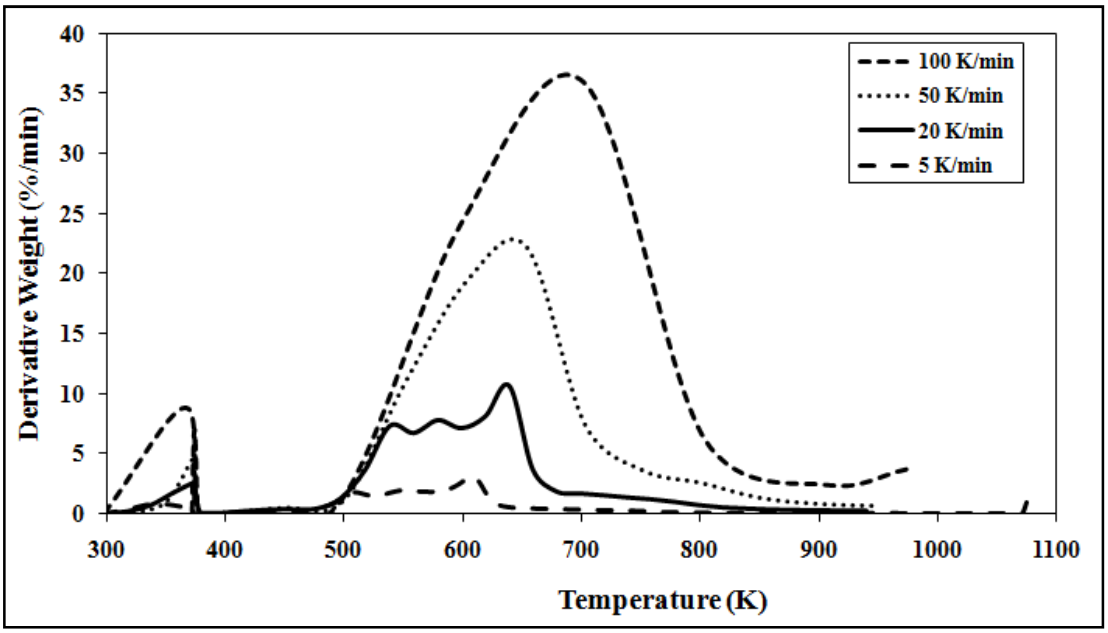

Figure 7.11: The effects of heating rate on thermal decomposition of sugarcane bagasse (Nitrogen gas flow rate: 50 cm^3/min)

Effect of Gas Flow Rate

Effect of gas flow rate on thermal decomposition of sugarcane bagasse sample was investigated for two different gas flow rate (50 and 100 cm^3/min) in N_2 atmosphere. The representative TG and DTG curves of the samples, relative to the change of flow rate were plotted in Figure 7.12. Total weight loss was slightly increased by the

increase of gas flow rate. For example, weight losses for the thermal decomposition with 50 cm^3/min gas flow rate at the heating rate of 20 and 50 K/min were 79.4% and 79.5 %, whereas they were obtained to be 79.1 and 79.3 % in case of the gas flow rate of 100 cm^3/min, respectively. Especially, the increased flow rate enhances the diffusion of the N_2 molecules into the lignocellulosic structure, and causes an increase of the weight loss. But since 40 cm^3/min and higher flow rates are enough for a thermal decomposition reaction to begin, weight loss stays approximately the same. Maximum peak temperatures were nearly the same by an increase in the gas flow rate.

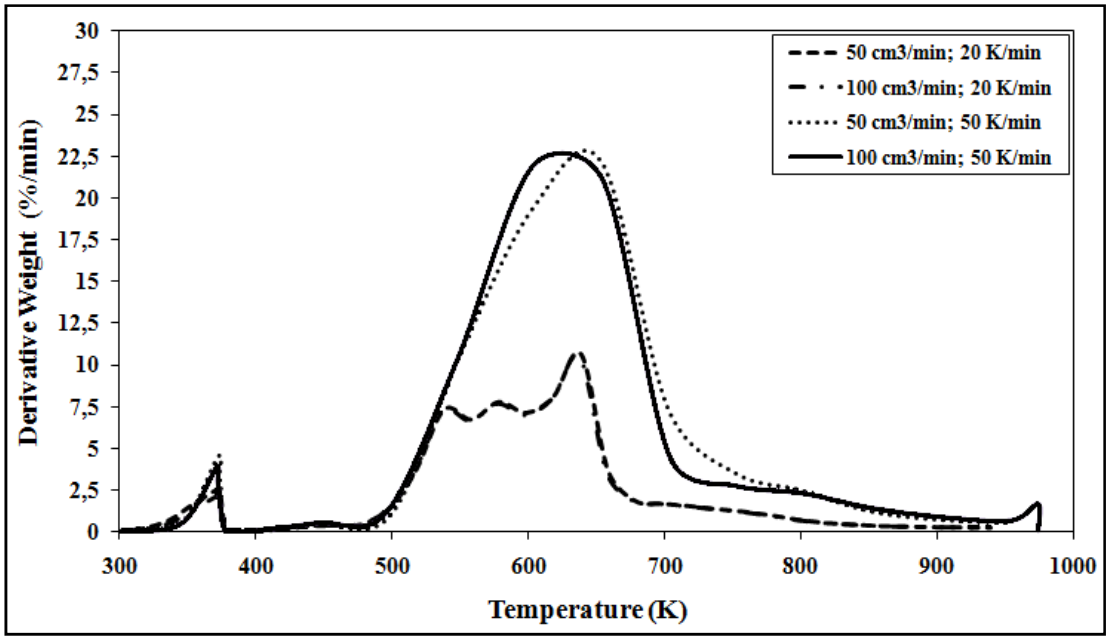

Figure 7.12: The effects of gas flow rate on thermal decomposition of sugarcane bagasse

7.5. Calculation of Kinetic Parameters and Results

For all samples, kinetic parameters have been evaluated under nitrogen atmosphere with heating rates of 5, 20 and 50 K/min, separately. The overall kinetic parameters for all biomass species (lignin, holocellulose and cellulose) have been investigated. E_a (activation energy) and A (frequency factor) values are tabulated in Table 7.5.1 through 7.5.12. For thermal decomposition mechanism function f(α), (1-α) has been selected and the calculations are carried out according to the assumption that, thermal decomposition mechanism of this four biomass samples are chemically controlled. A careful investigation of correlation coefficients, would display that this assumption

was reasonable since the R^2 values were fairly high. In order to be specific, out of 36 kinetic parameters, 28 of them were in the range of 0.97-0.99.

All the calculations were carried out in duplicate, and the coefficient of correlation (R^2) values were given on the right hand side of the tables.

In Tables 7.5.1 through 7.5.3 the kinetic parameters calculated for hazelnut shell under three different heating rates were tabulated.

Table 7.5.1: Calculated kinetic parameters for Hazelnut Shell under 5 K/min

Structural Component	n	E_a (kJ/mol)	A (1/s)	R^2
Hemicellulose	1.0000	1.44 - 1.30	6.68-5.85	0.9458-0.9472
Cellulose	1.0000	5.18 - 4.98	52.06-48.29	0.9896-0.9818
Lignin	1.0000	3.31 - 3.38	23.21-23.91	0.9902-0.9895

Table 7.5.2: Calculated kinetic parameters for Hazelnut Shell under 20 K/min

Structural Component	n	E_a (kJ/mol)	A (1/s)	R^2
Hemicellulose	0.0000	23.74 - 24.59	0.01 - 0.01	0.9443-0.9460
Cellulose	1.0000	4.97 - 4.98	187.04 - 188.02	0.9853-0.9858
Lignin	1.0000	4.12 - 4.14	132.28 - 133.43	0.9924-0.9927

Table 7.5.3: Calculated kinetic parameters for Hazelnut Shell under 50 K/min

Structural Component	n	E_a (kJ/mol)	A (1/s)	R^2
Hemicellulose	0.0000	30.17 - 32.19	0.03 - 0.04	0.9991-0.9999
Cellulose	1.0000	4.74 - 4.77	156.89 - 168.80	0.9827-0.9849
Lignin	0.0000	-9.97- -9.87	-10^{-5}- -10^{-5}	0.9729-0.9741

Cellulose was found to decompose with the 1st order reaction under all heating rates. Since cellulose has been reported to decompose via 1st order reaction by most of the authors, this result was consistent with the studies conducted in the literature [58]. Hemicellulose is usually thought to follow a 1st order reaction order, while for some cases the reaction order might lie between 0-1 [58,44,63]. Lignin generally decomposes with a reaction order between 1-3 based on the several studies reported in the literature [44]. As the heating rate was increased from 5 K/min to 50 K/min the activation energy values for hemicellulose was increased. On the contrary, activation energy for cellulose decomposition was decreased with increasing heating rate. In case of lignin, a general comment on the trend of activation energy could not be mentioned. It is interesting to come up with a ngative activation energy for lignin

since this has not been reported in the literature by any researchers yet. Howewer, having a negative sign is not meaningless in terms of reaction engineering point of view. Actually, a negative sign means the reaction does not require any energy input to proceed. In other words, lignin decomposition under 50 K/min could be viewed as a autocatalytic reaction. At 5 K/min the activation energy for hemicellulose decomposition was the lowest, meaning that the most reactive part was hemicellulose [60]. But, for 20 K/min and 50 K/min it is clear that the activation energy values for hemicellulose decomposition were higher than that of cellulose and lignin decomposition.

Table 7.5.4: Calculated kinetic parameters for Olive Cake under 5 K/min

Structural Component	n	E_a (kJ/mol)	A (1/s)	R^2
Hemicellulose	1.0000	1.54 – 1.49	29.32 - 27.93	0.9417 -0.9428
Cellulose	1.0000	6.03 - 5.85	290.30 – 272.27	0.9831 -0.9762
Lignin	1.0000	3.66 – 3.76	110.55 – 115.98	0.9700 - 0.9627

Table 7.5.5: Calculated kinetic parameters for Olive Cake under 20 K/min

Structural Component	n	E_a (kJ/mol)	A (1/s)	R^2
Hemicellulose	1.0000	1.80 – 1.80	36 – 36.06	0.9538 - 0.9538
Cellulose	1.0000	5.46 – 5.58	227.26 – 238.18	0.9838 - 0.9835
Lignin	1.0000	3.82 – 4.17	117.96 – 137.25	0.9948 – 0.9923

Table 7.5.6: Calculated kinetic parameters for Olive Cake under 50 K/min

Structural Component	n	E_a (kJ/mol)	A (1/s)	R^2
Hemicellulose	3.0000	58.76 – 60.49	29.15 - 40.68	0.9805 - 0.9815
Cellulose	1.0000	4.68 - 4.65	164.21 - 162.03	0.9811 - 0.9812
Lignin	0.0000	-10.67 - -10.69	-10^{-5} - -10^{-5}	0.9930 - 0.9928

In Tables 7.5.4 through 7.5.6, the data corresponding to olive cake pyrolysis kinetic parameres were presented. The trend of activation energy for hemicellulose decomposition under three different heating rates was just the same as that of hazelnut shell. In order to be specific, E_a values displayed an increasing trend as the heating rate was increased. In addition to that, the hemicellulose once again followed the 1st order reaction for 5 and 20 K/min, while the reaction order has been calculated to be 3 for the heating rate 50 K/min. This is a different behavior when compared to hazelnut shell hemicellulose decomposition. For the cellulose decomposition, the

trend observed in Tables 7.5.1 through 7.5.3 has also been valid for cellulosic part of olive cake. The order of the reaction for cellulose decomposition was once again consistent with the literature data cited above [58,44,63]. At 5 and 20 K/min the activation energy for hemicellulose decomposition was the lowest, meaning that the most reactive part was hemicellulose.

Table 7.5.7: Calculated kinetic parameters for Corn Cob under 5 K/min

Structural Component	n	E_a (kJ/mol)	A (1/s)	R^2
Hemicellulose	1.0000	0.94 - 0.92	15.66 – 15.21	0.9719-0.9764
Cellulose	1.0000	3.37 - 3.39	95.34 – 96.49	0.9976-0.9969
Lignin	1.0000	3.18 – 3.21	88.30 – 89.31	0.9921-0.9918

Table 7.5.8: Calculated kinetic parameters for Corn Cob under 20 K/min

Structural Component	n	E_a (kJ/mol)	A (1/s)	R^2
Hemicellulose	1.0000	1.09 - 1.09	18.72 – 18.79	0.9428 - 0.9427
Cellulose	1.0000	3.50 - 3.60	100.02 - 105.27	0.9986 - 0.9981
Lignin	1.0000	4.35 - 5.08	145.76 – 194.28	0.9980-0.9977

Table 7.5.9: Calculated kinetic parameters for Corn Cob under 50 K/min

Structural Component	n	E_a (kJ/mol)	A (1/s)	R^2
Hemicellulose	1.0000	1.49 - 1.51	1.49 - 1.51	0.9526 - 0.9519
Cellulose	1.0000	3.78 - 3.82	112.45 - 114.68	1.0000 - 1.0000
Lignin	3.0000	50.03 – 51.21	7.11 – 8.92	0.9961 - 0.9963

In Tables 7.5.7 through 7.5.9, the data corresponding to corn cob pyrolysis kinetic parameres were presented. The trend of activation energy for hemicellulose decomposition under three different heating rates was just the same as that of hazelnut shell and olive cake. In addition to that, the hemicellulose followed the 1st order reaction for all heating rates. This is a different behavior when compared to hazelnut shell and olive cake hemicellulose decomposition. Referring back to tables 7.5.3 and 7.5.6, one can see that the order of reaction for the former was 0, while it was 3 for the latter. For the cellulose decomposition, the trend observed in Tables 7.5.1 through 7.5.6 was not valid for cellulosic part of corn cob. As could be seen in Tables 7.5.6 through 7.5.9 activation energy for cellulose show an increasing trend with the increasing heating rate. The situation is just the opposite with hazelnut shell and olive cake. The order of the reaction for cellulose decomposition was once again

consistent with the literature data cited above [58,44,63]. At all heating rates, the activation energy for hemicellulose decomposition was the lowest, meaning that the most reactive part was hemicellulose. Different behaviors related to the magnitude of activation energy, with respect to the three-psudo components have been reported in literature in several studies [58,57,64,65]

Table 7.5.10: Calculated kinetic parameters for Sugarcane Bagasse under 5 K/min

Structural Component	n	E_a (kJ/mol)	A (1/s)	R^2
Hemicellulose	1.0000	1.69 - 1.60	33.46 – 31.23	0.9813-0.9789
Cellulose	1.0000	4.57 - 4.29	166.07 – 147.79	0.9860 - 0.9719
Lignin	1.0000	2.77 - 2.87	70.84 – 75.16	0.9929 - 0.9923

Table 7.5.11: Calculated kinetic parameters for Sugarcane Bagasse under 20 K/min

Structural Component	n	E_a (kJ/mol)	A (1/s)	R^2
Hemicellulose	1.0000	1.95 – 1.94	40.75 – 40.64	0.9792 - 0.9791
Cellulose	1.0000	4.62 – 5.05	166.24 – 198.86	0.9818 - 0.9900
Lignin	1.0000	5.07 – 4.66	193.12 – 166.57	0.9894 - 0.9896

Table 7.5.12: Calculated kinetic parameters for Sugarcane Bagasse under 50 K/min

Structural Component	n	E_a (kJ/mol)	A (1/s)	R^2
Hemicellulose	0.0000	23.94 - 23.63	0.01 - 0.01	0.9960 - 0.9981
Cellulose	1.0000	3.87 – 3.74	119.37 - 111.38	0.9765 - 0.9954
Lignin	0.0000	-11.26 - -10.78	10^{-5}- 10^{-5}	0.9934 - 0.9908

In Tables 7.5.10 through 7.5.12, the data corresponding to sugarcane bagasse pyrolysis kinetic parameres were presented. The trend of activation energy for hemicellulose decomposition under three different heating rates was just the same as that of hazelnut shell, olive cake and corn cob. Howewer, the reaction order of hemicellulose decomposition displayed minor difference with the data presented in advance. As could be followed from the tables 7.5.10 through 7.5.12 hemicellulose was decomposed according to 1st order reaction order for 5 and 20 K/min. The order of the reaction was reported to be 0 for 50 K/min in Table 7.5.12. This is a different behavior when compared to hazelnut shell, olive cake and corn cob hemicellulose decomposition. Actually, hemicellulose and lignin parts of all the biomass feedstocks stuided in this thesis, displayed different decomposition characteristics under the observed heating rates. For the cellulose decomposition, the trend observed in Tables 7.5.1 through 7.5.6 was not valid for cellulosic part of sugarcane bagasse. As

could be seen in Tables 7.5.6 through 7.5.9 activation energy for cellulose showed an increasing trend with the increasing heating rate, while in Tables 7.5.10 through 7.5.12 the trend was just different from the ones discussed in case of hazelnut shell, olive cake and corn cob. But, the order of the reaction for cellulose decomposition was once again consistent with the literature data cited above, as well as the experiemental findings extracted from this study. At 5 and 20 K/min, the activation energy for hemicellulose decomposition was the lowest, meaning that the most reactive part was hemicellulose. This behavior was the same as that of observed for olive cake.

8. OVERALL RESULTS AND RECOMMENDATIONS

In this study, the thermal decomposition characteristics of biomass samples (hazelnut shell, olive cake, corn cob and sugarcane bagasse) were investigated via thermogravimetry (TG) at four different heating rates (5, 20, 50 and 100 K/min) and under two nitrogen gas atmospheres (50 and 100 cm^3/min). The kinetic parameters (activation energy (E_a), frequency factor, A and order of the reaction, n) were also determined by Coats Redfern method. The relationship between the feedstock's calculated kinetic parameters and the data from DTG curves have also been compared.

8.1 Concluding remarks

1. The proximate analyses results of the selected biomass samples indicate that the range of moisture, volatile matter, fixed carbon and ash contents of the samples vary between 7.48-9.72 %, 71.72-78.39 %, 8.61-17.07 % and 1.77-5.44 %, respectively.

2. The extractive matter contents of the sample vary between 84.83-99.72% and the lignin contents vary between 4.73-44.40%. Sugarcane bagasse has the highest hemicellulose whereas olive cake has the lowest. Olive cake has the highest α-cellulose where hazelnut shell has the lowest.

3. The heating rate is one of the most important parameters influencing the thermal decomposition characteristics. At the lower value of the interval of heating rate, the maximum rate of weight loss of the hazelnut sample was so low that it was only 2.8 %/min for 5 K/min. As the heating rate increased, maximum rates of weight losses also increased so obviously that they were determined as 10.2, 22.3 and 45.6 %/min for the heating rates of 20, 50 and 100 K/min, respectively.

4. Total weight losses from the hazelnut sample were determined as 75.3, 75, 74.7, and 75.2 % on original basis at the heating rates of 5, 20, 50 and 100 K/min,

respectively. The increase in heating rate did not cause an important change in weight loss.

5. The temperatures at which volatile evolution reaches a maximum (maximum peak temperature) during thermal decomposition process were also affected from the variation of the heating rate. They were determined as 612, 619, 649 and 705 K for the heating rates of 5, 20, 50 and 100 K/min, respectively.

6. Total weight loss of the hazelnut sample was slightly increased by the increase of gas flow rate.

7. As the heating rate increased, maximum rates of weight losses of the olive cake sample also increased so obviously that they were determined as 3.7, 13.7, 26.7 and 53.3 %/min for the heating rates of 5, 20, 50 and 100 K/min respectively.

8. Total weight losses from the olive cake sample were determined as 78.8, 78.5, 78.9, and 78.3 % on original basis at the heating rates of 5, 20, 50 and 100 K/min, respectively. The increase in heating rate did not cause an important change in weight loss.

9. The maximum peak temperatures for olive cake sample were determined as 608, 639, 654 and 700 K for the heating rates of 5, 20, 50 and 100 K/min, respectively. The increase in heating rate from 5 K/min to 100 K/min induced the peak temperatures shifted to higher values.

10. Total weight loss of the olive cake sample was slightly increased by the increase of gas flow rate (from 50 to 100 cm^3/min).

11. As the heating rate increased, maximum rates of weight losses of the corn cob sample also increased so obviously that they were determined as 2.8, 9.3, 19.2 and 37.5 %/min for the heating rates of 5, 20, 50 and 100 K/min, respectively.

12. Total weight losses from the corn cob sample were determined as 78.4, 78.3, 77.9, and 77.6 % on original basis at the heating rates of 5, 20, 50 and 100 K/min, respectively. The increase in heating rate did not cause an important change in weight loss.

13. The maximum peak temperatures for corn cob sample were determined as 557, 578, 599 and 701 K for the heating rates of 5, 20, 50 and 100 K/min,

respectively. The increase in heating rate from 5 K/min to 100 K/min induced the peak temperatures shifted to higher values.

14. Total weight loss of the corn cob sample was slightly increased by the increase of gas flow rate (from 50 to 100 cm^3/min).

15. As the heating rate increased, maximum rates of weight losses of the sugarcane bagasse sample increased so obviously that they were determined as 3.1, 10.6, 21.9 and 35.9 %/min for the heating rates of 20, 50 and 100 K/min, respectively.

16. Total weight losses from the sugarcane bagasse sample were determined as 79.6, 79.1, 79.3, and 79.6 % on original basis at the heating rates of 5, 20, 50 and 100 K/min, respectively.

17. The maximum peak temperatures for sugarcane bagasse sample were determined as 598, 638, 603 and 701 K for the heating rates of 5, 20, 50 and 100 K/min, respectively. The increase in heating rate from 5 K/min to 100 K/min induced the peak temperatures shifted to higher values.

18. Total weight loss of the sugarcane bagasse sample was slightly increased by the increase of gas flow rate (from 50 to 100 cm^3/min).

19. General trend for lignin decomposition from the reaction order point of view were: 1,1,0 for the heating rates 5, 20 and 50 K/min.

20. General trend for cellulose decomposition from the reaction order point of view were: 1,1,1 for the heating rates 5, 20 and 50 K/min.

21. For hemicellulose decomposition, a general trend could not be mentioned.

22. E_a value for hemicellulose decomposition increased for all samples as the heating rate was increased from 5 to 50 K/min.

23. R_2, the coefficient of correlation was found to be between 0.9417-1.0000 for all calculations.

24. For hemicellulose decomposition, E_a values varied between 0.94-60.49 kJ/mol.

25. For cellulose decomposition, E_a values varied between 3.37-6.03 kJ/mol.

26. For lignin decomposition, E_a values varied between -10.87-51.21 kJ/mol.

27. As the heating rate was increased;

- peak temperature was also increased for all samples.

- maximum temperature shifted to the right (higher T zones)

- maxiumum rate of weight loss was increased

28. As the heating rate was increased, lignin decomposition temperature interval was decreased for all samples.

29. As the heating rate was increased, cellulose decomposition temperature interval was increased for all samples (except Corn Cob).

30. As the heating rate was increased from 5 to 20 K/min, hemicellulose decomposition temperature interval was increased for all samples (except Sugarcane Bagasse).

8.2 Recommendations

1. Analysis of the thermal decomposition gases for biomass samples should be carried out and the data obtained should also be examined to clarify thermal decomposition mechanism.

2. Effect of carbon dioxide on the thermal decomposition mechanism should be investigated.

3. The characteristics of biomass samples, thermal decomposition conditions and the kinetic parameters evaluated should be collected in a database and should be kept up to date.

4. The thermogravimetric analysis of commercial pseudocomponents might be investigated, such that the thermal decomposition behavior of the biomass (including the three decomposition zones, namely hemicelluloses, cellulose and lignin) could be compared with that of obtained from the findings of this thesis.

REFERENCES

[1] **Hegerl, G.C., F. W. Zwiers, P. Braconnot, N.P. Gillett, Y. Luo, J.A. Marengo Orsini, N. Nicholls, J.E. Penner and P.A. Stott**, 2007. Understanding and Attributing Climate Change. In: *Climate Change 2007: The Physical Science Basis. Contribution of Working Group I to the Fourth Assessment Report of the Intergovernmental Panel on Climate Change* [Solomon, S., D. Qin, M. Manning, Z. Chen, M. Marquis, K.B. Averyt, M. Tignor and H.L. Miller (eds.)]. Cambridge University Press, Cambridge, United Kingdom and New York, NY, USA.

[2] **Ugurlu O.,** 2006. "Türkiye'de Çevresel Güvenlik Bağlamında Sürdürülebilir Enerji Politikaları", *Ph. D. Thesis,* Ankara University.

[3] **Izmirlioglu et al.,** 2000. "İklim Değişikliği Özel İhtisas Komisyon Raporu", DPT 8. Beş Yıllık Kalkınma Planı

[4] <http://www.eia.doe.gov/oiaf/ieo/world.html> , accessed at 14.12.2009.

[5] **Shell Annual Report,** 2009. <http://www-static.shell.com/static/ public/ downloads/brochures/corporate_pkg/scenarios/shell_energy_scenarios_2050.pdf>, accessed at 21.12.2009.

[6] **WEC Report,** 2009.<http://www.worldenergy.org/documents/ scenarios studyonline1.pdf>, accessed at 10.12.2009

[7] **Exxon Mobil Report The Outlook for Energy A View to 2030** <http://www.exxonmobil.com/corporate/files/news_pub_2008_energyoutlook.pdf> , accessed at 11.12.2009

[8] <http://www.iea.org/textbase/nppdf/free/2009/key_stats_2009.pdf>, accessed at 12.12.2009.

[9] **BP Statistical Review of World Energy 2010**, <http://www. bp.com/statisticalreview>, accessed at 03.06.2010.

[10] <http://www.wtrg.com/prices.htm >, accessed at 14.12.2009.

[11] ***ICCI Conference,*** 2009.

[12] **Krohn S., Morhorst P., Awerbuch S.,** 2009. The Economics of Wind Energy, European Wind Energy Association Report.

[13] ***TKİ- KÖMÜR GAZLAŞTIRMA VE YAKMA TEKNOLOJİLERİ KURSU*** 2008.

[14] ***Micro Cogeneration System Seminar,*** 2010.

[15] ***World Energy Council Turkish National Committee***, 2010, Energy Report.

[16] **Atakul, H.,** 2006. "An Overview of Energy Resources Of Turkey", Seminar I, Gasification and Gas Cleaning Technologies, 18-20th January 2006.

[17] **TETC (Turkish Electric Transmission Company)**, http://www.teias.gov.tr, accessed at 06.01.2010.

[18] **Selvitop O.,** "GLOBAL EKONOMİK KRİZİN ENERJİ SEKTÖRÜ ÜZERİNDEKİ ETKİLERİ" http://www.osbuk.org/haber/uplfiles /osbuk_ -_oselvitop_-_etkb(1).ppt, accessed at 07.01.2010.

[19] **ENSM (Energy&Natural Sources Ministry)** <http://www.enerji.gov.tr/index.php?dil=tr&sf=webpages&b=y_istatistik &bn=244&hn=244&id=398 > accessed at 08.01.2010.

[20] **Akpulat O.,** 2009. Co-Combustion of Coal and Olive Cake In a Fluidized Bed with Limestone Addition and Freeboard Extension, , *MSc. Thesis*, Environmental Engineering, METU.

[21] **Demirbas A.,** 2008. Importance of biomass energy sources for Turkey, *Energy Policy*, pp.834-842.

[22] **Kumar A. , Jones D.D., Hanna A.M.,** 2009. Thermochemical biomass gasification: A review of the current status of the technology, *Energies*, Vol.2 ,pp, 556-581.

[23] **Olgun H.,** 2008. Turkish American Clean Energy Conference,.

[24] **Belen I.,** 2009. Orman Biyokütlesinden Enerji Üretimi, pp, 1-70.

[25] **McKendry P.,** 2002. Energy production from biomass (part 2): conversion technologies", *Bioresource Technology*, pp. 47-54.

[26] **Klass D.L.,** 1998. Biomass for renewable energy, fuels and chemicals, pp. 159-331, San Diego Academic Pres,

[27] **Agbontalr E.A.,** 2007. Overview of Various Biomass Conversion Routes, *American-Eurasian J.Agric.&Environ.Sci* Vol 6, pp. 662-671. <http://www.idosi.org/aejaes/jaes2(6)/8.pdf>, accessed at 29.01.2010.

[28] Gasification Redefining Clean Energy, <http://www.gasification.org/Docs/Final_whitepaper.pdf>, accessed at 21.01.2010.

[29] **Stiegel G.J.,** 2005. Clean, Secure and Affordable Energy Systems, IGCC Clean Coal Technologies Conference. <http://www.turbinetech.com /rss/documents/stiegel060905.pdf>, accessed at 21.01.2010.

[30] **Higman C., Van Der Burgt M.,** 2003. Gasification, pp. 1-85, Gulf Professional Publishing.

[31] **Kural O.,** 1998. Kömür Özellikleri, Teknolojisi ve Çevre İlişkileri, pp. 533- 556, Özgün Publishing.

[32] **Phillips J.,** 2006. The Gas Turbine Handbook, pp. 98-109, NETL. <http://www.netl.doe.gov/technologies/coalpower/turbines/refshelf/handbook/1.2.1.pdf>, accessed at 05.04.2010

[33] **Bain R.L.,** 2006. Biomass Gasification, USDA Thermochemical Conversion Workshop Pacific Northwest National Laboratory. <http://www.ars.usda.gov/sp2UserFiles/Program/307/biomasstoDiesel/RichBainpresentationslides.pdf>, accessed at 05.04.2010.

[34] **Okutan H. C. ,** 2009. *ATIKTAN ENERJİYE Yakma, Gazlaştırma, Piroliz Uygulamaları*, <http://www.rewistanbul.com/sunumlar2009/ATIKTAN ENERJIYE/Hasan_Can_Okutan_REW_Istanbul_2009.ppt>, accessed at 10.12.2009.

[35] **Hemminger W. et al.,** "Recommendations for names and definitions in thermal analysis and calorimetry", ICTAC nomenclature committee, <http://www.ictac.org/ictacnews/articles/dec98/ind98030.pdf>, accessed at 25.05.2010.

[36] **Elving P.J.** 1974. Thermal Methods of Analysis, pp. 488-495, John Wiley&Sons,

[37] **Ozawa T.,** 2000. Thermal Analysis- review and prospect, *Thermochimica Acta*, Vol. 355, pp. 35-42.

[38] <http://iocg.ignou.ac.in/wiki/images/1/1c/UNIT_10_THERMOGRAVIMETRICANALYSIS.pdf >, accessed at, 27.05.2010.

[39] <http://www.msm.cam.ac.uk/Teaching/PtIII/T1/T1H.pdf>, accessed at, 28.05.2010.

[40] **Ozdemir B.,** 2009. Aktif Karbon Üretim Sürecinin Termogravimetrik Analiz İle İncelenmesi, *MSc. Thesis,* Energy Institute, ITU

[41] **Coats, A.W., Redfern, J. P.,** 1964. Kinetic parameters from thermogravimetric data, *Nature*, Vol. 201, pp. 68-79.

[42] **Aboulkas A., El harfi K., El bouadili A., Nadifiyine M., Benchanaa M., Mokhlisse A.,** 2009. Pyrolysis kinetics of olive oil residue /plastic mixture by non-isothermal thermogravimetry. *Fuel.* Vol. 90, pp. 722-728.

[43] **Varhegyi G., Chen H., Godoy S.,** 2009. Thermal decomposition of wheat, oat, barley and brassica carinata straws: A kinetic study. *Energy&Fuels***.** Vol. 23, pp. 646-652.

[44] **Liu., Zhao W., Qian J., Liu C., Zhu Q., Zhao G.,** 2009. Analysis of coals and biomass pyrolysis using the distributed activation energy model. *Bioresource Technology*. Vol. 100, pp. 948-952.

[45] **Munir S., Daood S.S., Nimmo W., Cunliffe A.M., Gibbs B.M.**, 2009. Thermal analysis and devolatilization kinetics of cotton stalk, sugarcane bagasse and shea meal under nitrogen and atmosphere. *Bioresource Technology.* Vol. 100, pp. 1413-1418.

[46] **Khalil R., Varhegyi G., Jashcke S., Gronli M., Hustad J.,** 2009. CO_2 gasification of biomass chars: A kinetic study. *Energy&Fuels.* Vol. 23, pp. 94-100.

[47] **Kumar A., Wang L., Dzeni Y.A., Jones D.D., Hanna M.A.,** 2008. Thermogravimetric characterization of corn stover as gasification and pyrolysis feedstock. *Biomass&Bioenergy*. Vol. 32, pp. 460-467.

[48] **Lester E., Cheung W. H., Lee V.K.C., McKay G.,** 2008. Kinetic study on bamboo pyrolysis. *Ind. Eng. Chem. Res.* Vol. 47, pp. 5710-5722.

[49] **Lester E., Gong M., Thompson A.,** 2007. A method for source appointment in biomass/coal blends using thermogravimetric analysis. *Journal of Analytical and Applied Pyrolysis.* Vol. 80, pp. 111-117.

[50] **Sennecca O.,** 2007. Kinetics of pyrolysis, combustion and gasification of three biomass fuels. *Fuel Processing Technology.* Vol. 88, pp. 87-97.

[51] **Yang H., Yan R., Chen H., Lee D.H., Zheng C.,** 2007. Characteristics of hemicellulose, cellulose and lignin pyrolysis. *Fuel.* Vol. 86, pp. 1781-1788.

[52] **Garcı´a-Iban˜ez P., Sa´nchez M., Cabanillas M.,** 2006. Thermogravimetric analysis of olive-oil residue in air atmosphere. *Fuel Processing Technology.* Vol. 87, pp. 103-107.

[53] **Cetin E., Moghtaderi B., Gupta R., Wall T.F.,** 2005. Biomass gasification kinetics: influences of pressure and char structure. *Combustion Science and Technology*. Vol. 177, pp. 765-791.

[54] **Varhegyi G., Grønli M.G., Di Blasi C.,** 2004. Effects of sample origin, extraction, and hot-water washing on the devolatilization kinetics of chestnut wood. *Ind. Eng. Chem. Res.* Vol. 43, pp. 2356-2367.

[55] **Ollero P., Serrera A., Arjona R, Alcantarilla S.,** 2003. The CO_2 gasification kinetics of oil residue. *Biomass&Bioenergy*. Vol. 24, pp. 151-161.

[56] **Ghaly A.E., Mansaray K.G.,** 1999. Comparative study on the thermal degradation of rica husks in various atmospheres. *Energy Sources.* Vol. 21, pp. 867-881.

[57] **Lee S.B., Fasina O.,** 2009. TG-FTIR analysis of switchgrass pyrolysis. *Journal of Analytical and Applied Pyrolysis.* Vol. 86, pp. 39-43.

[58] **Hu S., Jess A., Xu M.,** 2007. Kinetic study of Chinese biomass slow pyrolysis: comparison of different kinetic models. *Fuel.* Vol. 86, pp. 2778-2788.

[59] **Wilson L., Yang W., Blasiak W., John G.R., Mhilu C.F.,** 2011. Thermal characterization of tropical biomass feedstocks. *Energy Conversion and Management.* Vol. 52, pp. 191-198.

[60] **Biagini E., Fantei A., Tognotti L.,** 2008. Effect of the heating rate on the devolatilization of biomass residues. *Thermochimica Acta.* Vol. 472, pp. 55-63.

[61] **Jeguirim M., Trouve G.,** 2009. Pyrolysis characteristic and kinetics of Arundo donax using thermogravimetric analysis. *Bioresource Technology*. Vol. 100, pp. 4026-4031.

[62] **TAPPI T204 om-88,** 1992. Anonymous, Tappi Test Methods, Tappi Press Atlanta, GA.

[63] **Varhegyi G., Antal J.M., Jakab E., Szabo P.,** 1997: Kinetic modeling of biomass pyrolysis, *Journal of Analytical and Applied Pyrolysis,* Vol 42, pp. 73-87.

[64] **Müller-Hagedorn M., Bockhorn H.,** 2007: Pyrolytic behavior of different biomasses (angiosperms) (maize plnts, straws and wood) in low temperature pyrolysis, *Journal of Analytical and Applied Pyrolysis,* Vol 79, pp. 136-146.

[65] **Kastanaki E., Vamvuka D., Grammelis P., Kakaras E.,** 2002: Thermogravimetric studies of the behavior of lignite-biomass blends during devolatilization, *Fuel Processing Technology*, Vol. 77-78, pp. 159-166.

CURRICULUM VITAE

Mustafa Can Celebi was born in 1987, in Istanbul. He graduated Dogus Primary School in 2001 and started high school in Huseyin Avni Sozen Anatolian College the same year. He received his BSc. Degreee from Middle East Technical University Chemical Engineering Department in 2008. Subsequent to his graduation, he started his master of science studies in Istanbul Technical University Energy Institute.